Phosphorus forms, transformation, sorption, and release in sediments of Walnut Creek watershed, Iowa

by

Suroso Rahutomo

A dissertation submitted to the graduate faculty

in partial fulfillment of the requirements for the degree of

DOCTOR OF PHILOSOPHY

Major: Soil Science (Soil Chemistry)

Program of Study Committee:
Michael L. Thompson, Major Professor
John L. Kovar
C. Lee Burras
David A. Laird
Thomas E. Loynachan

Iowa State University

Ames, Iowa

2016

TABLE OF CONTENTS

LIST OF FIGURES

LIST OF TABLES

ACKNOWLEDGMENTS

First and foremost, I sincerely thank my major professor, Dr. Michael Thompson, and Dr. John Kovar; there is nothing much I could have done to accomplish my study without them. I would also like to thank the members of my committee: Dr. David Laird, Dr. Thomas Loynachan, and Dr. Lee Burras, for inspiring me with their passion for soil science. Moreover, I will never forget Indonesian Oil Palm Research Institute for giving me a chance to enjoy my adventures at Iowa State University. My research is part of the project funded by Agriculture and Food Research Initiative Competitive Grant no. 2013-67019-21393 from the USDA National Institute of Food and Agriculture, I am grateful to the institutions. I also greatly appreciate the family of Rupert Rudolph Hunziker who recognized my interest in soil science by awarding me the 2014 Rupert and Judith Hunziker Graduate Scholarship.

I am so pleased to all members of "Walnut Creek Research Group" (Dr. Richard Schultz, Dr. Thomas Isenhart, Dr. Keith Schilling, Dr. Mark Tomer, Dr. Pete Moore, Dr. Kevin Cole, Dr. James Russell, Jason Palmer, Leigh Ann, William Beck), from whom I learn how a research group work in efficient ways and all members support each other. I am indebted to all of my lab mates and friends: Dr. Teresita Chua, Fritzie Rivas, Taslima Stephen, Llewin Froome, Yili Meng, Kendria Peterson, and Lara Schenck who have never been reluctant to give a hand and more importantly, to give me everlasting friendships. Special thank also goes to many other people that give me supports in thousand different ways. Lastly, my family is the best gift I've ever had, especially my wife, Eva, and my son, Nabil. Without them I am just nothing, and I can't wait to begin our new adventure!

ABSTRACT

The dynamics of phosphorus (P) reactions in stream water have received much attention due to their potential to trigger eutrophication. This study aimed to explore the dynamics of P in Walnut Creek, Jasper County, Iowa. The Walnut Creek watershed supports a variety of land uses (row crop production, grazing, and riparian buffer zones), and the alluvial cross section is composed of a sequence of sediments that contribute differentially to the amounts and forms of P entering the stream. The experiments were focused on the distribution and transformations of solid-phase P in the sediments, P sink/source status of the sediments under varying physicochemical conditions, potential P release from the sediments to the stream water at varying redox potentials, and a comparison of methods for determining P concentration in diverse matrices.

Twenty-five sediment samples from Walnut Creek watershed (classified into three groups: bank, in-stream, and floodplain deposits) were sequentially extracted for P. The distribution of P among organic and inorganic solid phases varied among the stream sediments. Across all 25 sediments, the inorganic P (*Pi*) fractions followed the order: Fe bound *Pi* > Ca bound *Pi* > reductant soluble *Pi* > Al bound *Pi* > soluble and loosely bound *Pi*. For the organic (*Po*) fractions, the order was nonlabile *Po* > fulvic acid bound *Po* > humic acid bound *Po* > labile *Po* > moderately labile *Po*. The ranges of total P (TP), Mehlich-3 extractable P (P-M_3), and ammonium oxalate extractable P (P_{ox}) were 386-1,134, 5-85, and 60-823 mg kg^{-1}, respectively. Among the groups, the highest concentrations of TP, P-M_3, and P_{ox} were in the in-stream deposits. TP was significantly correlated with Fe oxides, clay, and soil organic matter, especially in the bank and floodplain deposits.

The sink-source status for P mobility of the twenty-five sediments in Walnut Creek watershed was predicted for a variety of physicochemical treatments (including variations in solid-to-solution ratio, redox potential, and shaking energy intensity to design treatments of oxic, anoxic, high shaking energy intensity, and low solid-to-solution ratio). The physicochemical treatments resulted in variation in the values of equilibrium phosphorus concentration (EPC) and phosphorus buffering capacity (PBC), and consequently, changed the predictions of the sink-source status of the sediments. Under all physicochemical treatments, it was more likely that the in-stream deposits would act as sources than would the bank sediments or the floodplain soils. It was predicted that most of the twenty-five sediments would act as sources by releasing P to the stream water under an anoxic environment. Total P, Mehlich-3 extractable P, and ammonium oxalate extractable P were the sediment parameters correlated to the EPC values.

Other experiments in this study used four samples from the Walnut Creek bank sediments (the Camp Creek Member, the Roberts Creek Member, the Gunder Member (all three members of the Holocene De Forest Formation), and Pre-Illinoian Till. In the first experiment, the effects of anaerobic incubation and addition of glucose on PBC and EPC of the bank sediments were investigated. The experiment demonstrated that anaerobic incubation decreased Eh and increased pH, and these effects were exaggerated with presence of readily bioavailable carbon. The PBC and EPC varied among the major alluvial units of Walnut Creek bank sediments. In comparison to the treatment without anaerobic incubation, anaerobic incubation significantly increased PBC values of the Camp Creek and Gunder sediments. However, PBC values for the till dropped significantly from 970 L kg^{-1} (without anaerobic incubation) to 173 L kg^{-1} (with anaerobic incubation). Only the Gunder sediment

showed a significant increase in EPC when samples were equilibrated under anaerobic conditions. In the treatment of anaerobic incubation under abundance readily bioavailable carbon, in all sediments the PBC values were significantly lower and the EPC values were significantly higher than those in the treatment without anaerobic incubation.

The second experiment investigated the effects of oxic and anoxic conditions on the potential release of P from bank sediments. A reactor was specially designed to enclose sediment samples in 3,500 MWCO dialysis tubing, to be inserted into simulated stream water and rotated at a controlled velocity under oxic and anoxic conditions. The experiment demonstrated that variations in oxic and anoxic conditions governed Eh, pH, dissolved organic carbon, and release of P from sediment to the water. The highest dissolved P concentration in the water were exhibited by the Camp Creek and Roberts Creek sediments under anoxic conditions, indicating a higher potential for these sediments to function as an internal P source to an overlying water column under anoxic environments.

The effects of treatments of anaerobic incubation and the addition of readily bioavailable carbon on transformation of P forms in the bank sediments were investigated in the third experiment. The treatments resulted in changes in Eh and pH that were similar to those of the first experiment. The forms of P in four bank sediments of Walnut Creek were redistributed concomitantly with a decrease in Eh and an increase in pH due to anaerobic incubation and the addition of readily bioavailable carbon. Low redox potential increased concentration of labile *Pi* which coincided with a decrease in slowly cycling P that was associated with Fe. The distribution of slowly cycling P associated with Ca, stable P, and residue P did not significantly change at varying redox potential. Among the four bank sediments of Walnut Creek, the younger sediments with more organic matter, i.e., the Camp

Creek and Roberts Creek sediments, had greater labile and slowly cycling P associated with Fe, reflecting a greater potential to contribute to elevated levels of P in the stream water, especially if subjected to low redox potential in the stream.

Lastly, two experiments were conducted to investigate the use of the malachite green (MG) method for determining P concentrations in diverse matrices. The first experiment compared MG to the molybdate blue-ascorbic acid (AA) method to assess the sequential extraction of P during fractionation analysis, while the second compared MG to inductively coupled plasma atomic emission spectrometry (ICP-AES) for determining P_{ox}. The results showed that the MG and AA methods agreed for determining P concentration in the extracts of water, 1 *M* HCl, and concentrated H_2SO_4. However, a slight discrepancy between the two methods was found for extracts of 0.5 *M* $NaHCO_3$ and 0.1 *M* NaOH, and concentrated HCl. Furthermore, in the determination of P_{ox}, the MG method resulted in significantly higher values than those obtained by ICP analysis.

CHAPTER 1

GENERAL INTRODUCTION

Elevated levels of phosphorus in streams can cause eutrophication and, in turn, create imbalance in the aquatic ecosystem (Correll, 1998). High P levels in stream water are often associated with P movement through erosion and surface run off from agricultural land and pasture (Heathwaite and Dils, 2000; Tufekcioglu *et al.*, 2012). Most of crop cultivars in modern agriculture require high input of nutrients, including P, therefore regular application of P fertilizers to agricultural land is practiced to increase available P in soils. Some portion of P from the fertilizers may be retained in the soil and transported to streams together with eroded soil materials. Under certain circumstances, the solid-phase P in eroded materials from agricultural land or pasture may be released to the stream water. Another pathway for sediments containing P to enter stream water is bank erosion (Palmer *et al.*, 2014; Zaimes *et al.*, 2008). In Iowa, bank erosion is considered to be the main source of suspended sediments in stream water (Schilling and Wolter, 2000).

In contrast to the factors that contribute to elevated P in stream water, sediments may also act as "sinks" by adsorbing P from stream water. In the adsorption processes, negatively charged ionic P species are mostly adsorbed to sites of Fe or Al-oxyhydroxides. To a lesser extent, adsorption can occur on clay minerals and in association with Fe oxide - organic matter complexes as well as on the surface of Ca and Mg carbonates in calcareous soils (Holford, 1997). Meanwhile, the distribution of solid-phase P in the sediments is an important factor affecting the potential P release from the sediments. Sediments containing more labile-P fractions may have a greater potential for releasing P to the stream water than

the sediments which are dominated by stable-P fractions. In addition, composition of solid-phase P fractions in soils may change due to physicochemical changes in the soil environment (Hedley *et al.*, 1982; Schrijver *et al*., 2012; Sui *et al*., 1999a; Varinderpal-Singh *et al*., 2007).

As in other stream environments, there is also a growing concern about P dynamics in Walnut Creek, Jasper County, Iowa. The Walnut Creek watershed supports a variety of land uses, including row crop production, grazing, and riparian buffer zones. The alluvial cross section is composed of a characteristic sequence of sediments that have a potential to contribute differentially to the amounts and forms of P entering the stream. A range of physicochemical properties (e.g., total suspended solids, redox potential, and kinetic energy of stream flow) in the system of sediment-stream water may exist occasionally along the creek due to storm events, groundwater discharge to the stream, or blocking of stream flow by debris or beaver dams. Previous studies have been conducted to investigate the dynamics of P in the Walnut Creek watershed, for example, studies of the variation of total P content in stream water over a 5-year monitoring period (Schilling *et al*., 2006a), the variation of total P content by lithostratigraphic unit (Schilling *et al.*, 2009), and potential for P contribution from groundwater discharge to the stream (Schilling and Jacobson, 2008b).

With the aim of contributing to a better understanding of the dynamics of P in the Walnut Creek watershed, the present study focused on the factors of solid-phase P distribution in the sediments and its transformation, P adsorption-desorption reactions, and the potential for P release from the sediments to the water column under physicochemical environments that are likely to occur along the creek. Examining those factors is essential for robust modeling predictions of the fate of P at the interface of sediments and stream

water. It is also generally recognized that assessing the dynamics of P requires a rapid and sensitive method for determining phosphate in diverse matrices. Therefore, the objectives of this study were to:

- characterize the properties of sediments in the Walnut Creek watershed and their relationships
- describe the distribution of solid-phase P in the sediments of the Walnut Creek watershed
- predict the sink/source behavior of sediments from the Walnut Creek watershed under a variety of physicochemical treatments
- investigate the effects of varying redox potential on P sorption indices, transformations of solid-phase P fractions, and P release from the Walnut Creek bank sediments
- compare a rapid and sensitive method, the malachite green method, to other methods for determining phosphate concentration in diverse matrices.

CHAPTER 2

LITERATURE REVIEW

Scope of the Review

The review in this chapter consists of eight parts. The first part concentrates on the environmental issues related to P in water bodies and the main pathways for P to enter stream water with emphasis on the Mississippi River. All samples in this study were collected from Walnut Creek watershed, and a review from previous studies of the watershed constitutes the second part. The third part is about environmental thresholds derived from the degree of phosphorus saturation and soil test P. The fourth part reviews the two methods for P fractionation used in this study and previous studies that are related to transformation of solid-phase P in soils/sediments. Quantity/intensity analysis as a mathematical model for studying P adsorption/desorption is the main focus in the fifth part, while methods used in previous studies for investigating P release from sediments are reviewed in the sixth part. Related to the fifth and the sixth parts, methods for varying redox potential in a lab experiment are reviewed in the seventh part. Finally, the eighth part reviews the malachite green method, the molybdate blue-ascorbic acid method, and the ICP-AES method, i.e., the three methods used to determine P concentrations in the soil extracts analyzed in this study.

Phosphorus in Freshwater Bodies and its Environmental Significance

Phosphorus (P) is an essential nutrient for phytoplankton. Especially when sufficient nitrogen is present, phytoplankton growth may be enhanced by even a small increment of P (Upreti *et al.*, 2015). This reflects the small stoichiometric ratio of P to other major nutrients

necessary for phytoplankton growth. The classic example is the atomic ratio 106C:16N:1P for phytoplankton in marine environments (Redfield, 1958). Though the ratio may be different in other ecosystems (e.g. Cleveland and Liptzin, 2007; Ptacnik *et al.*, 2010; Stelzer and Lamberti, 2001), it describes the significant role of elevated P in triggering phytoplankton blooms.

Phytoplankton blooms in eutrophic water could be harmful to species balance in aquatic ecosystems (Correll, 1998). Other examples of water quality impairments due to eutrophication are increased in turbidity, low dissolved oxygen, unpleasant odor and taste, and toxins which may be produced by some species of cyanobacteria (CCME, 2004). For Canadian rivers and lakes, the range of total phosphorus concentrations that trigger eutrophic status is 35-100 $\mu g\ L^{-1}$ (CCME, 2004). In the US, the Environmental Protection Agency's water quality criteria recommend that total P concentrations should not exceed 25, 50, and 100 $\mu g\ L^{-1}$ in lakes/reservoirs, stream entering lakes, and stream/rivers, respectively, to minimize phytoplankton growth (USEPA, 1986).

Phosphorus in the water bodies may originate from nonpoint or from point sources. In general, a primary nonpoint sources is agricultural activities, e.g. in the Mississippi River (Jacobson *et al.*, 2011). Alexander *et al.* (2008) estimated that 80% of P entering the Mississippi River is from agricultural sources, while the contribution from nonagricultural sources was 20%. Modern agricultural systems may require high inputs of P, either in the form of highly soluble phosphate (e.g., monocalcium phosphate) or organic waste (e.g., animal manure) to increase available P. Besides direct runoff from agriculturally managed lands, P may enter streams in the Mississippi River basin through stream bed and bank erosion (Schilling *et al*., 2011; Wilson *et al*., 2008). Bank erosion may make a significant

contribution to the suspended sediments in stream waters, especially in Iowa (Schilling and Wolter, 2000), carrying particulate P into the stream water.

Another potential pathway for P to enter streams is through solution phase movement in the soil or leaching (Sinaj *et al.*, 2002). Normally, the amount of P loss through leaching from agricultural land is small (Sims *et al.*, 1998) compared to P transport from surface run-off and erosion. This is due to the very small quantity of P in soil solution compared to total P (Holford, 1997), as well as affinity of P to be retained by soil particle surfaces. However, loss of P through leaching may be favored when manure has been applied to soil (McDowell and Sharpley, 2001b), in soils which have high permeability (Kang *et al.*, 2011), or in paddy soils which receive high rates of P fertilizer (Zhang *et al.*, 2003). Therefore, along with erosion and run off, leaching should be considered as one of the P transport mechanisms from soil with a potential to cause eutrophication in water bodies (Turner and Haygarth, 2000). An example of potential eutrophication in groundwater fed wetlands due to P leaching had been reviewed by Smolders *et al.* (2010).

Walnut Creek Watershed

Walnut Creek is located in Jasper County, Iowa (Fig. 1). According to Schilling *et al.* (2006b), Walnut Creek drains 7,951 ha area and discharges into the Des Moines River at the upper end of the Red Rock Reservoir. It supports a variety of land uses, including row crop production, grazing, and riparian buffer zones in the Neil Smith National Wildlife Refuge, a large-scale project prairie restoration project in Iowa. The watersheds of Walnut Creek are part of the Southern Iowa Drift Plain, where steeply rolling hills and well-developed drainage systems are commonly found. Most soils in the watersheds of the Southern Iowa Drift Plain

were formed in loess and till, whereas dominant soil textures are silty clay loams, silt loams or clay loams. Palmer *et al.* (2014) reported that annual streambank recession rates in Walnut Creek in 2005-2011 were 0.6 cm yr^{-1} and 28.2 cm yr^{-1} during years of hydrological inactivity and during seasons with high discharge rates, respectively. They also reported that the overall average for total bank erosion sediment was 5,299 Mg yr^{-1}, suggesting that streambank erosion made major contribution to sediment discharged from Walnut Creek watershed.

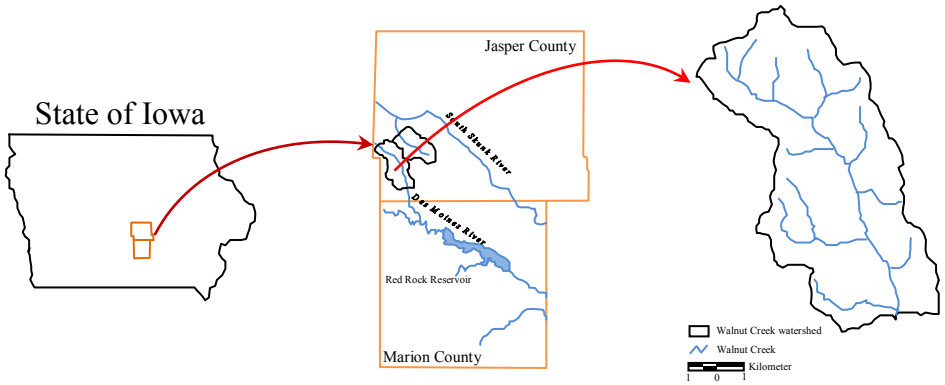

Figure 1. Walnut Creek watershed in Jasper County, Iowa, adapted from Schilling *et al.* (2006b).

The alluvial cross section of Walnut Creek is composed of a characteristic sequence of sediments with potential to contribute differentially to the amounts and forms of P entering the stream. An example of the alluvial cross section is given in Fig. 2 and illustrates the six stratigraphic units of the Walnut Creek watershed (Camp Creek Member, Roberts Creek Member, Gunder Member, Pre-Gunder alluvium, Wisconsinan loess, and Pre-Illinoian Till). Schilling *et al.* (2006b) described that the first three alluvial units (the Camp Creek, the Roberts Creek, and the Gunder) as members of the De Forest Formation; the fourth alluvial

unit (the Pre-Gunder) is older than the oldest member of the De Forest formation. The last two units (the loess and the Pre-Illinoian Till) are commonly found on hill slope locations, but the stream may also cut through them. Four out of the six stratigraphic units (the Camp Creek Member, the Robert Creek Member, the Gunder Member, and the Pre-Illinoian Till) are major stratigraphic units of alluvium in Walnut Creek bank sediments (Schilling *et al.*, 2004).

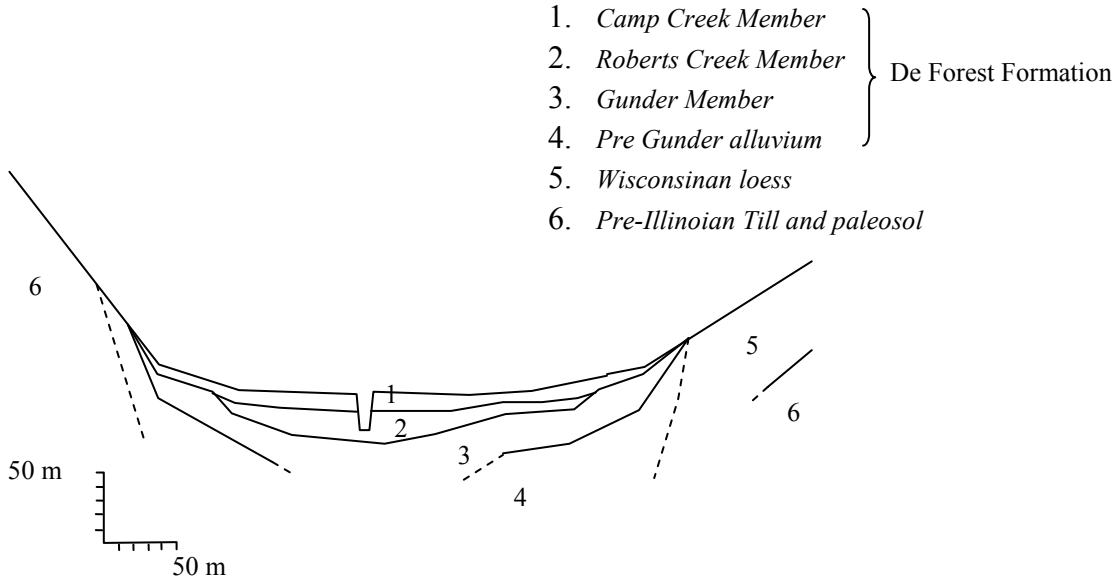

Figure 2. An example of alluvial cross section from a transect in Walnut Creek watershed, adapted from Schilling *et al.* (2004) and Schilling *et al.* (2006b).

The De Forest formation represents the Holocene Interglacial stage over the last 11,000 years BP, and it occurs throughout Iowa. As Baker *et al.* (1996) reported in detail, the Gunder Member, the Roberts Creek Member, and the Camp Creek Member date from 11,000 to 4,000 yr BP, 4000 to 400 yr BP, and the last 380 yr, respectively. The fourth alluvial unit, Pre-Illinoian Till, was deposited sometime between 2,000,000 to 500,000 years BP. The Camp Creek Member consists of post-settlement alluvial and colluvial materials

deposited in the stream valley and range from approximately 0. 6 to 2 m in thickness (Schilling *et al*., 2006b). Due to different geomorphological processes, each stratigraphic unit has a set of unique characteristics. Examples are the variations in particle size distribution and hydraulic conductivity that were described by Schilling *et al.* (2004) and are presented in Table 1.

Table 1. Particle size distribution (PSD) and hydraulic conductivity (HC) of major stratigraphic units in Walnut Creek, adapted from Schilling *et al.* (2004). Numbers in parentheses are standard deviation.

Alluvium	PSD (%)				HC ($m\ s^{-1}$)
	Sand	Coarse Silt	Fine Silt	Clay	
Camp Creek[†]	3.2 (2.3)	36.2 (6.8)	36.6 (11.1)	24.1(10.7)	5.57×10^{-5}
Roberts Creek[‡]	4.7 (3.1)	31.8 (10.1)	48.8 (21.3)	14.8(13.7)	1.70×10^{-6} (1.46×10^{-6})
Gunder[§]	12.3 (13.5)	35.5 (13.6)	25.2 (10.8)	27.0(11.7)	4.93×10^{-6} (5.90×10^{-6})
Pre-Illinoian Till[œ]	41.9 (3.0)	20.3 (5.2)	20.5 (9.4)	17.4(10.5)	1.99×10^{-7} (1.75×10^{-7})

[†] *n (number of samples) = 5 for PSD and 1 for HC;* [‡]*n= 8 for PSD and 6 for HC;* [§]*n= 12 for PSD and 15 for HC;* [œ] *n= 3 for PSD and 4 for HC.*

DPS and Soil Test P as Indicators of Environmental Risks

The Degree of Phosphorus Saturation (DPS) is a statistic that compares the amount of P that is bound to a soil to an index of the potential capacity of the soil to adsorb P (Renneson *et al.,* 2015). Therefore, equations to calculate DPS commonly represent the ratio of P extractable with an extracting solution to the concentration of certain metals extractable with the same extracting solution. For example, DPS indices have been developed that compare the amount of extractable P to the concentration of Fe+Al in ammonium oxalate (Hooda *et al.*, 2000; Yan *et al.*, 2013), in the Mehlich-1 extractant (Nair *et al.*, 2004), in Mehlich-3 extractant (Sims *et al.*, 2002), and in the Bray extracting solution (Dayton *et al.*, 2014). In the Mehlich-3 extracting solution, some studies have used the ratio of extractable P to extractable

Al (Sims *et al.*, 1998), and others have compared extractable P to extractable Ca+Mg (Ige *et al.*, 2005; Xue *et al.*, 2014). It should be noted that related coefficient, the α value, may be employed to improve the estimate of the concentration of metals that might be associated with P sorption (for example is $DPS_{ox} = [P_{ox}/ \alpha(Al_{ox} + Fe_{ox})]*100$, where P_{ox}, Al_{ox}, and Fe_{ox} are ammonium oxalate extractable P, Al, and Fe, respectively). Some α values have been proposed, for example α = 1 (Kleinman and Sharpley, 2002), α = 0.5 (Leinweber *et al.*, 1997), and α = 0.25 (Nair *et al*., 2004). In addition, an alternative equation was used by Pöthig *et al.* (2010) to calculate DPS in more than 400 soils from Germany and Switzerland, where only water-soluble P was used in the mathematical equation.

The use of DPS in soil and environmental studies has been increasing rapidly due to its potential to integrate an assessment of the intensity of P accumulation as referred to the finite capacity of a soil to adsorb P as well as to describe the potential of P to desorb from the solid phase to solution phase (Beauchemin and Simard, 1999). In environmental studies, the DPS is widely used to assess P environmental risk (Casson *et al.*, 2006; Hooda *et al.*, 2000). It is generally accepted that soils with high DPS values are more susceptible to loss P due to low capacity to retain additional P (Alleoni *et al.*, 2014). Some DPS values have been suggested as thresholds for environmental risks (Table 2). The threshold values vary in this table depending on parameters used to calculate DPS, objectives, and soil types.

Besides DPS values, soil test P can be used to assess potential P release. The use of soil test P as an indicator of environmental risks may be simple and applicable since soil test P is a part of routine analysis in many soil labs. However, Sharpley *et al.* (2003) suggested that soil test P should be interpreted carefully for environmental purposes since the P status (low, medium, or high) known on soil test reports are based on the expected response of a

Table 2. Degree of Phosphorus Saturation (DPS) values as indicator of environmental risk from previous studies.

DPS (%)	Parameters used to estimate DPS	Note	Reference
8	P_{ox}, Al_{ox}, and Fe_{ox}	DPS value suggested as a threshold for ability of an Ultisol amended with inorganic P fertilizers in the field to release P.	Gikonyo *et al.* (2011)
9	P_{M3} and Al_{M3}	DPS proposed as the threshold for the A horizon of agricultural soils in Quebec with the surface water quality objective of 0.03 mg total P L^{-1}.	Sims *et al*. (1998)
10	P_{ox}, Al_{ox}, and Fe_{ox}	DPS value suggested as a critical point in a number of soils in the UK. Less P desorption when DPS was <10%, a linear increase in P leachate losses when DPS was >10%.	Hooda *et al.* (2000)
15	P_{ox}, Al_{ox}, and Fe_{ox}	DPS value suggested as a critical point for agricultural soils in the northeastern region of the United States; above this value water soluble P could be expected to increase rapidly with additional P loading.	Ohno *et al.* (2007)
15	P_{M3}, Fe_{M3}, and Al_{M3}	DPS used as a threshold in Delaware soils to minimize the risk of nonpoint-source P pollution	Sims *et al*. (2002)
22	P_{M3}, Fe_{M3}, and Al_{M3}	DPS value corresponded to a critical concentration of water extractable P of 1 mg L^{-1} in Minnesota soils.	Laboski and Lamb (2004)
22	P_{ox}, Al_{ox}, and Fe_{ox}	DPS value suggested as a threshold for ability of an Ultisol amended with inorganic P fertilizers in a lab incubation to release P.	Gikonyo *et al*. (2011)
25	P_{ox}, Al_{ox}, and Fe_{ox}	DPS set as threshold for noncalcareous sandy soils in Netherland with the surface water quality objective of 0.15 mg total P L^{-1}.	(Breeuwsma *et al*. (1995)
25	P_{ox}, Al_{ox}, and Fe_{ox}	DPS value corresponded to 50 mg Mehlich-1 P kg^{-1}, an excessive P level in Delaware soils.	Pautler and Sims (2000)
<30, 30-60, >60	P_{M1}, Fe_{M1}, and Al_{M1}	DPS values to assign different P loss ratings in the Florida P Index.	Nair *et al*. (2004)

Notes: P_{ox}, Al_{ox}, and Fe_{ox} are acidified ammonium oxalate extractable P, Al, and Fe, respectively. P_{M3}, Al_{M3}, and Fe_{M3} are Mehlich-3 extractable P, Al, and Fe, respectively. P_{M1}, Al_{M1}, and Fe_{M1} are Mehlich-1 extractable P, Al, and Fe, respectively

crop to P. Critical values used to predict P loss usually range from less than 2 to 4 times of the critical value for optimum crop yield (Sharpley *et al.*, 2003). Several values of soil test P have been suggested in different states in the United States. For example, 150 mg Bray-P kg^{-1} is the threshold to recommend no additional P application in Ohio (Dayton *et al.*, 2014). Pautler and Sims (2000) suggested that soils in Delaware with >50 mg Mehlich-1 P kg^{-1} would have excessive P for crop production. Using calcareous soils in the Minnesota River Basin, Fang *et al.* (2002) suggested that the critical levels for soil Mehlich-3 P and Olsen P were 65-85 and 40-55 mg kg^{-1}, respectively. Other environmental thresholds for soil test P in the US have been summarized by Sharpley *et al.* (2003).

Phosphorus Fractionation in Soils/Sediments

Phosphorus in soil and sediments is distributed among various fractions of organic P *(Po)* and inorganic P *(Pi)*. The solid phase P can be classified into three general groups: labile P, slowly cycling P, and stable P (Schrijver *et al.*, 2012; Tiessen and Moir, 2008) . Labile P is soil P capable of readily entering the soil solution, while slowly cycling P is thought to be a P associated with Fe/Al oxide, Ca, and organic compounds and which is not readily available for plant uptake. Stable P fraction is more tightly bound to mineral and organic compounds than is slowly cycling P. Stable P also includes P that is bound to highly recalcitrant compounds in the soil. In term of P dynamics in stream water and sediments, characterizing these fractions is important to predict potential releases of P from the sediments into the stream water.

General principle of laboratory analysis for soil P fractionation is sequential extraction using different extracting solutions. In the method of Tiessen and Moir (2008),

labile *Pi* fraction, slowly cycling *Pi,* stable *Pi* fraction, and residue P are sequentially extracted using 0.5 *M* $NaHCO_3$, 0.1 *M* NaOH and 1 *M* HCl, concentrated HCl, and H_2SO_4, respectively. In another method particularly for non-calcareous soils, Zhang and Kovar (2009) described that soluble and loosely bound P, Al bound-*Pi*, Fe bound-*Pi*, reductant soluble-*Pi*, and Ca bound-*Pi* are sequentially extracted using 1 *M* NH_4Cl, 0.5 *M* NH_4F, 0.1 *M* NaOH, CBD (citrate bicarbonate dithionite), and 0.25 M H_2SO_4, respectively.

For each step in the sequential extraction, *Pi* and *Pt* (total P) are measured directly in the extract, while *Po* is calculated by subtracting *Pi* from *Pt*. It should be noted that the procedures for determining *Po* fractions in the method of Tiessen and Moir (2008) are different from those of Zhang and Kovar (2009). First, *Pi* and *Po* in the method of Tiessen and Moir (2008) are determined in a single scheme of sequential extraction. By contrast, sequential extraction for *Po* fractionation in the method of Zhang and Kovar (2009) is separate from the scheme for *Pi* fractionation, where labile *Po,* moderately labile *Po,* humic acid and fulvic acid-*Po,* and nonlabile *Po* are extracted using 0.5 *M* $NaHCO_3$, 1 *M* HCl, 0.5 *M* NaOH, and 1 *M* H_2SO_4, respectively. Second, in the method of Tiessen and Moir (2008), *Pt* is measured after digestion of the extract with ammonium persulfate in an autoclave at 121°C, while potassium persulfate is recommended in the method of Zhang and Kovar (2009) and digestion of the extract takes place on a hot plate at 150°C.

The distribution of solid-phase P may change due to cultivation practices or change may be induced by treatments applied in laboratory incubations. Examples of land management practices that have been shown to change the distribution of P among solid-phase fractions include long-term fertilization (Varinderpal-Singh *et al.*, 2007), application of biosolids (Sui *et al*., 1999a), and reforestation of farmlands (Schrijver *et al.*, 2012). In a 108-

day incubation study, He *et al.* (2004) reported that *Pi* extractable with 0.5 *M* $NaHCO_3$ and 0.1 *M* NaOH increased with addition of manure and fertilizers. Other studies have suggested that transformation of P fractions in incubation studies mostly relate to microbial activities triggered by the addition of energy sources. In a 9-month laboratory incubation, Hedley *et al.* (1982) reported the decrease of labile *Pi* in soil amended with cellulose and N. In this study, they suggested that adding cellulose and N increased microbial activity and in turn promoted the immobilization of *Pi* to microbial P. A similar result was reported by Du *et al.* (2011) who found a decrease in water-soluble P after 72-h incubation of sediments treated with glucose.

Phosphorus Adsorption and Desorption

Phosphorus adsorption refers to the retention of phosphate at or near adsorption sites of solid-phase soil components. In contrast, P desorption refers to the release of phosphate from the solid phase to the solution phase. In terms of P dynamics in stream water, sediments may adsorb P from the stream water (acting as "sinks") or desorb P to the stream water (acting as "sources"). A batch adsorption study is commonly used to evaluate the sink/source status of the sediments. Principally, such a study describes the amount of phosphate adsorbed onto sorption sites in the sediments (solid phase P, commonly abbreviated as Q) as a function of phosphate concentration in the solution (liquid phase P, commonly abbreviated as C) at constant temperature after equilibrium has been reached. There are various mathematical models to analyze the relationship between Q and C, but for the purpose of evaluating stream sediments as sinks or sources of phosphate,

quantity/intensity (Q/I) analysis is widely used, since a range of low P concentrations can be employed to represent P concentration under natural conditions.

In the Q/I analysis, linear regression is determined from the relationship of Q as a function of C (Hongthanat *et al.,* 2011). The slope of this linear regression is the PBC or phosphorus buffering capacity, while C at Q = 0 is the EPC or equilibrium phosphorus concentration. PBC indicates the capability of sediment to buffer P adsorption and desorption, while EPC indicates a condition where adsorption and desorption processes are in equilibrium. Sink/source status of sediments in the stream water can be predicted by comparing EPC to the dissolved P in the stream water. Phosphorus desorption from stream sediments to the stream water is favored when EPC is greater than dissolved P in the stream water. Conversely, P adsorption is predicted to be dominant when EPC is lower than dissolved P in the stream water.

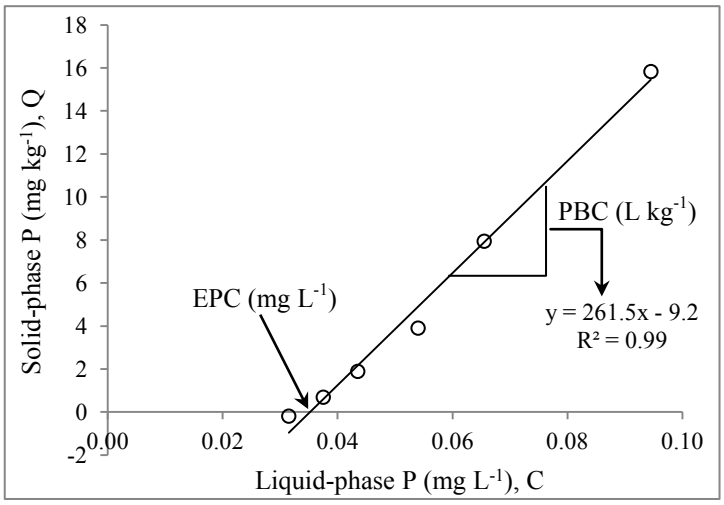

Figure 3. An example of Q/I analysis, the liquid phase P (C) is plotted against P in the solid phase (Q) to determine phosphorus buffering capacity (PBC) and equilibrium phosphorus concentration (EPC). In this example, PBC and EPC are 261.5 L kg^{-1} and 0.035 mg L^{-1}, respectively.

Several factors may control P adsorption and desorption, e.g., sorption sites available in the sediments, pH, potential redox, ionic strength, and the presence of competing organic compounds. Sorption sites for P adsorption are mainly from iron(III) (hydr)oxides, hydrous aluminum oxides, and clay minerals (Stumm and Morgan, 1970). Other sorption sites may occur on manganese oxide (MnO_2) surfaces, especially when the concentration of MnO_2 is greater than the concentration of iron and aluminum oxides (Yao and Millero, 1996). However, the point of zero charge of manganese oxides is about 2.8 (Gadde and Laitinen, 1974). The pH of the stream water is around neutral, therefore Mn oxides surfaces will have a net negative surface charge and may contribute negligibly to limited P adsorption.

Solution pH plays an important role in controlling P adsorption/desorption since it can drive the dominant species of phosphate in stream water, dominant charges in the edges of iron oxides, and the competition between HCO_3^- and phosphate ion (Bar-Yosef *et al.*, 1988). In general, P adsorption increases under acidic conditions due to the dominantly positive charges on the surfaces of Fe and Al-oxides. For potential redox, adsorption is more likely to occur under high redox potential. Pant and Reddy (2001) suggested that under aerobic conditions, more P sorption sites are available from the amorphous and poorly crystalline forms of Fe oxides. Conversely, anaerobic conditions promote the reduction of Fe^{3+} to Fe^{2+} and dissolution of Fe oxides, resulting in fewer sorption sites and the release of Fe-bound P.

Phosphorus adsorption is also influenced by ionic strength and the presence of dissolved organic compounds. For example, in a study using a range of ionic strengths in a base solution, Lucci *et al.* (2010) showed that higher P adsorption was found when the base solution had higher ionic strength. However, the influence of ionic strength on P adsorption

also depends on pH, as reported by Arai and Sparks (2001). They found that P adsorption on ferrihydrite increased with increasing ionic strength at pHs greater than 7.5 but not at pHs between 4 – 7.5. The effects of humic acid on P adsorption were mainly due to the competition for adsorption in the sorption sites. The suppression of phosphate adsorption by the presence of soil humic acid had been reported by Antelo *et al.* (2007) for goethite and by Yao and Millero (1996) for manganese oxide.

Study of Potential P Release from Soil/Sediments

Study of potential release of P through water movement in soils or sediments can be carried out in the field or lab experiment. For field experiments, groundwater samples are collected in lysimeters (McDowell and Sharpley, 2001b; Sinaj *et al*., 2002; Sui *et al*., 1999b; Turner and Haygarth, 2000), in the tile drain outlets (Heckrath *et al.*, 1995), or in the monitoring wells (Schilling and Jacobson, 2008a; Schilling and Jacobson, 2014). In lab experiments, P release can be mimicked by flowing water through a packed soil column, and the flow can be designed move upward (Frossard *et al.*, 2014) or downward (Glaesner *et al.*, 2012). In other lab experiments, water is not passed through sediments but a system is designed to incubate sediment and overlying water for a selected incubation period. The apparatus used for such incubations include glass tubes (Jiang *et al.*, 2008), 1000-mL beakers (Li *et al.*, 2013), or Plexiglas tubes (Wang *et al.*, 2008).

The advantages of studying P release in a lab experiment are the ease in manipulating the physicochemical properties of sediment/solution and minimizing unknown parameters. For example, Favaretto *et al.* (2012) applied gypsum to packed soil columns to diminish P transport through flowing water, while Frossard *et al.* (2014) labeled soils with ^{33}P to model

the P transport in soil. In an incubation study, Li *et al.* (2013) designed a range of pH, temperature, dissolved oxygen, and flow rate to investigate the effects of these factors on P release at the sediment-water interface. Lai and Lam (2008) and Wang *et al.* (2008) created oxic and anoxic environments in sediment and overlying water to examine factor of redox potential, while sterilized/non-sterilized sediments and dark/light cycles were applied in the study by Jiang *et al.* (2008) to investigate the effects of biological activity and light on P release from river sediments.

Varying Redox Potential for Studying P in a Laboratory Experiment

Redox potential has been investigated numerous times in the study of P dynamics in soils or sediments. Redox potential governs the oxidation state of Fe in the structure of poorly crystalline sesquioxide minerals that commonly bind P. In a classic P cycling model, low redox potential in an anoxic environment reduces Fe(III) in iron oxides to soluble Fe(II)-ions, promoting release of P from the iron oxides (Pant and Reddy (2001). In contrast, a high redox potential under oxic environments promotes oxidation of Fe(II)-ions and precipitation of insoluble Fe(III)-oxides, resulting in more sorption sites for P binding.

Oxic conditions in a lab experiment can be maintained by aerating the system continuously with room air (e.g., Lai and Lam, 2008). By contrast, methods for creating anoxic environments may be more complicated. A common method for decreasing redox potential in a lab experiment is by saturating the system with nitrogen and minimizing oxygen infiltration into the system. For example, Pant and Reddy (2001) applied this method to investigate the effects of redox potential on P sorption indices. Lai and Lam (2008) and Wang *et al.* (2008) also studied P release from sediments under decreasing redox potential.

Under saturated nitrogen in the system, remaining oxygen will be utilized by aerobic microorganisms as an electron acceptor. When oxygen is ultimately depleted, anaerobic microorganisms will be more active due to their ability to use nitrate, Mn^{4+}, and Fe^{3+} as electron acceptors (Schlesinger and Bernhardt, 2013), resulting in lower redox potential. Since this process involves microorganisms in the utilization of oxygen, nitrate, Mn^{4+}, and Fe^{3+}, the mechanisms may be exaggerated when there is an abundance of energy sources and electron donors in the system.

An alternative for decreasing redox potential in a lab experiment is by using microorganisms that are able to stimulate oxygen depletion and then utilize Fe(III) as the sole electron acceptor (Upreti *et al.*, 2015). A facultatively anaerobic bacterium, *Sewanella putrefaciens* CN32 (Jaisi *et al*., 2005), is an example of a microorganism that can be used for this purpose. According to Upreti *et al.* (2015), *Sewanella putrefaciens* CN32 utilizes dissolved oxygen first before switching to use Fe(III) as electron acceptor, therefore a gradual change in redox potential can be achieved. However, this method may not be as simple as the method of saturating the system with nitrogen. In addition, the microorganisms may not be present in the natural environment. When introduced microorganisms become dominant, the composition of the microbial community in the lab experiment may not represent natural conditions in the field.

Malachite Green, Molybdate Blue-Ascorbic Acid, and ICP-AES Methods

A very general method to determine the concentration of phosphate in an aqueous extract is the molybdate blue-ascorbic acid method (Watanabe and Olsen, 1965). The method is a colorimetric method and is based on the complexation of phosphate and

molybdate ions to form a colored complex. Ascorbic acid is added as a reducing reagent to develop the blue color. This method is simple and very popular in many laboratories around the world. However, it is time consuming, laborious, creates significant chemical waste, and the reagents are not stable under room temperature for more than 24 hours. In addition, the blue color develops very weakly in the extract of acidified ammonium oxalate.

In many studies (e.g. Bell *et al.*, 2005; Dayton and Basta, 2005; Yoo *et al.*, 2006), inductively coupled plasma-atomic emission spectrometry (ICP-AES) has been used to measure ammonium oxalate-extractable P. ICP-AES is an automated technique, and it has advantages for the simultaneous or sequential analysis of multiple elements (Jarvis and Jarvis, 1992; Olesik, 1991; Rommers and Boumans, 1996). However, as in other automated techniques, the equipment is very expensive (Huerta-Diaz *et al.*, 2005), and considerable technical expertise is required with the ICP-AES. Rommers and Boumans (1996) also suggested that the accuracy of the ICP-AES technique may not be high.

An alternative colorimetric method for determining phosphate in solution is the malachite green method. It is based on the complexation of malachite green with phosphomolybdate (Ohno and Zibilske, 1991; Subba Rao *et al.*, 1997). Compared to other basic dyes (e.g., safranin, brilliant green, fuchsin red, methylene blue, and methyl violet), Itaya and Ui (1966) stated that malachite green was most favorable for micro-determination of phosphate due to the high intensity of the color as well as the typical change of the absorption maximum by exposure to phosphomolybdate. The malachite green colorimetric method has been reported to work well in studies of phosphate adsorption by inorganic colloids in environmental water samples (Van Moorleghem *et al.*, 2011), for analysis of low concentrations of P in soil extracts (Ohno and Zibilske, 1991), lipid P (Zhou and Arthur,

1992), alkaline phosphatase activity (Baykov *et al.*, 1988), and ammonium oxalate-extractable P (Pizzeghelloa *et al.*, 2011). Absorbance in the malachite green method can be read using a 96-well microplate reader (D'Angelo *et al.*, 2001). Therefore, this method can be faster, require less labor, and create much less chemical waste than the molybdate blue-ascorbic acid method. It is also an alternative to ICP-AES analysis to measure ammonium oxalate-extractable P (P_{ox}).

CHAPTER 3

POTENTIAL CONTRIBUTIONS OF INORGANIC AND ORGANIC PHOSPHORUS IN SEDIMENTS TO P LOADS OF WALNUT CREEK, IOWA

Introduction

Past studies have linked nutrients discharged through the Mississippi River in the Midwestern United States to extensive hypoxia in the Gulf of Mexico (Bianchi *et al.*, 2010; Royer *et al.*, 2006). Nitrogen is widely accepted as a major contributing nutrient to the hypoxia (Rabalais *et al.*, 2002), however Sylvan *et al.* (2006) suggested that phosphorus (P) is also important in promoting the hypoxic zone in the Gulf of Mexico. Phosphorus loads in the Mississippi River are often associated with intensive agricultural activities in the tributary watersheds (Jacobson *et al.*, 2011). A model developed by Alexander *et al.* (2008) estimated the contribution of pasture land, row crop land, and other crop land as 37, 25, and 18%, respectively; the contribution of all agricultural sources was higher than from urban sources (12%). Besides direct runoff from agriculturally managed lands, another pathway for P to enter the Mississippi River is through stream bed and bank erosion (Schilling *et al*., 2011; Wilson *et al*., 2008). In Iowa, streambank erosion is considered to be the main source of suspended sediments in stream water (Schilling and Wolter, 2000). Certainly, P transport in the solution phase of the soil may occur (Sinaj *et al.*, 2002; Turner and Haygarth, 2000), though the quantity is commonly less than P transport through eroded sediments.

In eroded sediments, P occurs in both inorganic P *(Pi)* and organic P (*Po)* forms. Inorganic P (*Pi*) consists of soluble or loosely bound fractions as well as fractions that are precipitated with or adsorbed to Al, Fe, and Ca components or as hydroxyapatite (Hedley *et al.*, 1982; Tiessen and Moir, 2008; Zhang and Kovar, 2009). For *Po* fractions, the dominant

compounds in soils are inositol phosphates; phospholipids, nucleic acids, phosphoproteins, and sugar phosphate usually occur in smaller concentrations (Dalal, 1977). Williams and Steinbergs (1958) suggested that the *Po* fraction could be present in soil as a component of humified organic matter. Predicting the potential release of P from eroded sediments by reliance only on total P concentrations is not likely to be accurate (Kisand, 2005), therefore characterizing *Pi* and *Po* fractions could be valuable to predict the fate of P in eroded materials entering the stream.

The goals of the present study were to characterize *Pi* and *Po* fractions associated with eroded sediments in the Walnut Creek watersheds and to investigate its relationships with other sediment properties. Walnut Creek is in Jasper County, Iowa, drains about 7,951 ha area, and discharges into the Des Moines River, a tributary of the Mississippi River, at the upper end of the Red Rock Reservoir (Schilling *et al*., 2006b). It supports a variety of land uses, including row crop production, grazing, and riparian buffer zones in the Neil Smith National Wildlife Refuge, a large-scale project prairie restoration project in Iowa. The alluvial cross section is composed of a characteristic sequence of sediments with potential to contribute differentially to the amounts and forms of P entering the stream. The characterization and differentiation of such sediments is essential for robust modeling predictions of the fate of P in Midwestern streams.

Materials and Methods

Sediment sampling and characterization

Twenty-five sediment samples were collected from the corridor and floodplain of Walnut Creek (coordinates of sampling site are in Appendix B1). These samples were grouped into three categories: bank, in-stream deposits, and floodplain deposits (Table 3).

Samples from the streambanks were based on the major stratigraphic units in Walnut Creek: Camp Creek, Roberts Creek, and Gunder are all members of the Holocene De Forest Formation, with dates from the last 380 yr, 4000 to 400 yr BP, and 11,000 to 4,000 yr BP, respectively. The fourth material sampled, Pre-Illinois Till, is associated with glaciation that occurred between 2,000,000 to 500,000 yr BP (Baker *et al.*, 1996; Schilling *et al.*, 2004). Sampled in-stream deposits consisted of materials found in a debris dam, a sand bar, in-stream slumps, a beaver dam, and stream bottom sediment. Floodplain samples were collected at 0-20 cm depth at sites in row crop production (soybean and corn fields), grazing (pasture), and riparian buffer zones (forest). Immediately after transported to the lab, the samples were air dried and sieved to pass a 2-mm screen; coarse mineral fragments and organic materials were sorted out.

Table 3. The twenty-five samples collected in the study. Numbers in parentheses following sample description represent different sampling site (coordinates of sampling sites are in Appendix B1).

Bank		In-stream deposit		Floodplain	
Code	Description	Code	Description	Code	Description
B-2	Camp Creek (1)	I-4	Stream bottom sediment (1)	F-1	Pasture
B-3	Roberts Creek (1)	I-5	Slump, debris dam	F-9	Forest (1)
B-7	Till (1)	I-6	Stream bed sediments, debris dam	F-10	Forest (2)
B-17	Camp Creek (2)	I-8	Sand bar	F-14	Corn Field, tillage
B-18	Roberts Creek (2)	I-11	Stream bottom sediment (2)	F-15	Soybean field
B-19	Gunder	I-12	Slump (1)	F-16	Corn Field, no tillage
B-20	Till, calcareous (2)	I-13	Bar		
B-21	Camp Creek (3)	I-23	Slump (2)		
B-22	Roberts Creek (3)	I-24	Stream bottom sediment (3)		
		I-25	Beaver dam		

Total carbon and total nitrogen were analyzed using high-temperature dry combustion (Nelson and Sommers, 1996), particle size distribution was determined gravimetrically

(Kettler *et al.*, 2001), and pH was determined potentiometrically at a soil to water ratio of 1:1. Total organic matter was determined using the loss-on-ignition method (Konen *et al.*, 2002). The perchloric acid digestion method (Kuo, 1996) was used to extract total P (TP), and the P concentration in the digest was determined by using the molybdate blue-ascorbic acid method (Watanabe and Olsen, 1965). The molybdate blue-ascorbic method was also used to determine P in Mehlich-3 extracts (Mehlich, 1984) (P_{M3}), while Ca in this extraction (Ca_{M3}) was determined by using inductively coupled plasma-atomic emission spectrometry (ICP-AES). Citrate-bicarbonate-dithionite extractable Fe (Fe_{CBD}) was determined by atomic absorption spectroscopy (Shang and Zelasny, 2008). Ammonium oxalate extractable Fe, Al, and Mn (Fe_{ox}, Al_{ox}, and Mn_{ox}) were determined using ICP-AES, and P (P_{ox}) in this extraction was determined using a malachite green method (D'Angelo *et al.*, 2001).

Phosphorus fractionation

Inorganic P (*Pi*) and organic P (*Po*) were sequentially extracted using different extracting solutions following the methods of Zhang and Kovar (2009) (Fig. 4 and Fig. 5). For *Pi* fractionation, 0.5 g of air-dried sediment (<2 mm) was sequentially extracted with 1 *M* NH_4Cl, 0.5 *M* NH_4F, 0.1 *M* NaOH, citrate-bicarbonate-dithionite (CBD), and 0.25 *M* H_2SO_4. A different scheme was used for *Po* fractionation: 0.5 g of air-dried sediment (<2mm) was sequentially extracted with 0.5 *M* $NaHCO_3$, 1.0 *M* HCl and 0.5 *M* NaOH, after which the samples were ignited at 550°C and then extracted with 1.0 *M* H_2SO_4. A modification from the original method was applied for determining *Pt*, in which ammonium persulfate was used for the digestion in an autoclave instead of potassium persulfate on a hot plate. Phosphorus concentration in the extracts was determined using the molybdate blue-ascorbic acid method

(Watanabe and Olsen, 1965); the absorbance was read at λ 880 nm using a spectrophotometer. *Pi* and *Pt* were determined directly from the extracts, whereas *Po* fractions were determined by subtracting *Pi* from the total P (*Pt*).

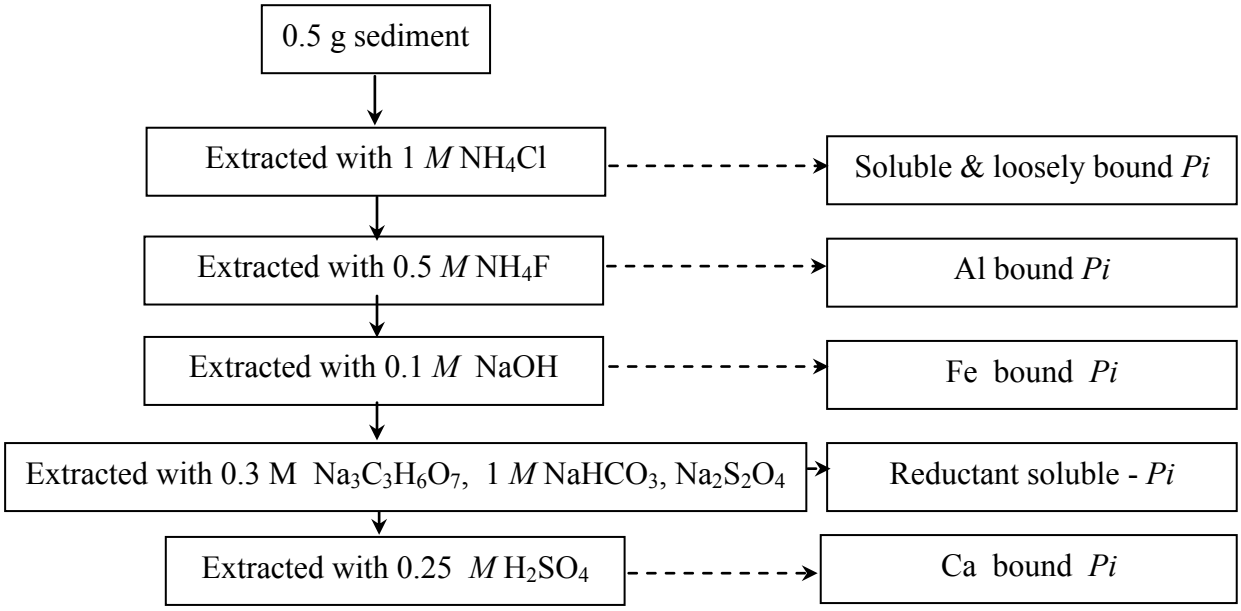

Figure 4. Scheme of inorganic P sequential extraction, adapted from Zhang and Kovar (2009).

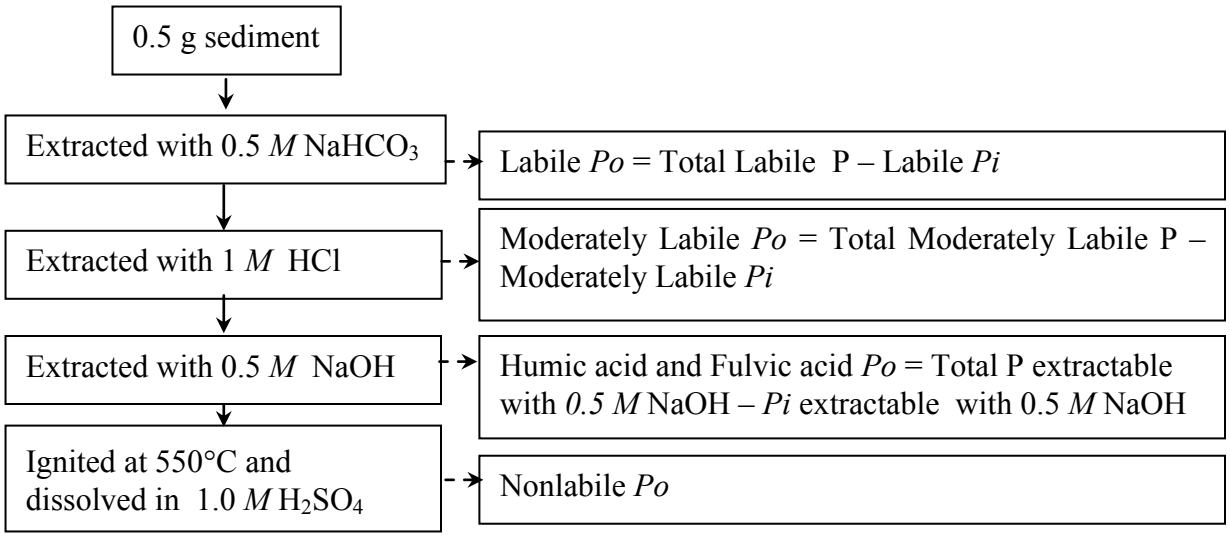

Figure 5. Scheme of organic P sequential extraction, adapted from Zhang and Kovar (2009).

Results and Discussion

Sediment characteristics

Table 4 shows that sediment characteristics varied greatly across all 25 samples. The ranges of TP, P_{M3}, and P_{ox} were 386-1,134 , 5-85, and 60-823 mg kg^{-1}, respectively. Fe_{ox}, Al_{ox}, Mn_{ox}, and Ca_{M3} ranged from 743-9,903, 235-1,542, 154-9,794, and 1,927-6,750 mg kg^{-1}, respectively. Organic matter ranged from 1.51 to 7.53%. The pH values ranged from 5.5 to 8.1, indicating a wide range of sediment acidity. The clay fraction ranged from 15 to 36%, while sand fraction was from 2 to 52%. Among the three groups, the in-stream deposit had the highest TP, P_{M3}, and P_{ox} (Fig. 6), indicating a potential major contributor to P leaving the watershed from bed sediment re-suspension during high-flow events. Furthermore, the in-stream deposit group had the highest average of Fe_{ox} and Mn_{ox}, while floodplain and bank deposits had the highest Al_{ox} and Ca_{M3}, respectively.

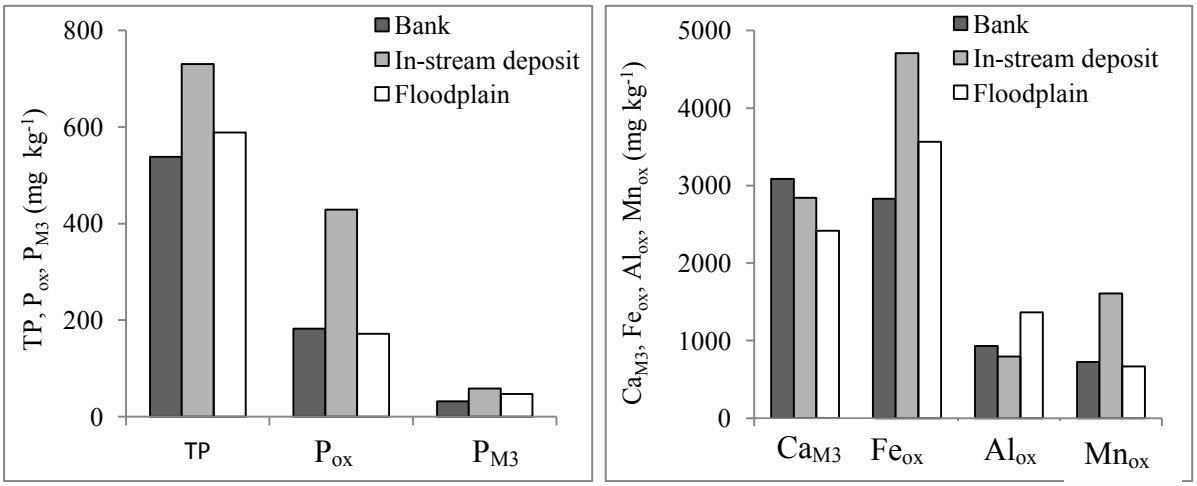

Figure 6. Average of TP, P_{ox}, P_{M3}, Ca_{M3}, Fe_{ox}, Al_{ox}, and Mn_{ox} in the group of bank (*n=9*), in-stream deposit (*n=10*), and floodplain (*n=6*) sediments.

Table 4. Selected sediment properties, where OM = organic matter, C= total C, N= total N, TP = total P, $Fe_{ox}/Al_{ox}/Mn_{ox}/P_{ox}$ = ammonium oxalate extractable Fe/Al/Mn/P, Fe_{CBD} = citrate bicarbonate dithionite extractable Fe, Ca_{M3}/P_{M3} = Mehlich 3 extractable Ca/P.

Group	Sample Code	Description	OM	C	N	Sand	Silt	Clay	pH H_2O (1:1)	TP mg kg^{-1}
			----------%----------							
Banks	B-2	Camp Creek (1)	4.52	1.54	0.16	6	73	21	5.7	499
	B-3	Roberts Creek (1)	7.53	3.12	0.25	2	62	36	6.0	847
	B-7	Till (1)	1.65	0.25	0.06	49	28	23	7.1	370
	B-17	Camp Creek (2)	3.38	1.32	0.14	11	64	25	6.2	491
	B-18	Roberts Creek (2)	4.51	1.84	0.14	13	60	27	6.3	588
	B-19	Gunder (1)	1.51	0.31	0.06	6	72	22	7.4	484
	B-20	Till, calcareous (2)	1.71	1.06	0.03	49	30	21	8.1	473
	B-21	Camp Creek (3)	4.38	1.66	0.13	19	59	22	6.0	573
	B-22	Roberts Creek (3)	4.23	1.54	0.14	6	69	25	5.7	522
In-stream deposit	I-4	Stream bottom sediment (1)	3.19	0.88	0.15	9	59	32	6.7	666
	I-5	Slump, debris dam	5.59	2.06	0.16	6	60	34	5.9	386
	I-6	Stream bed sediments, debris dam	3.64	1.00	0.10	22	53	25	7.2	966
	I-8	Sand bar	2.98	0.99	0.10	52	33	15	7.2	566
	I-11	Stream bottom sediment (2)	2.57	0.84	0.10	30	51	19	5.9	974
	I-12	Slump (1)	3.87	1.49	0.14	34	51	15	6.6	558
	I-13	Bar	4.25	1.47	0.12	6	63	31	6.5	1,134
	I-23	Slump (2)	2.33	0.34	0.05	33	37	30	6.3	815
	I-24	Stream bottom sediment (3)	5.90	2.40	0.19	13	63	24	5.9	566
	I-25	Beaver dam	4.52	1.71	0.16	27	56	17	7.1	673
Floodplain	F-1	Pasture	5.19	2.23	0.24	1	81	18	5.6	567
	F-9	Forest (1)	5.09	1.95	0.20	18	63	19	5.7	556
	F-10	Forest (2)	6.41	2.52	0.24	4	70	26	6.1	730
	F-14	Corn Field, tillage	4.21	1.49	0.15	10	67	23	6.3	559
	F-15	Soybean field	4.38	1.59	0.16	17	61	22	6.5	505
	F-16	Corn Field, no tillage	4.69	1.91	0.18	22	57	21	6.2	617

Table 4. Continued.

Group	Sample Code	Description	Fe_{ox}	Al_{ox}	Mn_{ox}	P_{ox}	Fe_{CBD}	Ca_{M3}	P_{M3}
			-----mg kg^{-1}------						
Banks	B-2	Camp Creek (1)	2,816	1,321	595	127	8,620	2,646	39
	B-3	Roberts Creek (1)	4,424	1,742	2,182	479	7,274	5,170	55
	B-7	Till (1)	1,665	496	267	124	11,858	1,927	26
	B-17	Camp Creek (2)	3,348	1,002	702	158	6,825	1,975	29
	B-18	Roberts Creek (2)	3,947	1,076	1,263	193	5,862	2,983	41
	B-19	Gunder (1)	1,967	445	154	137	3,813	2,135	28
	B-20	Till (2)	743	235	166	106	10,124	6,750	5
	B-21	Camp Creek (3)	3,925	1,116	801	188	8,745	2,243	35
	B-22	Roberts Creek (3)	2,654	947	403	129	7,272	1,965	29
In-stream deposit	I-4	Stream bottom sediment (1)	3,068	837	9,794	499	5,095	3,729	61
	I-5	Slump, debris dam	1,951	1,542	689	60	4,294	4,038	13
	I-6	Stream bed sediments, debris dam	9,903	1,058	1,290	655	15,571	2,905	58
	I-8	Sand bar	3,948	602	919	351	6,888	2,278	76
	I-11	Stream bottom sediment (2)	4,009	455	532	648	7,404	1,976	85
	I-12	Slump (1)	3,947	678	740	329	7,338	2,380	84
	I-13	Bar	6,310	585	147	823	8,426	3,129	67
	I-23	Slump (2)	4,340	649	872	297	15,948	2,764	45
	I-24	Stream bottom sediment (3)	6,169	957	423	275	7,562	2,144	27
	I-25	Beaver dam	3,431	609	672	353	7,401	3,065	71
Floodplain	F-1	Pasture	3,914	1,367	511	160	7,341	2,387	34
	F-9	Forest (1)	3,348	1,379	809	170	8,171	2,242	56
	F-10	Forest (2)	4,228	1,319	618	292	8,615	2,897	55
	F-14	Corn Field, tillage	3,496	1,451	740	129	8,557	2,417	37
	F-15	Soybean field	3,644	1,453	852	119	8,876	2,282	30
	F-16	Corn Field, no tillage	2,751	1,216	471	161	9,195	2,271	72

Simple correlations between sediment properties related to P are summarized in Table 5, and several details may be inferred. First, TP was not significantly correlated with clay or OM when all data (n = 25) were used. This observation does not agree with the assumption that total P concentrations would be higher in soils with higher clay and OM content due to its contribution on *Pi* retention and *Po* fractions, respectively (e.g. Dalal, 1977; Deng and Dixon, 2002; Holford, 1997; Kirkby *et al.*, 2011; Quintero *et al.*, 1999). However, TP was significantly correlated with clay and OM when the analysis used only the data set from the bank and the floodplain deposits (n=15), i.e., excluding the heterogeneous in-stream deposits. Second, excluding data set from the in-stream deposits also resulted in significant correlation between P_{M3} and pH as well as between P_{ox} and Fe_{ox}. The higher correlation coefficients obtained by excluding data from the in-stream deposits indicated that processes of P adsorption/desorption, mineral precipitation/dissolution, and mineralization/immobilization would be less predictable for the in-stream deposits compared to the other groups. Regular contact with the flowing stream flow may have had an impact on characteristics of the in-stream deposits compared with the bank sediments and floodplain soils.

Third, while P_{M3} was not significantly correlated to Ca_{M3}, the fraction of P_{M3} to TP (P_{M3} / TP) was significantly correlated to Ca_{M3} (n=*25* or n=15). Fourth, TP was not significantly correlated with Fe_{CBD}, but it was positively correlated with Fe_{ox} (n=*25* or n=15). This result is likely due to the different forms of Fe extracted by CBD and ammonium oxalate. While the CBD extraction is targeted to measure total free Fe / Al / Mn oxides, the ammonium oxalate extraction is targeted to measure the poorly crystalline (Fe/Al/Mn) sesquioxides, which have a high capacity for P binding (Kleinman and Sharpley, 2002; Rotterdam *et al*., 2012). Last, a slightly higher Pearson's r was identified when P_{ox} was

Table 5. Simple correlation between sediment characteristics related to P. Clay and OM are in %, TP, P_{M3}, P_{ox}, Fe_{CBD}, Fe_{ox}, Al_{ox}, and Mn_{ox} are in mg kg^{-1}.

Y	X	Pearson's *r*	*P* value	Significance
Total P	Clay†	0.29	0.1669	NS
	Clay‡	0.66	0.0074	**
	OM†	0.12	0.5530	NS
	OM‡	0.88	<0.0001	*
	Fe_{CBD}†	0.33	0.1069	NS
	Fe_{CBD}‡	-0.23	0.4138	NS
	Fe_{ox}†	0.70	0.0001	**
	Fe_{ox}‡	0.70	0.0036	**
	Fe_{ox} + Al_{ox}†	0.64	0.0006	**
	Fe_{ox} + Al_{ox}‡	0.71	0.0029	**
	Fe_{ox}+Al_{ox}+Mn_{ox}†	0.52	0.0083	**
	Fe_{ox}+Al_{ox}+Mn_{ox}‡	0.76	0.0029	**
	P_{M3}†	0.61	0.0013	**
	P_{M3}‡	0.66	0.0070	**
	P_{ox}†	0.92	<0.0001	**
	P_{ox}‡	0.90	<0.0001	**
P_{M3}	pH†	0.04	0.9548	NS
	pH‡	0.60	0.0189	*
	Ca_{M3}†	-0.25	0.2366	NS
	Ca_{M3}‡	-0.25	0.3684	NS
P_{ox}	Fe_{ox}†	0.26	0.2114	NS
	Fe_{ox}‡	0.52	0.0472	*
	Fe_{ox} + Al_{ox}†	0.59	0.0019	**
	Fe_{ox} + Al_{ox}‡	0.60	0.0214	*
	Fe_{ox}+Al_{ox}+Mn_{ox}†	0.60	0.0014	**
	Fe_{ox}+Al_{ox}+Mn_{ox}‡	0.69	0.0048	**
P_{M3}/TP	Ca_{M3}†	-0.41	0.0407	*
	Ca_{M3}‡	-0.56	0.0295	*
P_{ox}/TP	Fe_{ox}†	-0.34	0.0978	NS
	Fe_{ox}‡	0.37	0.1766	NS
	Fe_{ox} + Al_{ox}†	0.49	0.0130	*
	Fe_{ox} + Al_{ox}‡	0.48	0.0693	NS
	Fe_{ox}+Al_{ox}+Mn_{ox}†	0.65	0.0004	**
	Fe_{ox}+Al_{ox}+Mn_{ox}‡	0.59	0.0219	*

*Note = † using all sediment samples data (n=25), ‡ using only data for sediment within bank and floodplain group (n=15), * = significant at α=0.05, **= significant at α=0.01, NS=not significant.*

correlated to the sum of poorly crystalline sesquioxides (Fe_{ox}+Al_{ox}+Mn_{ox}) than only to Fe_{ox} or (Fe_{ox}+Al_{ox}), especially when data from the in-stream deposits were excluded (*n*=15).

Phosphorus adsorption by manganese oxides (MnO_2) is possible when MnO_2 occurs in considerable concentrations (Yao and Millero, 1996); however, Gadde and Laitinen (1974) suggested that this is less likely to happen at most soil pH values since the PZC (point of zero charge) of MnO_2 is ~2.8.

Phosphorus fractionation

Comparison of sum of all fractions (TP_{sum}) and TP

Figure 7 shows a significant correlation between sum of all individual P fractions (TP_{sum}) and total P extracted with perchloric acid and nitric acid (TP). Thus we conclude that the fractionation method used in this study reasonably recovered total P in the individual *Pi* and *Po* fractions. However, across all 25 samples, most of TP_{sum} was lower than TP, which is possibly related to three factors. First, the accuracy of sequential extraction in determining a specific P fraction could be low due to reorganization of P fractions during a prior extraction, to reagents which are nonselective for the target phases, and to residual P that is not completely extracted (Wang *et al.*, 2010). Second, TP was determined in a single step of digestion with perchloric acid and nitric acid, suggesting less possible loss of P than in TP_{sum} which was determined by sequential extraction. Third, *Po* fractions could be underestimated due to hydrolysis of *Po* to *Pi*, especially with strong extracting solutions (Blake *et al.*, 2003).

Inorganic P fractions

Following the method of Zhang and Kovar (2009), inorganic fractions of P in this study were classified as soluble and loosely bound *Pi* (SL-*Pi*), Al-bound Pi (Al-*Pi*), Fe-bound *Pi* (Fe-*Pi*), reductant-soluble *Pi* (RS-*Pi*), and Ca-bound *Pi* (Ca-*Pi*), as seen in Fig. 8 .

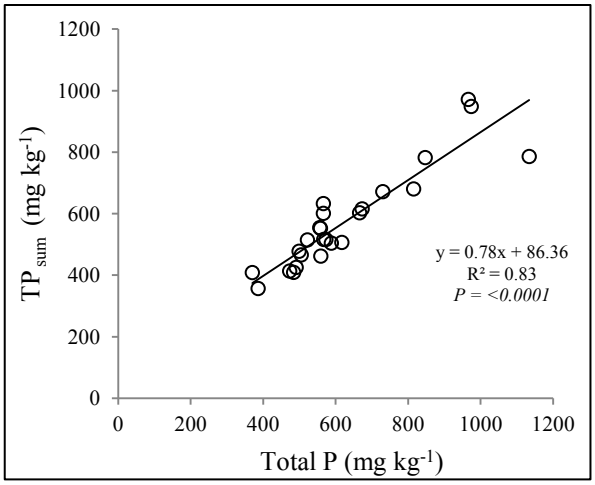

Figure 7. Comparison of total P extracted with nitric acid + perchloric acid (TP) and sum of all individual P fractions (TP_{sum}), *n=25*.

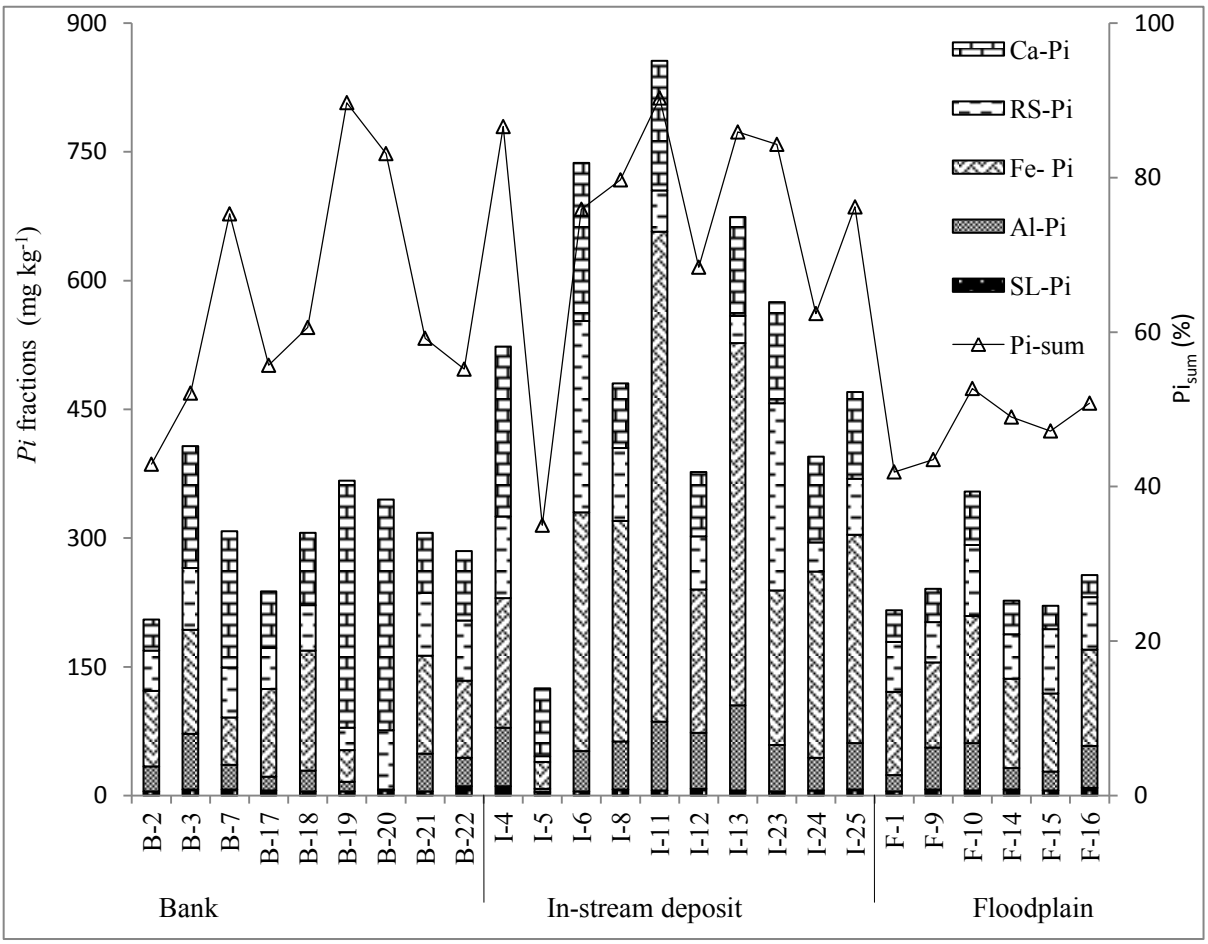

Figure 8. Distribution of *Pi* fractions in all twenty-five sediment samples. Bar chart represents all *Pi* fractions (in mg kg^{-1}), line chart represents percentage of Pi_{sum} to TP_{sum}.

The total of all individual *Pi* fractions (Pi_{sum}) ranged between 125 and 856 mg kg^{-1} or 35 to 90% of TP_{sum}. Moreover, SL-*Pi* ranged from 4 to 11 mg kg^{-1} or 0.7 to 3.5% of Pi_{sum}. For each group of sediments, SL-*Pi* averaged 6 mg kg^{-1} in the bank, and it was 7 mg kg^{-1} in the floodplain and the in-stream deposits (Table 6). The small portion of SL-*Pi* in this study agreed with a previous study by Wang *et al.* (2010) for the surface sediments of a river system in China, however the value was much less than the SL-*Pi* values reported by Kisand (2005) for sediment in Lake Verevi, a eutrophic temperate lake in South Estonia. Although the SL portion was almost negligible compared to Pi_{sum}, SL-*Pi* is the solid-phase P which may be released first when sediments are re-suspended during the high-flow events, therefore its impact on causing impairment of water quality may be more straightforward than that of other P fractions.

The Al-*Pi* and Fe-*Pi* values ranged from 0 to 99 mg kg^{-1} and from 1 to 571 mg kg^{-1}, respectively. Fe-*Pi* has a potential to elevate soluble P levels in the water column under anaerobic condition when Fe^{3+} is reduced to Fe^{2+} and the sorbing Fe oxides are dissolved (Pettersson, 1998). Moreover, the lowest value of Al-*Pi* and Fe-*Pi* was in B-20, possibly due to the characteristics of this sediment: pH (8.1), calcareous, and low Al_{ox}. RS-*Pi* ranged from 7 mg kg^{-1} (I-5) to 223 mg kg^{-1} (I-6), both the lowest and the highest RS-*Pi* were in the in-stream deposit. Of the three groups, the in-stream deposits had the highest average Al-*Pi,* Fe-*Pi,* and RS-*Pi*. Ca-*Pi* ranged from 26 mg kg^{-1} (F-16) to 288 mg kg^{-1} (B-19). Unlike other *Pi* fractions, the highest average of Ca-*Pi* was in the bank sediments. Moreover, Ca-*Pi* concentration in the bank sediments followed the order: Camp Creek < Roberts Creek < till < Gunder, indicating a lower Ca-*Pi* concentration in the youngest sediments.

Averaged for the 25 sediments in this study, the inorganic P (*Pi*) fractions followed the order: Fe-*Pi* > Ca-*Pi* > RS-*Pi* > Al-*Pi* > SL-*Pi*. This order was fairly similar to the distribution of P phases reported for Washington tidal river sediments which followed the order: Fe-P > Ca-P > Al-P (Huanxin *et al.*, 1997). The composite average order was also similar to that in the in-stream deposits (Table 6). However, it was different from that in the floodplain soils and the bank deposits. The *Pi* factions followed the order: Fe-*Pi* > RS-*Pi* > Ca-*Pi* > Al-*Pi* > SL-*Pi* in the floodplain, and the order was Ca-*Pi* > Fe-*Pi* > RS-*Pi* > Al-*Pi* > SL-*Pi* in the bank.

Table 6. Mean of *Pi* fractions in the bank (n= 9), the in-stream deposit (n=10), and the floodplain (n=6). Numbers in parentheses are standard deviation.

Pi fractions	Bank		In-stream deposit		Floodplain	
	mg kg^{-1}	%	mg kg^{-1}	%	mg kg^{-1}	%
SL-*Pi*	6 (1.9)	2	7 (2.0)	1	7 (1.4)	3
Al-*Pi*	28 (19.0)	9	57 (25.3)	11	37 (16.1)	14
Fe-*Pi*	83 (44.3)	27	252 (150.6)	48	109 (20.6)	43
RS-*Pi*	57 (15.6)	19	87 (75.0)	17	63 (13.8)	25
Ca-*Pi*	133 (91.0)	43	120 (44.3)	23	38 (13.0)	15
Pi_{sum}	307 (61.9)	100	523 (206.3)	100	254 (51.8)	100

Organic P fractions

Organic P (*Po*) fractions in this study were classified as labile *Po* (Lab-*Po*), moderately labile *Po* (MLab-*Po*), humic acid bound *Po* (HA-*Po*), fulvic acid bound *Po* (FA-*Po*), and nonlabile *Po* (NLab-*Po*), as presented in Fig. 9. The Lab-*Po* ranged from 2 to 47 mg kg^{-1} or 0.5 to 8.5% of the total of all individual *Po* fractions (Po_{sum}). Averaged over each group, Lab-*Po* was 20, 14, and 32 mg kg^{-1} in the bank deposits, the in-stream deposits, and the floodplain soils, respectively (Table 7). Especially in the bank sediments, Lab-*Po* for Camp Creek and Roberts Creek were higher than for Gunder and the till. As stated by Xu *et*

al. (2013), the decrease of Lab-*Po* with increasing depth likely indicates a transformation of the labile *Po* fraction into nonlabile *Po* pools over time.

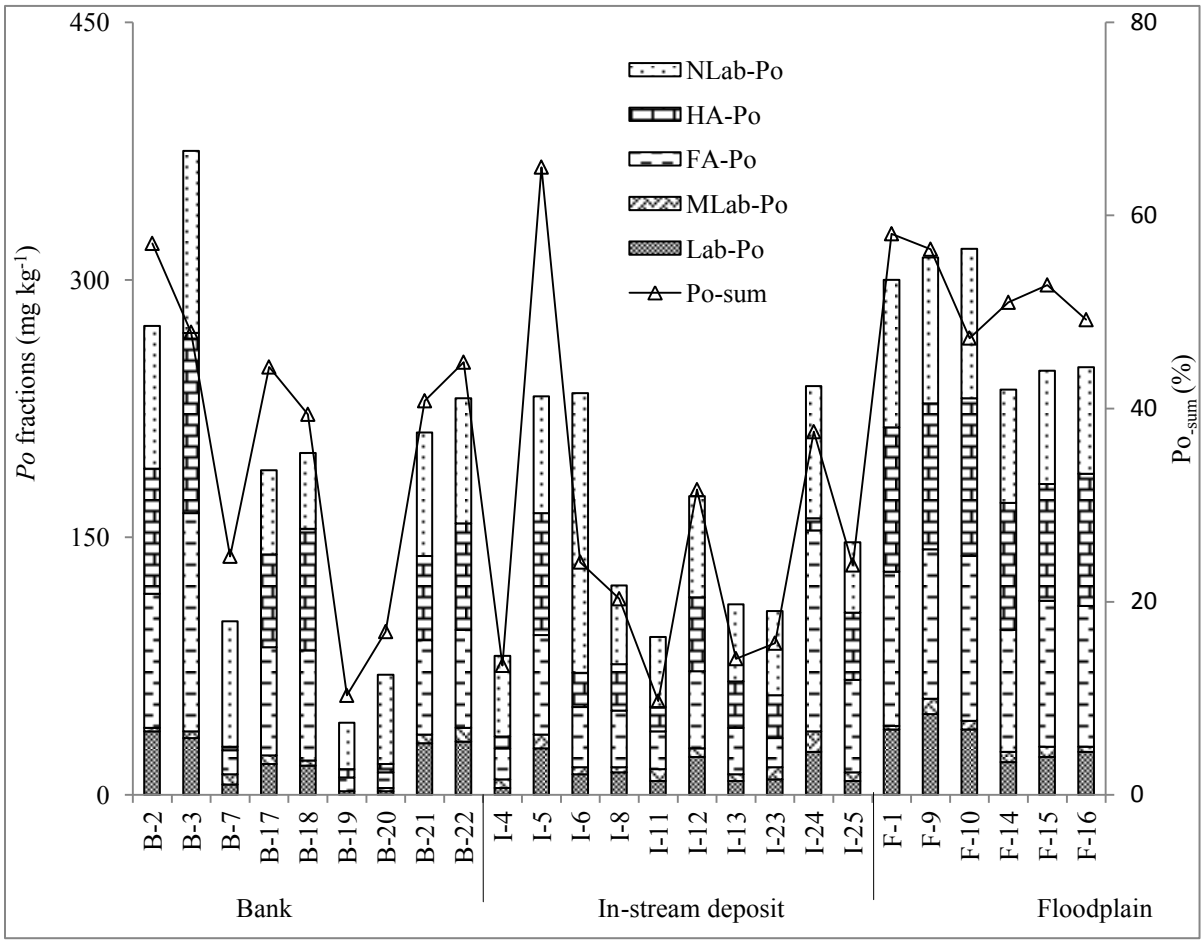

Figure 9. Distribution of *Po* fractions in all twenty-five sediment samples. Bar chart represents *Po* fractions (in mg kg^{-1}), line chart represents percentage of Po_{sum} to TP_{sum}.

In general, Lab-*Po* was higher than MLab-*Po*, likely because of differences in the pH of the extracting solution for each fraction. As suggested by You *et al.* (2006), soil organic matter (SOM) fractions are more readily extractable from soil/sediment samples with the higher pH of the extracting solution. Lab-*Po* was fractionated by extraction with 0.5 *M* $NaHCO_3$ at pH 8.5, while MLab-*Po* was extracted with 1 *M* HCl at pH -1. In the sequential

extraction method of Tiessen and Moir (2008), *Po* extractable with 1 *M* HCl was not determined because it was usually low.

Table 7. Mean of *Po* fractions in the bank (*n*= 9), the in-stream deposit (*n*=10), and the floodplain (*n*=6). Numbers in parentheses are standard deviation.

Po fractions	Bank		In-stream deposit		Floodplain	
	mg kg^{-1}	%	mg kg^{-1}	%	mg kg^{-1}	%
Lab-*Po*	20 (13.9)	11	14 (8.1)	9	32 (11.1)	11
MLab-*Po*	4 (2.4)	2	6 (2.6)	4	5 (2.5)	2
FA-*Po*	53 (38.4)	28	43 (29.8)	28	85 (8.4)	31
HA-*Po*	47 (36.1)	25	28 (19.3)	18	80 (8.7)	29
NLab-*Po*	64 (23.7)	34	64 (36.9)	41	75 (11.8)	27
Po_{sum}	188 (104.6)	100	155 (61.7)	100	277 (37.1)	100

FA-*Po* and HA-*Po* are two fractions which are extractable with alkaline extracting solution (0.5 *M* NaOH) and are associated with humic substances. Across all 25 sediments, the ranges of FA-*Po* and HA-*Po* were 8-127 and 2-105 mg kg^{-1}, respectively. On average, the percentage of FA-*Po* and HA-*Po* in the total Po_{sum} was 29 and 24%, respectively. Paing *et al.* (1999) reported FA-*Po* and HA-*Po* values of 58-60 and 19-28%, respectively, for sediments in a very different ecological setting, two Mediterranean French coastal lagoons. Hong and Yamane (1980) reported that about 60% of FA-*Po* was inositol hexakisphosphate, and the rest was other forms of *Po.* However, further fractionation of FA-*Po* or HA-*Po* was beyond the scope of the present study. The last *Po* fraction in this study was NLab-*Po, Po* fractions associated with nonhumic substances. These values ranged between 27 and 163 mg kg^{-1}. Especially for the bank and the in-stream deposit, NLab-*Po* comprised the greatest portion of Po_{sum}.

In general, the *Po* fractions followed the order: NLab-*Po* > FA-*Po* > HA-*Po* > Lab-*Po* > MLab-*Po*. The overall order was similar to that in the bank and the in-stream deposits.

Nevertheless, *Po* fractions in the floodplain soils followed a different order: FA-*Po* > HA-*Po* > NLab-*Po* > Lab-*Po* > MLab-*Po*. Interestingly, whether in the bank sediments, the in-stream deposits, or the floodplain soils, the ratio of (NLab-*Po* + FA-*Po* + HA-*Po*) to (Lab-*Po* + MLab-*Po*) was 87:13. This indicates that proportion of (Lab-*Po* + MLab-*Po*) to Po_{sum} remained stable across the groups, although the reason is unclear.

The sum of all individual *Po* fractions (Po_{sum}) in this study ranged from ~10% to 65% of TP_{sum}. Po_{sum} was strongly correlated with organic matter content determined by the LOI method (Fig. 10). The positive correlation suggested that more *Po* was found in samples with higher organic matter concentrations, and it agreed with a previous study by Phiri *et al.* (2001). For samples in the floodplain, it was reasonable that about half of TP_{sum} would be organic P since all samples in this group were collected from the soil surface where organic matter generally accumulates. On the other hand, there was also a vertical discrepancy of Po_{sum} among the major stratigraphic units in the streambank in Walnut Creek. The OM content and the fraction of Po_{sum} in the youngest materials, Camp Creek (B-2, B-17, and B-21) and the Roberts Creek (B-3, B-18, B-22) sediments, in the upper part of the stratigraphic column were greater than those in older Gunder (B-19) and till (B-7 and B-20) deposits.

Figure 11 shows a significant correlation between Po_{sum} and total C, and this agrees with previous research by Kirkby *et al.* (2011) for Australian soils and other world soils. However, a stronger correlation was obtained when the data from the in-stream deposits were excluded. Furthermore, the average C:Po_{sum} ratio in the bank sediments and the floodplain soils were similar (68:1 and 69:1, respectively), while in the in-stream deposits it was 88:1. This indicates that properties of the organic P in the in-stream deposits were likely different from those of the other groups. As noted earlier, characteristics of the group of in-stream

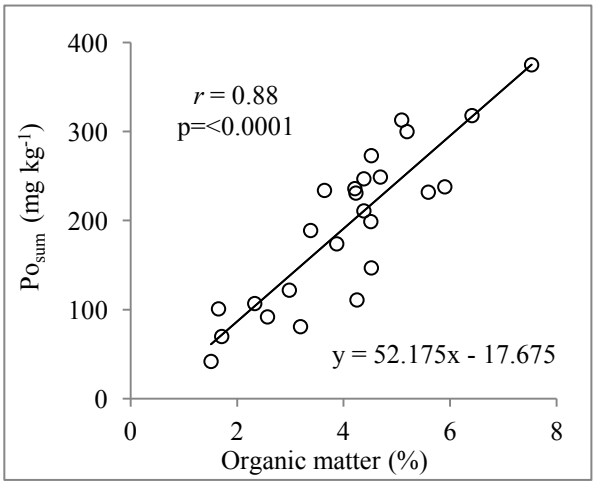

Figure 10. Correlation between organic matter content determined with LOI method and sum of all individual *Po* fractions (Po_{sum}), *n*:25.

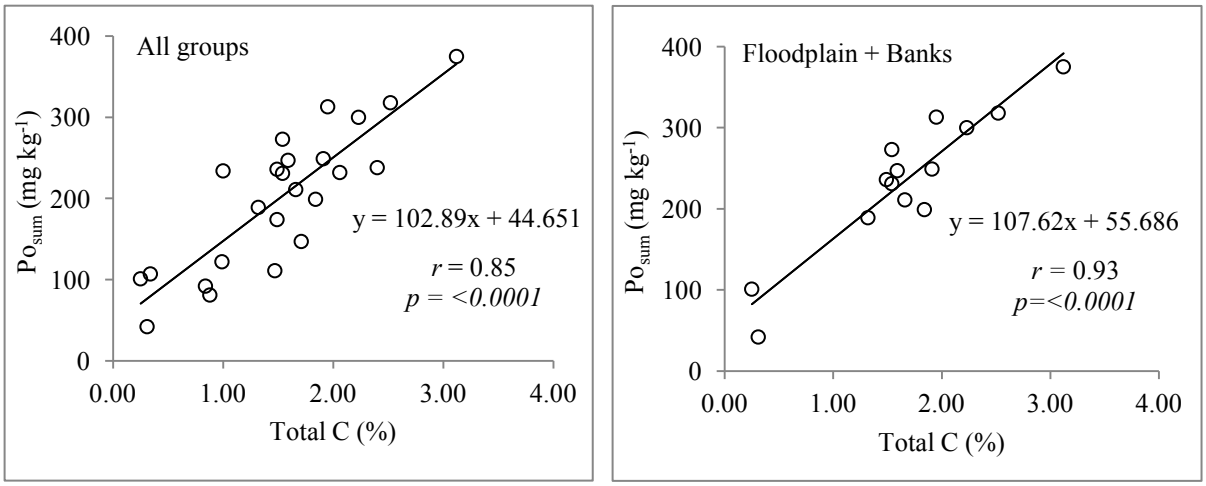

Figure 11. Relationship between total C and Po_{sum} when data sets from all three groups were used (left) and data set from the in-stream deposits was excluded (right). Data from B-20 were excluded.

deposits may have been affected by more regular contact with the flowing stream. We speculate that the relative physical stability of the bank sediments and floodplain deposits led to a more constant C:P ratio than in the in-stream deposits. This is based on assumption that organic matter in soil profiles could be more subject to normal processes of pedogenesis,

while organic matter in the in-stream deposits was affected by a continuous process of transporting, sorting, and depositing by stream flow. In addition, microbial communities in the soil profile might be different from those in the in-stream deposits, leading to a different $C:Po_{sum}$. The C:P ratio of soil microbial biomass can vary greatly (between 23-333, according to Manzoni *et al.*, 2010), however it may be even greater in a freshwater ecosystem. According to Cross *et al.* (2005), the C:P ratio for fungi and bacteria was 5-370 and 300-1190, respectively, in a freshwater benthic system. Nevertheless, a *Po* fractionation associated with microorganisms is beyond the scope of this study.

Conclusions

Sediment characteristics as well as P forms associated with eroded sediments in Walnut Creek watershed varied greatly across all twenty-five sediments in this study. Among the groups, the highest concentrations of TP, P_{M3}, and P_{ox} were in the in-stream deposits, indicating a potential major contributor to P leaving the watershed from bed sediment re-suspension during high-flow events. By using data set from only bank sediments and floodplain soils, we found a better correlation between P forms and other sediment properties. Across all 25 sediments, the inorganic P (*Pi*) fractions followed the order: Fe bound *Pi* > Ca bound *Pi* > reductant soluble *Pi* > Al bound *Pi* > soluble and loosely bound *Pi*. For the organic (*Po*) fractions, the order was nonlabile *Po* > fulvic acid bound *Po* > humic acid bound *Po* > labile *Po* > moderately labile *Po*.

CHAPTER 4

PREDICTING P SOURCE-SINK STATUS OF WALNUT CREEK SEDIMENTS IN VARYING PHYSICOCHEMICAL CONDITIONS

Introduction

Eroded sediments entering tributary streams of the Mississippi River often carry a considerable amount of P and become a potential source for elevating the level of P in the stream water (Fang *et al.*, 2002; Hubbard *et al.*, 2011; Jacobson *et al.*, 2011; Lerch *et al.*, 2015). Nevertheless, P mobility from eroded sediments is not simply controlled by the total amount of P (Kisand, 2005). Mobility of P is a complex process involving interrelated physical, chemical, and biological factors. Phosphorus adsorption and desorption are important processes that involve both the solid and solution phases (Zhou and Li, 2001). Although true equilibrium is difficult to achieve and whole solid-solution system is simplified in the adsorption-desorption model (Koski-Vähälä and Hartikainen, 2001), Taylor and Kunishi (1971) found that the model was useful to predict P release from sediment to ambient water.

In the adsorption-desorption model, phosphorus buffering capacity (PBC) and equilibrium phosphorus concentration (EPC) are two sorption indices frequently used to assess P release from sediments (Haggard *et al.*, 2007; Hongthanat *et al.*, 2011; Jarvie *et al.*, 2005). The PBC is valuable to assess the capability of sediment to buffer the adsorption-desorption process. The EPC is valuable to predict whether sediments are likely to act as a sink or a source for P in the water column. Phosphorus adsorption is favored when the EPC is less than the concentration of dissolved P in the stream water. In that circumstance, to

maintain chemical equilibrium, the sediment would act as a "sink" by decreasing the P concentration in the water that suspends the sediment. Conversely when EPC is greater than the dissolved P concentration, P desorption is favored; that is, the sediment may act as a "source" by releasing P to the water until a new equilibrium is reached. Therefore, both the EPC value of the sediment and the dissolved P concentration of the water have an impact on the overall mobility of P in stream water. Since physicochemical properties in a stream ecosystem are dynamic, P adsorption-desorption processes likely occur simultaneously. Adsorption may be more dominant under some circumstances, while under other conditions desorption may be dominant (Hongthanat *et al.*, 2011).

The present study investigated the P adsorption-desorption behavior of sediments collected from the Walnut Creek watershed in Jasper County, Iowa. The Walnut Creek watershed supports various land uses (pasture, row crop production, prairie wildlife conservation, and riparian forest), drains 7,951 ha area, and discharges into the Des Moines River, a tributary of the Mississippi River, at the upper end of the Red Rock Reservoir (Schilling *et al*., 2006b). The alluvial cross section is composed of a predictable sequence of sediments that potentially have different P adsorption/desorption characteristics. Moreover, physicochemical properties along the creek are likely to be dynamic. Sediment concentrations as well as P levels in the stream water fluctuate throughout the year (Schilling *et al*., 2006b; Schilling *et al*., 2011). An increase in P load to the stream may occur seasonally, for example during large storm (e.g. Hubbard *et al.*, 2011; Royer *et al.*, 2006) or in response to repeated freezing and thawing (e.g. Bechmann *et al.,* 2005). In addition, the kinetic energy of flowing water during large storms would differ from that of normal discharge events. At several sites along Walnut Creek, flowing water has been blocked by

debris and beaver dams, leading to slower water flow, more sediment deposition, and perhaps localized anaerobic environments (e.g. Briggs *et al.,* 2013*;* Burchsted *et al.*, 2010). The variability of sediment types and possible physicochemical properties in the stream ecosystem were considered in this study to investigate the two P sorption indices, PBC and EPC, in the sediments of Walnut Creek.

Materials and Methods

Sediment sampling and characterization

Twenty-five sediment samples were collected from corridor and floodplain of Walnut Creek in Jasper County, Iowa (Table 8, coordinates of sampling sites are in Appendix B1). These samples were classified as bank, in-stream, and floodplain deposits. Sediments sampled to represent the bank deposits consisted of major stratigraphic units in the Walnut Creek valley. Vertically from the surface, they are the Camp Creek Member, the Roberts Creek Member, the Gunder Member, and Pre-Illinoian Till (Schilling *et al.*, 2004). According to Schilling *et al.* (2006b), three alluvial units in the stratigraphy of Walnut Creek banks (Camp Creek (samples B-2, B-17, B-21), Roberts Creek (samples B-3, B-18, B-22), and Gunder (sample B-19)) are the members of De Forest Formation. The De Forest formation occurs throughout Iowa, and the Pre-Illinoian Till (samples B-7 and B-20) is commonly exposed at hill slope locations in southern Iowa. The De Forest formation was formed during the Holocene Interglacial over the last 11,000 years BP, while Pre-Illinoian Till was deposited between 2,000,000 and 500,000 years BP. Baker *et al.* (1996) reported that the Gunder Member, the Roberts Creek member, and the Camp Creek Member date from 11,000 to 4,000 yr BP, 4000 to 400 yr BP, and the last 380 yr, respectively.

Table 8. The twenty-five samples collected in the study. Numbers in parentheses following sample description represent different sampling site (coordinates of sampling sites are in Appendix B1).

Bank		In-stream deposit		Floodplain	
Code	Description	Code	Description	Code	Description
B-2	Camp Creek (1)	I-4	Stream bottom sediment (1)	F-1	Pasture
B-3	Roberts Creek (1)	I-5	Slump, debris dam	F-9	Forest (1)
B-7	Till (1)	I-6	Stream bed sediments, debris dam	F-10	Forest (2)
B-17	Camp Creek (2)	I-8	Sand bar	F-14	Corn Field, tillage
B-18	Roberts Creek (2)	I-11	Stream bottom sediment (2)	F-15	Soybean field
B-19	Gunder	I-12	Slump (1)	F-16	Corn Field, no tillage
B-20	Till, calcareous (2)	I-13	Bar		
B-21	Camp Creek (3)	I-23	Slump (2)		
B-22	Roberts Creek (3)	I-24	Stream bottom sediment (3)		
		I-25	Beaver dam		

For the in-stream deposits, samples were differentiated as debris dam, bar, slump, beaver dam, and stream bottom sediment. In the floodplain soils group, samples were collected at 0-20 cm depth at the sites representing row crop production (soybean and corn field), grazing (pasture), and riparian buffer zones (forest). Most of the samples in the floodplain were collected in the soil mapping unit of Ackmore soil series (fine-silty, mixed, superactive, nonacid, mesic Mollic Fluvaquent (silt loam, 0-2% slope); only sample F-10 was collected from a Lawson-Nodaway-Colo (Aquic Cumulic Hapludoll, Mollic Udifluvent, and Cumulic Endoaquoll) complex mapping unit (Soil Survey Staff). Immediately after transport to laboratory, one portion from each sample was subsampled to be stored in a cold room, while another portion was air dried and sieved to pass a 2-mm screen. The samples stored in the cold room were prepared for the adsorption study, and the <2mm air dried samples were

allocated for sediment characterization. For most of the sampling sites, intact core samples were collected at the same time of sampling to determine bulk density.

Particle size distribution and bulk density were determined gravimetrically (Kettler *et al.*, 2001), while pH was determined at a soil to water ratio of 1:1. Total carbon and total nitrogen were analyzed using high-temperature dry combustion (Nelson and Sommers, 1996). Total organic matter was determined using the loss-on-ignition method (Konen *et al.*, 2002). The perchloric acid digestion method (Kuo, 1996) was used to determine total P, and concentrations were determined in the digest using the molybdate blue-ascorbic acid method (Watanabe and Olsen, 1965). Mehlich-3 solution (Mehlich, 1984) was used to extract exchangeable cations (Ca_{M3}, Mg_{M3}, K_{M3}, Na_{M3}), and the concentrations were determined using inductively coupled plasma-atomic emission spectrometry (ICP-AES). Mehlich-3 solution was also used to extract P (P_{M3}) and the concentrations were determined using the molybdate blue-ascorbic acid method (Watanabe and Olsen, 1965). Citrate-bicarbonate-dithionite-extractable Fe (Fe_{CBD}) was determined by atomic absorption spectroscopy (Shang and Zelasny, 2008). Ammonium oxalate extractable Fe, Al, and Mn (Fe_{ox}, Al_{ox}, Mn_{ox}) were determined by ICP-AES, and P (P_{ox}) in this extraction was determined using a malachite green method (D'Angelo *et al.*, 2001). P_{M3} and Ca_{M3} were used to calculate the degree of P saturation ($DPS_{(Ca\text{-}M3)}$) as well as P_{ox}, Fe_{ox}, and Al_{ox} for $DPS_{(Al\text{-}ox + Fe\text{-}ox)}$. The formulas to calculate DPS are described in equation 1 and 2, units in all variables are mmol kg^{-1} (Hongthanat *et al*., 2011; Kleinman and Sharpley, 2002).

$$DPS_{(Ca-M3)} = \frac{P_{M3}}{[Ca_{M3}]} \times 100 \quad \text{(Equation 1)}$$

$$DPS_{(Fe-ox+Al-ox)} = \frac{P_{ox}}{[Fe_{ox} + Al_{ox}]} \times 100 \quad \text{(Equation 2)}$$

Isotherm adsorption study

A batch isotherm adsorption study was conducted to assess amount of phosphate adsorbed by stream sediments (solid phase P, abbreviated as Q) as a function of phosphate concentration in the solution (liquid phase P, abbreviated as C) at equilibrium at a constant temperature. To serve as a base solution for the experiments, stream water from Walnut Creek was filtered through a 0.45-μm cellulose-acetate membrane. Stream water is preferred for such experiments to represent the ionic strength and chemical composition of natural conditions (Lucci *et al.*, 2010). Three subsamples of the stream water were characterized by pH of 8.0 (±0.1), electrical conductivity (EC) of 0.45 (±0.04) dS m^{-1}, dissolved P of 0.050 (±0.009) mg L^{-1}, and K, Ca, Mg, Na of 1.3 (±0.40), 56.3 (±4.2), 23.0 (±2.0), 5.7 (±0.2) mg L^{-1}, respectively (values in the parentheses are standard deviations). All sediments listed in Table 8 were used in this study. To mimic possible physicochemical aspects during the process of sediment erosion in stream water, four physicochemical treatments were designed by varying the solid-to-solution ratio, shaking energy, and redox potential, as summarized in Table 9. The physicochemical treatments are referred to oxic environment (OX), anoxic environment (AN), high shaking energy (HE), and low solid-to-solution ratio (LS).

Table 9. Physicochemical treatments designed for evaluation of PBC and EPC.

Designated term	Symbol	Solid-to-solution ratio	Shaking energy	Anaerobic incubation
Oxic environment	OX	1:20	Low	Not incubated
Anoxic environment	AN	1:20	Low	Incubated
High shaking energy	HE	1:20	High	Not incubated
Low solid-to-solution ratio	LS	1:200	Low	Not incubated

The adsorption study used 50-mL centrifuge tubes to obtain an equilibrium state between solid and solution. The volume of base solution added in all treatments was 30 mL per tube, spiked with 0, 0.05, 0.10, 0.20, 0.40, and 0.80 mg P L^{-1}. The mass of moist sediments were equivalent to the oven-dried mass of 1.5 g (under OX, AN, and HE) and 0.15 g (under LS) for solid-to-solution ratios of 1:20 and 1:200, respectively. In the anaerobic (AN) incubation, the cap of the centrifuge tube was lined with a rubber septum to allow access for nitrogen purging. N_2 gas was pumped into individual centrifuge tubes on the first day of the incubation and repeated weekly. After N_2 purging, the surface of the rubber septum and the bottom part of the cap was rubbed with silicone glue to minimize air infiltration. Incubation was carried out for 30 days in a chamber flooded with N_2.

The equilibrium state was achieved by shaking the samples on a reciprocating shaker for 24 hours. A slow shaking speed (200 excursions per minute) was applied under OX, AN, and LS, while fast shaking speed (300 excursions per minute) was applied under HE to result in high shaking energy. After the sediments settled, Eh and pH were measured by inserting the Eh or pH probe in the tube so that the edge of the probe was about 2 cm above the surface of the settled sediment. In the anaerobic treatment, Eh and pH were measured in a glove box

which was flooded with N_2. Afterward, each tube was centrifuged at 4,300 x *g* for 15 minutes, followed by filtering the supernatant through Whatman 42 filter paper. The P concentration in the solution at equilibrium was determined using the malachite green method (D'Angelo *et al.*, 2001). Equilibrium phosphorus concentration (EPC) and phosphorus buffering capacity (PBC) were determined following the method of Hongthanat *et al.* (2011) where P in the liquid phase (C) was plotted against P in the solid phase (Q), and a line was fit to the data using simple linear regression.

To better understand relationship between EPC and sediment properties, a simple correlation analysis was performed using SAS 12.0 software. The same software was used for mean comparison of pH, Eh, PBC, and EPC at each of physicochemical properties design. Moreover, two approaches were used for assessing sink-source status of the sediments in the different treatments. First, the EPC values were directly compared to average values of dissolved P in Walnut Creek stream water determined in this study. As noted earlier, sediments are predicted to act as sinks when the EPC is less than dissolved P concentration and as sources when EPC is greater than the dissolved P concentrations in the stream water. The second approach was to compare the predicted pore water P concentration of in situ stream sediments (C_{pw}) to the dissolved P in infiltrating stream water. This comparison would be relevant in the context where the stream stage rises slowly enough that in-stream or bank sediments are not physically eroded or where overbank flooding leads stream water to infiltrate floodplain soils. In situ saturated sediment or soil could be a sink when C_{pw} is less than dissolved P and a source when C_{pw} is greater than dissolved P in the stream water. C_{pw} was predicted using the following equation:

$$C_{pw} = (S_a/[(\theta_v / \rho_b) + PBC] \qquad \text{(Equation 3)}$$

where C_{pw} = pore water P concentration (mg L^{-1}), S_a = concentration of active P in the sediment (mg kg^{-1}), we assumed the values were similar to soluble and loosely bound P (SL-*Pi*, data in Table 10), θ_v = volumetric water content (L L^{-1}), ρ_b= bulk density (kg L^{-1}), and PBC= phosphorus buffering capacity (L kg^{-1}). In these calculations, we assumed that the sediments would be water saturated, i.e., θ_v = total porosity.

Results and Discussion

Characteristics of the sediments

Characteristics of the twenty-five sediments are summarized in Table 10. The in-stream deposits and the floodplain soils had a narrow range of pH values (5.6 to 7.2), while the bank sediments had a wider pH range (5.7 to 8.1). The B-20 sample (developed from Pre-Illinoian Till) had the highest pH value, and it was also calcareous. Total C ranged from 0.25 to 3.12%, and organic matter ranged from 1.51 to 7.53%. The B-20 and B-17 samples had relatively similar organic matter contents (1.71 and 1.65 %, respectively), however total C in B-20 was about four times that of B-7, indicting the presence of inorganic carbon in sample B-20. Total N in samples from the floodplain soils tended to be higher than in the other groups, possibly due to fertilizer application in the row crops (samples F-14, F-15, and F-16), accumulation of manure from the pasture rangeland (sample F-1), or accumulation of runoff in the riparian buffer from adjacent row crop fields (samples F-9 and F-10). Samples from the floodplain had less variation of Mehlich-3 extractable cations, ammonium oxalate-extractable metals (Fe_{ox}, Al_{ox}, Mn_{ox}), and CBD-extractable Fe compared to the bank and in-stream deposits.

Table 10. Selected sediment properties, where OM = organic matter, C= total C, N= total N, TP = total P, $Fe_{ox}/Al_{ox}/Mn_{ox}/P_{ox}$ = ammonium oxalate extractable Fe/Al/Mn/P, Fe_{CBD} = citrate bicarbonate dithionite extractable Fe, SL-*Pi*= soluble and loosely bound inorganic P (1 *M* NH_4Cl extractable P), $Ca_{M3}/Mg_{M3}/K_{M3}/Na_{M3}/P_{M3}$ = Mehlich 3 extractable Ca/Mg/K/Na/P, $DPS_{(Al\text{-}ox + Fe\text{-}ox)}$ = degree of phosphorus saturation based on P_{ox}, Al_{ox}, and Fe_{ox}, $DPS_{(Ca\text{-}M3)}$ = DPS based on Ca_{M3} and P_{M3}, *n.a* = not available.

Group	Sample Code	Description	pH H_2O (1:1)	Sand	Silt	Clay	BD	TP	Fe_{ox}	Al_{ox}	Mn_{ox}	P_{ox}	Fe_{CBD}	SL-*Pi*
				------- % -------			g cm^{-3}	------- mg kg^{-1} -------						
Banks	B-2	Camp Creek (1)	5.7	6	73	21	1.30	499	2,816	1,321	595	127	8,620	5
	B-3	Roberts Creek (1)	6.0	2	62	36	*n.a*	847	4,424	1,742	2,182	479	7,274	7
	B-7	Till (1)	7.1	49	28	23	1.60	370	1,665	496	267	124	11,858	7
	B-17	Camp Creek (2)	6.2	11	64	25	1.23	491	3,348	1,002	702	158	6,825	6
	B-18	Roberts Creek (2)	6.3	13	60	27	1.29	588	3,947	1,076	1,263	193	5,862	5
	B-19	Gunder	7.4	6	72	22	1.57	484	1,967	445	154	137	3,813	5
	B-20	Till (2)	8.1	49	30	21	1.72	473	743	235	166	106	10,124	6
	B-21	Camp Creek (3)	6.0	19	59	22	*n.a*	573	3,925	1,116	801	188	8,745	5
	B-22	Roberts Creek (3)	5.7	6	69	25	*n.a*	522	2,654	947	403	129	7,272	11
In-stream deposit	I-4	Stream bottom sediment (1)	6.7	9	59	32	1.28	666	3,068	837	9,794	499	5,095	11
	I-5	Slump, debris dam	5.9	6	60	34	0.87	386	1,951	1,542	689	60	4,294	4
	I-6	Stream bed sediments, debris dam	7.2	22	53	25	*n.a*	966	9,903	1,058	1,290	655	15,571	5
	I-8	Sand bar	7.2	52	33	15	1.44	566	3,948	602	919	351	6,888	7
	I-11	Stream bottom sediment (2)	5.9	30	51	19	1.54	974	4,009	455	532	648	7,404	6
	I-12	Slump (1)	6.6	34	51	15	1.27	558	3,947	678	740	329	7,338	8
	I-13	Bar	6.5	6	63	31	1.15	1,134	6,310	585	147	823	8,426	6
	I-23	Slump (2)	6.3	33	37	30	*n.a*	815	4,340	649	872	297	15,948	5
	I-24	Stream bottom sediment (3)	5.9	13	63	24	*n.a*	566	6,169	957	423	275	7,562	6
	I-25	Beaver dam	7.1	27	56	17	*n.a*	673	3,431	609	672	353	7,401	7
Floodplain	F-1	Pasture	5.6	1	81	18	0.95	567	3,914	1,367	511	160	7,341	5
	F-9	Forest (1)	5.7	18	63	19	1.01	556	3,348	1,379	809	170	8,171	7
	F-10	Forest (2)	6.1	4	70	26	0.86	730	4,228	1,319	618	292	8,615	6
	F-14	Corn Field, tillage	6.3	10	67	23	1.41	559	3,496	1,451	740	129	8,557	7
	F-15	Soybean field	6.5	17	61	22	1.41	505	3,644	1,453	852	119	8,876	6
	F-16	Corn Field, no tillage	6.2	22	57	21	1.24	617	2,751	1,216	471	161	9,195	9

Table 10. Continued.

Group	Sample Code	Description	OM	C	N	C/N	Ca_{M3}	Mg_{M3}	K_{M3}	Na_{M3}	P_{M3}	DPS (Al-ox + Fe-ox)	DPS (Ca-M3)
			---- % ----				---------- mg kg^{-1} ----------					----- % -----	
Banks	B-2	Camp Creek (1)	4.52	1.54	0.16	9.63	2,646	537	142	69	39	4.14	1.90
	B-3	Roberts Creek (1)	7.53	3.12	0.25	12.48	5,170	1,186	173	104	55	10.75	1.37
	B-7	Till (1)	1.65	0.25	0.06	4.17	1,927	316	88	60	26	8.30	1.72
	B-17	Camp Creek (2)	3.38	1.32	0.14	9.43	1,975	463	100	70	29	5.27	1.87
	B-18	Roberts Creek (2)	4.51	1.84	0.14	13.14	2,983	558	145	89	41	5.64	1.78
	B-19	Gunder (1)	1.51	0.31	0.06	5.17	2,135	506	117	55	28	8.59	1.68
	B-20	Till (2)	1.71	1.06	0.03	35.33	6,750	288	103	57	5	15.52	0.10
	B-21	Camp Creek (3)	4.38	1.66	0.13	12.77	2,243	413	98	68	35	5.44	2.02
	B-22	Roberts Creek (3)	4.23	1.54	0.14	11.00	1,965	426	83	60	29	5.03	1.92
In-stream deposit	I-4	Stream bottom sediment (1)	3.19	0.88	0.15	5.87	3,729	968	191	87	61	18.76	2.12
	I-5	Slump, debris dam	5.59	2.06	0.16	12.88	4,038	670	143	85	13	2.11	0.41
	I-6	Stream bed sediments, debris dam	3.64	1.00	0.10	10.00	2,905	685	113	78	58	9.77	2.60
	I-8	Sand bar	2.98	0.99	0.10	9.90	2,278	405	112	68	76	12.20	4.33
	I-11	Stream bottom sediment (2)	2.57	0.84	0.10	8.40	1,976	425	67	57	85	23.61	5.54
	I-12	Slump (1)	3.87	1.49	0.14	10.64	2,380	454	134	70	84	11.08	4.59
	I-13	Bar	4.25	1.47	0.12	12.25	3,129	728	118	97	67	19.72	2.76
	I-23	Slump (3)	2.33	0.34	0.05	6.80	2,764	899	142	107	45	9.41	2.10
	I-24	Stream bottom sediment (3)	5.90	2.40	0.19	12.63	2,144	429	79	64	27	6.10	1.66
	I-25	Beaver dam	4.52	1.71	0.16	10.69	3,065	576	117	77	71	13.58	3.00
Floodplain	F-1	Pasture	5.19	2.23	0.24	9.29	2,387	434	146	63	34	4.28	1.85
	F-9	Forest (1)	5.09	1.95	0.20	9.75	2,242	352	177	67	56	4.93	3.26
	F-10	Forest (2)	6.41	2.52	0.24	10.50	2,897	577	171	78	55	7.58	2.48
	F-14	Corn Field, tillage	4.21	1.49	0.15	9.93	2,417	461	149	59	37	3.57	1.98
	F-15	Soybean field	4.38	1.59	0.16	9.94	2,282	423	113	53	30	3.23	1.71
	F-16	Corn Field, no tillage	4.69	1.91	0.18	10.61	2,271	400	189	74	72	5.52	4.09

The ranges of TP and P_{ox} were 386-1,134 and 60-823 mg kg^{-1}, respectively. The clay fraction was from 15-36%, while the sand fraction was from 2-52%. High sand concentration in samples B-7 and B-20 was comparable to the characteristics of Pre-Illinoian Till reported by Schilling *et al.* (2004). Six samples of the in-stream deposits (I-6, I-8, I-11, I-34, I-23, and I-25) were coarser than most of the other samples, reflecting differential transport of finer material with stream flow (McDowell and Sharpley, 2001a). The in-stream deposits had a wider range of clay concentration than did the bank sediments or the floodplain soils, also indicating variation in the deposition and transport of finer materials along the creek.

In general, characteristics of the sediments varied across the samples even within the same group. The variations were driven by the age and source of the deposits, by sediment transport and deposition, or by agronomic practices. Vertical variation in characteristics of the bank sediments reflected the sequence of Holocene alluvial events in Walnut Creek. Within the in-stream deposits group, the physical and chemical characteristics were related to the processes of sedimentation and transport of eroded materials. In the last group, floodplain soils, variations of sediment characteristics may have been associated with both recent overbank deposition and land use or agronomic practices at each sampling site.

Soil test P and DPS as indicators of environmental risk

Soil test P is a simple indicator to assess potential P release. Values for P_{M3} in this study ranged from 5 to 85 mg kg^{-1} (Table 10). In Ohio, 150 mg Bray-P kg^{-1} is the threshold to recommend no additional P application to a soil (Dayton *et al.*, 2014). Pautler and Sims (2000) suggested that Delaware soils with >50 mg Mehlich-1 P kg^{-1} would be excessive in P.

In a study of calcareous soils in the Minnesota River Basin, Fang *et al.* (2002) suggested that the critical levels for soil Mehlich-3 P and Olsen P were 65-85 and 40-55 mg kg^{-1}, respectively. Other environmental thresholds in the US that employ soil-test P values have been summarized by Sharpley *et al.* (2003). For Mehlich-3 extractable P, the threshold in several states ranges between 130 to 200 mg P kg^{-1}. Since environmental threshold values for these parameters have not been defined for soils in Iowa, threshold values from other studies were used to assess potential P loss from the samples. The P_{M3} levels in all samples were below the Mehlich-3 threshold values of 130-200 mg kg^{-1} as suggested by Sharpley *et al.* (2003). However, if compared to P_{M3} critical level of 65-85 mg kg^{-1} as suggested by Fang *et al.* (2002), six samples (I-8, I-11, I-12, I-13, I-25, and F-16) could be considered to pose a potential risk to water quality impairment.

Values for $DPS_{(Ca\text{-}M3)}$ and $DPS_{(Al\text{-}ox+Fe\text{-}ox)}$ ranged from 0.10 to 5.54% and from 2.11 to 23.61%, respectively (Table 10). The degree of P saturation (DPS) is an assessment of the portion of potential sorption sites that are bound with P to the number of sorption sites available for P sorption. Previous studies have used DPS values for assessing the environmental risks of P in soils or sediments. Some critical DPS values have been proposed, varying from 8 to 30% and depending on the method used to calculate DPS, the management objective, and kinds of soil under evaluation (Breeuwsma *et al.*, 1995; Casson *et al.*, 2006; Hooda *et al.*, 2000; Laboski and Lamb, 2004; Nair *et al.*, 2004; Ohno *et al.*, 2007; Pautler and Sims, 2000; Sims *et al.*, 1998; Sims *et al.*, 2002). The range of $DPS_{(Ca\text{-}M3)}$ in this study is comparable to the range of 0.05 to 8.58% (mean =1.65%) in the study by Ige *et al.*(2005) for calcareous soils in Manitoba. Unfortunately, so far there is no $DPS_{(Ca\text{-}M3)}$ value that has been set as a threshold to asses potential risk of P loss from soil or sediment.

By comparing the threshold value of 15% for $DPS_{(Al\text{-}ox+Fe\text{-}ox)}$ as suggested by Ohno *et al.* (2007), it could be predicted that P release to the stream water might be likely from four samples (B-20, I-4, I-11, I-13). Among the four samples with $DPS_{(Al\text{-}ox+Fe\text{-}ox)}$ greater than 15%, the B-20 sample (Pre-Illinoian Till) may need other parameters to fairly assess its potential for P loss since this sample also had the lowest P_{M3}.

pH and Eh at equilibrium

The mean of Eh and pH at equilibrium for each of treatments in this study are graphed in Fig. 12. In comparison with the oxic environment, raising the shaking energy from low to high did not result in a significant change in equilibrium pH. On the other hand, anaerobic incubation for 30 days resulted in significant lower Eh and a significantly higher pH, presumably associated with H^+ consumption under decreasing redox potential, as suggested by Ponnamperuma (1972). A significantly higher pH also occurred when the solid-to-solution ratio was lowered from 1:20 to 1:200, reflecting less desorption of H^+ ions from the smaller sediment mass.

Solution pH is one of the important factors controlling P adsorption and desorption (Bar-Yosef *et al.*, 1988). In general, P adsorption more likely occurs under acid conditions due to the dominantly positive charge on the surfaces of iron oxides in soil. In contrast, an increase in pH leads to P desorption as the positively charged sites diminish in number and ligand competition for the sorption sites by HCO_3^- increases. In nonalkaline soils, sites for P adsorption are mainly on Fe(III) and Al (hydr)oxides that occur in finer fractions in the particle size distribution (Stumm and Morgan, 1970). Using an experimental and modeling approach, Devau *et al.* (2009) demonstrated that pH can regulate P adsorption where iron

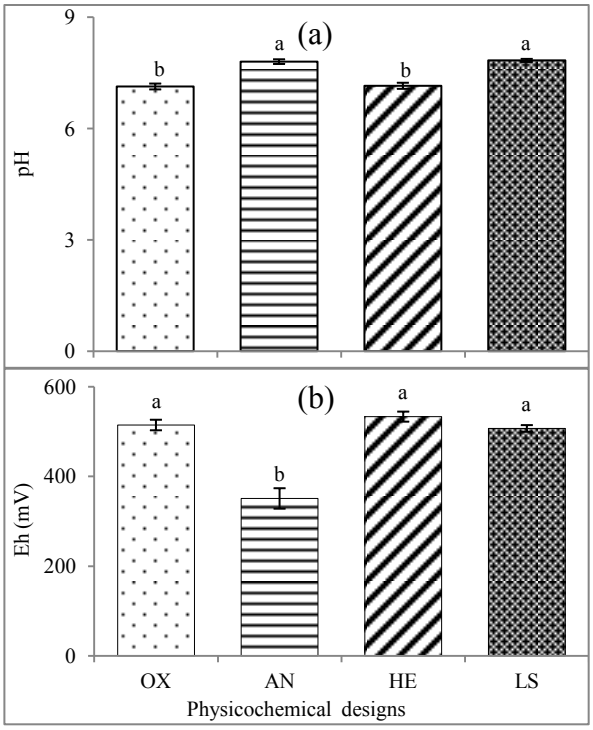

Figure 12. pH (a) and Eh (b) after equilibrium in the oxic environment (OX), anoxic environment (AN), high shaking energy (HE), and low solid-to-solution ratio (LS). Means with different letters were significantly different according to *t* test at $\alpha = 0.05$, n=25.

oxides, clay minerals, and gibbsite may be dominant at acidic, intermediate, and alkaline pHs, respectively. Redox potential (Eh) is another important factor driving P sorption-desorption, where low Eh is associated with enhanced dissolution of P as redox-sensitive minerals dissolve (Pratt *et al.*, 2007; Vadas and Sims, 1998).

PBC and EPC in varying physicochemical conditions

The PBC and EPC values of all twenty-five sediments under the four different physicochemical treatments are summarized in Table 11. Because of the variation of sediment properties, the PBC and EPC varied widely within a similar physicochemical treatment. A comparison of means showed that the four physicochemical treatments applied in this study did not have a significant, consistent effect on PBC (Fig. 13). The mean ± SE of

Table 11. Summary of two sorption indices, phosphorus buffering capacity (PBC) and equilibrium phosphorus concentration (EPC) for four treatments.

Group	Code	Description	PBC (L kg^{-1})				EPC (mg L^{-1})			
			OX†	AN†	HE†	LS††	OX†	AN†	HE†	LS††
Banks	B-2	Camp Creek (1)	173	242	172	275	0.040	0.110	0.051	0.028
	B-3	Roberts Creek (1)	83	98	98	173	0.166	0.330	0.197	0.117
	B-7	Till (1)	998	306	286	92	0.001	0.027	0.008	0.024
	B-17	Camp Creek (2)	181	321	194	235	0.035	0.047	0.041	0.049
	B-18	Roberts Creek (2)	338	570	438	392	0.027	0.041	0.034	0.045
	B-19	Gunder (1)	134	173	202	127	0.017	0.051	0.035	0.035
	B-20	Till (2)	1000	223	232	128	0.011	0.015	0.013	0.004
	B-21	Camp Creek (3)	212	449	243	223	0.057	0.091	0.056	0.076
	B-22	Roberts Creek (3)	283	456	256	267	0.040	0.075	0.041	0.045
In-stream deposit	I-4	Stream bottom sediment (1)	153	158	186	143	0.044	0.239	0.097	0.043
	I-5	Slump, debris dam	1401	893	525	495	0.007	0.061	0.011	0.004
	I-6	Stream bed sediments, debris dam	261	275	229	251	0.035	0.161	0.068	0.037
	I-8	Sand bar	166	124	169	296	0.039	0.364	0.087	0.059
	I-11	Stream bottom sediment (2)	1440	66	367	1819	0.004	0.151	0.018	0.005
	I-12	Slump (1)	75	96	60	176	0.224	0.514	0.259	0.129
	I-13	Bar	358	334	297	319	0.108	0.212	0.168	0.210
	I-23	Slump (3)	117	153	173	76	0.150	0.163	0.120	0.326
	I-24	Stream bottom sediment (3)	2121	708	2540	2766	0.008	0.041	0.015	0.007
	I-25	Beaver dam	441	146	476	231	0.055	0.182	0.074	0.107
Floodplain	F-1	Pasture	148	227	140	229	0.033	0.137	0.070	0.021
	F-9	Forest (1)	152	327	162	210	0.012	0.089	0.047	0.011
	F-10	Forest (2)	94	142	81	251	0.124	0.294	0.192	0.065
	F-14	Corn Field, tillage	267	255	207	197	0.013	0.058	0.044	0.063
	F-15	Soybean field	380	195	160	172	0.010	0.050	0.039	0.045
	F-16	Corn Field, no tillage	46	48	63	196	0.075	0.265	0.199	0.161

Note :
† 0, 0.05, 0.10, 0.20, 0.40, and 0.80 mg L^{-1} spiked P levels were used to determine PBC and EPC.
†† 0, 0.05, 0.10, and 0.20 L^{-1} spiked P levels were used to determine PBC and EPC, except for F-16 (0, 0.10, 0.20 mg L^{-1}), B-5 and B-20 (0, 0.05, 0.10 mg L^{-1})

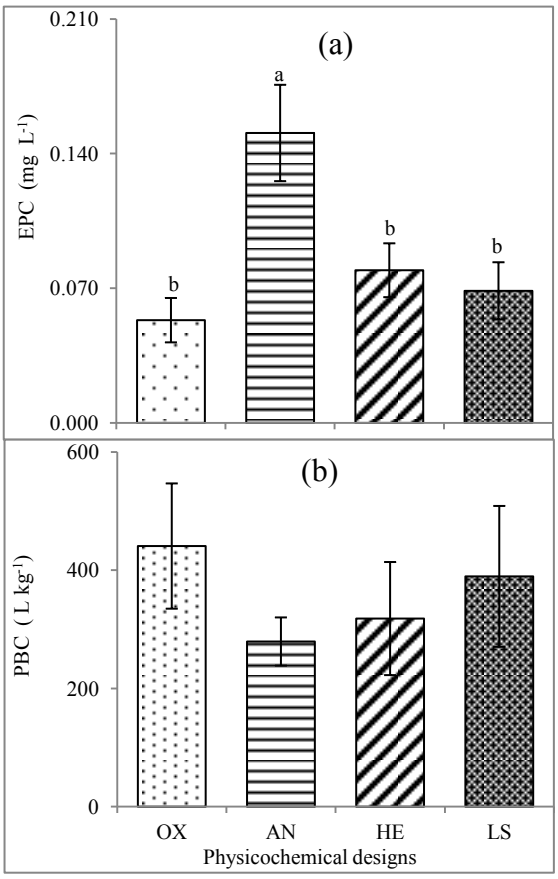

Figure 13. EPC (a) and PBC (b) after equilibrium in the oxic environment (OX), anoxic environment (AN), high shaking energy (HE), and low solid-to-solution ratio (LS). Means with different letters were significantly different according to *t* test at $\alpha = 0.05$, n=25.

PBC values under the oxic environment, anoxic environment, high-energy shaking, and low solid-to-solution ratio treatments were 441 ± 106, 279 ± 41, 318 ± 96, and 390 ± 119 L kg^{-1}, respectively. In contrast, a significant difference among the treatments was found in the EPC values (Fig. 13). The anoxic environment had the highest EPC mean value (0.15 ± 0.03 mg L^{-1}), which was significantly different from the EPC mean values in the other treatments.

Higher EPC values under anoxic conditions is a result comparable to a previous study by Pant and Reddy (2001) using sediments samples from the Indian River Lagoon. In their study, Pant and Reddy (2001) had associated the differences in maximum P sorption capacity and EPC at varying redox conditions with the dynamics of Fe in the sediments. Under oxic

environments, more P sorption sites from amorphous and poorly crystalline forms of Fe oxides are likely to be available. Conversely, anoxic environments promote the reduction of Fe^{3+} to Fe^{2+} and dissolution of Fe oxides, resulting in fewer sorption sites and the release of Fe-bound P. In addition, an increase in the pH at equilibrium under anoxic condition might have promoted release of P from binding with Al and Fe oxides. Moreover, some pH-sensitive organic P fractions may have contributed to the P measured in the solution phase (Koski-Vähälä and Hartikainen, 2001).

Furthermore, the mean ± SE of EPC values in the oxic environment, high-energy shaking, and low solid-to-solution ratio were 53 ± 12, 79 ± 14 and 69 ± 15 μg L^{-1}, respectively. There were no significant differences among the EPC mean values under these physicochemical treatments. This was not in accordance with the previous work by Sui and Thompson (2000) who reported that in a biosolids-amended Mollisol the amount of P desorbed increased as the solid-to-solution ratio decreased. In addition, in a study using deionized water as the base solution, Koski-Vähälä and Hartikainen (2001) reported that EPC values were 10, 13, and 51 μg L^{-1} for the solid concentrations of 1700, 170, and 17 mg L^{-1}, respectively, indicating an increase of EPC values under decreasing solid-to-solution ratio. Moreover, high shaking energy was expected to result in more dispersion of sediment aggregates and in turn to increase EPC values due to enhanced release of colloidal P. However, the hypothesis was not confirmed in the present study. The impact of pH as well as the type and availability of sorption sites in the 25 sediments probably overrode the influence of shaking energy and solid-to-solution ratio on EPC values in the oxic treatment.

Predicting P mobility

Variations in EPC under different physicochemical conditions may be used to predict P mobility from sediments to the stream water by comparing EPC values with concentration of dissolved P in the stream water. In the present study, for comparison purposes, the dissolved P value in the stream water was assumed to be 0.05 mg P L^{-1}, a value that was obtained as the average from water sampling in Walnut Creek during spring 2014 (data not shown). The results from this approach are presented in Fig. 14. In this figure, points plotted above the dashed line represent samples which could act as "sources" by releasing P to stream water. In contrast, points plotted below the dashed line represent samples that could act as "sinks" by adsorbing P to the sorption sites. Using this approach, it may be predicted that in anoxic environments most of sediment samples are likely to act as sources, and only five samples (B-7, B-18, B-9, B-20, and I-24) are likely to adsorb P from column water. In contrast, in oxic environments most samples could act as sinks, while eight samples (B-3, B-21, I-12, I-13, I-23, I-25, F-10, and F-16) could release P to the stream water. The number of samples which were likely act as sinks and sources under high-energy shaking is about equal: 12 and 13, respectively. At the low solid-to-solution ratio, more sediments could act as sinks than as sources: 15 and 10, respectively. In all four physicochemical treatments of this study, the in-stream deposits were more likely to act as sources than were the bank sediments or the floodplain soils.

We also used a second approach to evaluate source-sink risks. In this case, we compared a prediction of P concentration in pore water of the sediments (C_{pw}) to the dissolved P concentration in stream water. In this approach, in situ sediment or water-saturated soil would be predicted to be a sink when C_{pw} is less than dissolved P or a source

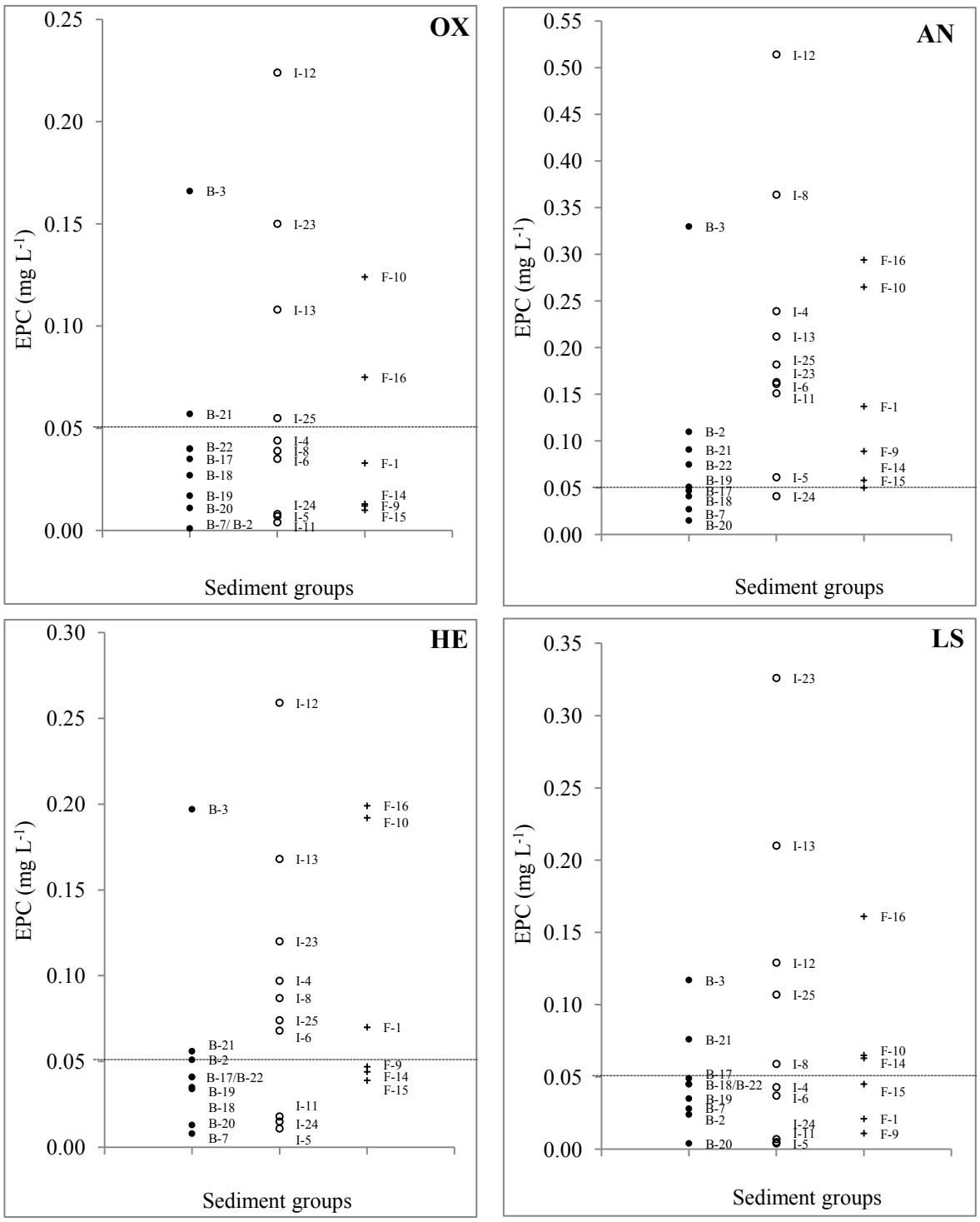

Figure 14. Sediments act as "sink" (below dashed line) or "source" (above dashed line) under physicochemical design of oxic environment (OX), anoxic environment (AN), high shaking energy (HE), and low solid to solution ratio (LS). Dashed line represents dissolved P concentration in stream water, assumed at 0.05 mg L^{-1}. Letters following the plot symbols are sample code, •B is sample from the bank (B), oI is sample from the in-stream deposit (I), and +F is from the floodplain (F).

when C_{pw} is greater than dissolved P in the stream water. As in the first approach, the dissolved P value was assumed to be 0.05 mg P L^{-1}. Due to limited availability of bulk density values, only 18 samples were used in this analysis; each group consisted of 6 samples. This approach is relevant to mimic conditions at base flow, when there is normally little suspended sediment in the stream, yet soluble P may be released to the stream as water passes over and through in-channel or near-channel sediments. Consequently, only the oxic environment, anoxic environment, and the low solid-to-solution ratio treatments were used in the analysis. The results from the second approach are presented in Fig. 15.

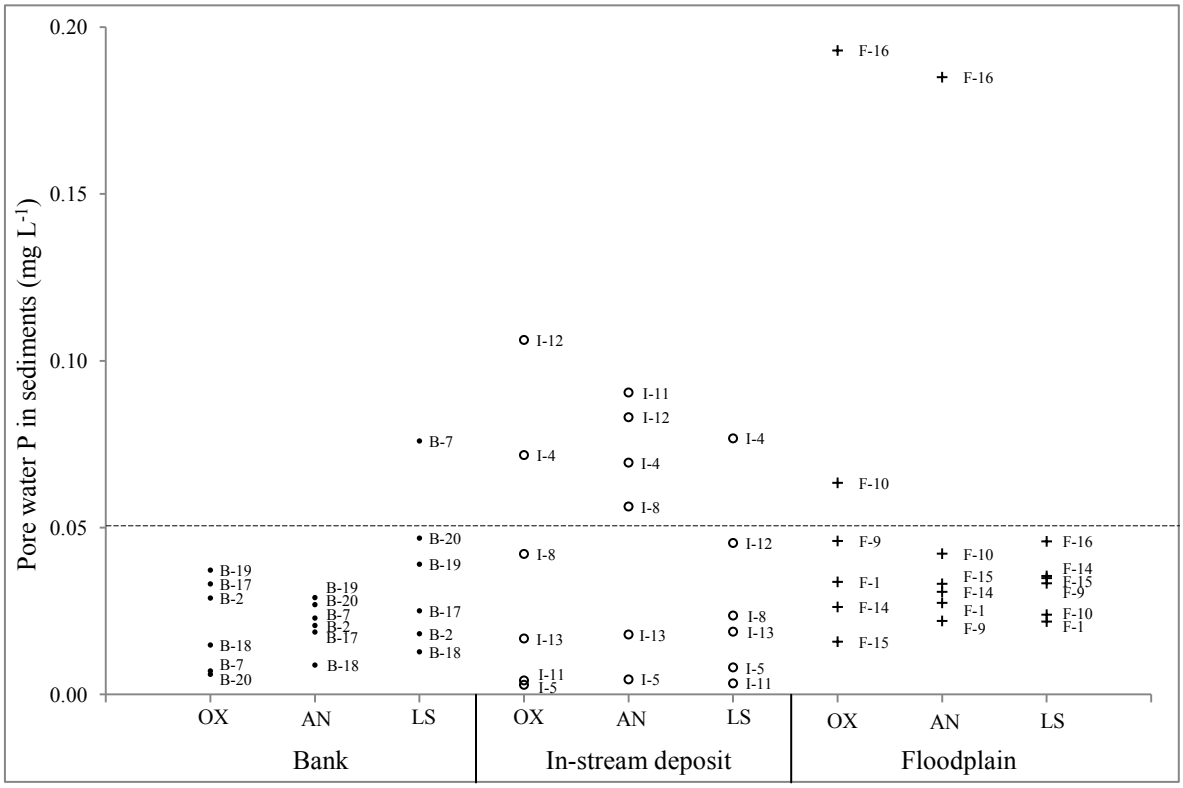

Figure 15. Predicting P mobility by comparing pore water P in sediment (C_{pw}) to dissolved P (represented by the dashed line, assumed at 0.05 mg L^{-1}). Below the dashed line sediments are predicted to be a sink, above the dashed line sediments are predicted to be a source. •B, ₒI, and +F are the code for samples from the bank, the in-stream deposit, and the floodplain, respectively. OX, AN, and LS are the treatments of oxic environment, anoxic environment, and low solid-to-solution ratio, respectively.

Figure 15 shows that for the bank sediments, only one sample (B-7) would be predicted to act as a source under the low solid-to-solution ratio, and the other samples would act as sinks in any of the treatments. Similarly, most samples in the floodplain could act as sinks in any of the treatments; only F-16 in the anoxic environment as well as F-10 and F-16 in the oxic environment could act as sources. On the other hand, more of the in-stream deposits could act as sources. There were two samples (I-12 and I-4), four samples (I-11, I-12, I-4, and I-8), and one sample (I-4) among the in-stream deposits that could be predicted to be sources under oxic conditions, anoxic conditions, and low solid-to-solution ratio, respectively.

Relationship between sediment properties and EPC

Simple correlation analyses between the sediment properties and EPC are summarized in Tables 12 and 13. All samples (n=25) were used for the correlation analysis summarized in Table 12, while only samples from the bank sediments and floodplain soils (n=15) were used for the correlation analysis summarized in Table 13. In general, there are more significant correlations between sediment properties and EPC values in the various physicochemical treatments for the restricted group of bank and floodplain samples (Table 13) than when all the samples are lumped (Table 12). This reflects the heterogeneity of characteristics in the recent in-stream deposits compared to the bank sediments and floodplain soils. The physicochemical processes associated with erosion, deposition, and stream flow are likely to shape the processes of P sorption/desorption, mineral P precipitation/dissolution, and mineralization/immobilization in the in-stream deposits. Those impacts are presumably less important in the bank sediments and floodplain soils. Therefore,

the dynamics of P in the in-stream deposits are likely to have a greater impact on stream P concentrations than processes that occur in the bank sediments or the floodplain soils.

Table 12. Simple correlation between equilibrium phosphorus concentration (EPC, *Y*) and sediment characteristics (*X*) under physicochemical design of oxic environment (OX), anoxic environment (AN), high shaking energy (HE), and low solid-to-solution ratio (LS). All samples (*n*=25) were used in the correlation analysis. Clay, sand, OM, C, and N are in %, TP, P_{M3}, P_{ox}, Fe_{CBD}, Fe_{ox}, Al_{ox}, and Mn_{ox} are in mg kg^{-1}.

X	Y							
	EPC under OX		EPC under AN		EPC under HE		EPC under LS	
	$r^{\dagger}$	$P^{\ddagger}$	r	$P^{\ddagger}$	r	$P^{\ddagger}$	r	$P^{\ddagger}$
Clay	0.17	0.4087 ns	-0.10	0.6214 ns	0.10	0.6485 ns	0.25	0.2289 ns
Sand	-0.03	0.0945 ns	0.14	0.5111 ns	-0.08	0.7180 ns	0.08	0.6865 ns
OM	0.27	0.1876 ns	0.23	0.2595 ns	0.35	0.0865 ns	-0.02	0.9092 ns
Silt	-0.05	0.8915 ns	-0.12	0.5675 ns	0.04	0.8395 ns	-0.20	0.3351 ns
C	0.22	0.2905 ns	0.19	0.3638 ns	0.31	0.1327 ns	-0.12	0.5646 ns
N	0.11	0.5941 ns	0.18	0.3770 ns	0.24	0.2399 ns	-0.03	0.8749 ns
pH	-0.08	0.6870 ns	0.02	0.9203 ns	-0.07	0.7294 ns	-0.00	0.9835 ns
Fe_{ox}	0.22	0.3003 ns	0.24	0.2496 ns	0.23	0.2609 ns	0.21	0.3178 ns
$Fe_{ox} + Al_{ox}$	0.21	0.3074 ns	0.22	0.2826 ns	0.25	0.2322 ns	0.17	0.4196 ns
$Fe_{ox}+Al_{ox}+Mn_{ox}$	0.18	0.3859 ns	0.31	0.1339 ns	0.25	0.2222 ns	0.09	0.6702 ns
Ca_{M3}	0.14	0.5160 ns	0.04	0.8637 ns	0.08	0.6915 ns	-0.01	0.9698 ns
TP	0.39	0.0555 ns	0.37	0.0666 ns	0.42	0.0366 *	0.48	0.0157*
P_{M3}	0.48	0.0146 *	0.78	<0.0001**	0.62	0.0008**	0.37	0.0727 ns
P_{ox}	0.33	0.1053 ns	0.46	0.0204*	0.38	0.0624 ns	0.31	0.1279 ns

*Note = † Pearson's r, ‡ P value, where *=significant at α=0.05, **= significant at α=0.01, ns=not significant.*

Table 13. Simple correlation between equilibrium phosphorus concentration (EPC) and sediment characteristics for the treatments of oxic environment (OX), anoxic environment (AN), high shaking energy (HE), and low solid-to-solution ratio (LS). Only samples from the streambanks and floodplain soils (n=15) were used in the correlation analysis. Clay, sand, OM, C, and N are in %, TP, P_{M3}, P_{ox}, Fe_{CBD}, Fe_{ox}, Al_{ox}, and Mn_{ox} are in mg kg^{-1}.

X	Y							
	EPC under OX		EPC under AN		EPC under HE		EPC under LS	
	$r^{\dagger}$	$P^{\ddagger}$	r	P	r	P	r	P
Clay	0.72	0.0023 *	0.48	0.0670 ns	0.46	0.0829 ns	0.44	0.1029 ns
Sand	-0.43	0.1057 ns	-0.42	0.1239 ns	-0.37	0.1779 ns	-0.22	0.4306 ns
Silt	0.24	0.3830 ns	0.30	0.2819 ns	0.25	0.3599 ns	0.11	0.7033 ns
OM	0.76	0.0010**	0.78	0.0006**	0.73	0.0021**	0.48	0.0678 ns
C	0.76	0.0011**	0.77	0.0009**	0.72	0.0022**	0.46	0.0852 ns
N	0.57	0.0251 *	0.71	0.0028**	0.66	0.0079**	0.47	0.0739 ns
pH	-0.35	0.2057 ns	-0.41	0.1311 ns	-0.34	0.2132 ns	-0.26	0.3554 ns
Fe_{ox}	0.54	0.0376 *	0.51	0.0534 ns	0.48	0.0711 ns	0.37	0.1686 ns
$Fe_{ox} + Al_{ox}$	0.55	0.0353 *	0.54	0.0365 *	0.51	0.0525 ns	0.40	0.1368 ns
$Fe_{ox}+Al_{ox}+Mn_{ox}$	0.60	0.0179 *	0.56	0.0304 *	0.52	0.0469 *	0.43	0.1091 ns
Ca_{M3}	0.30	0.2811 ns	0.17	0.5451 ns	0.15	0.5934 ns	-0.03	0.9131 ns
TP	0.91	0.0001**	0.87	<0.0001**	0.85	<0.0001**	0.62	0.0137 *
P_{M3}	0.59	0.0204 *	0.77	0.0008**	0.79	0.0004**	0.70	0.0036**
P_{ox}	0.91	0.0001**	0.79	0.0005**	0.73	0.0019**	0.50	0.0568 ns

*Note = † Pearson's r, ‡ P value, where *=significant at α=0.05, **= significant at α=0.01, ns=not significant.*

When all twenty-five samples in this study were pooled (Table 12), three sediment characteristics representing different forms of extractable P (TP, P_{M3}, and P_{ox}) were significantly correlated to EPC values in at least one of the treatments. In more detail, P_{M3} was significantly correlated to EPC under the oxic environment, anoxic environment, and

high-energy shaking environment. Total phosphorus (TP) was significantly correlated to EPC in the high-energy shaking and low solid-to-solution ratio treatments, while P_{ox} was significantly correlated to EPC only under anoxic conditions. When only data from the bank and the floodplain were used in the correlation analysis (n = 15, Table 13), the TP, P_{M3}, and P_{ox} were strongly and significantly correlated to EPC values in all the treatments, except for P_{ox} which was not significantly correlated to EPC values at low solid-to-solution ratios. $Fe_{ox}+Al_{ox}$ was significantly correlated to EPC under the oxic and anoxic environments. Clay was significantly correlated with EPC only in oxic environment, while Fe_{ox}, OM, C, N, and $Fe_{ox}+Al_{ox}+Mn_{ox}$ were significantly correlated to EPC in the oxic environment, anoxic environment, and at high-energy shaking, but not at the low solid-to-solution ratio.

The significant correlation between P_{M3} and EPC at all physicochemical treatments (except under low solid-to-solution ratio, especially when all sediments were used in the analysis) confirms that P_{M3} values are closely linked to EPC. P_{M3} is a soil test which is commonly used for both agronomic and environmental assessment, and it expected that P_{M3} is related to the pool of P involved in the dynamics of P sorption and desorption. Under anoxic condition, there was a significant correlation between P_{ox} and EPC even when all data were used in the analysis. The P_{ox} is believed to represent P that could be bound to poorly crystalline Fe/Al oxides; the release of such bound P could be associated with low redox potential, which would lead higher EPC values.

When the data set from the in-stream deposits were excluded from the correlation analysis, there was a strong and significant correlation between OM and EPC (as well as C and EPC) in the oxic, anoxic, and high shaking-energy environments. According to Antelo *et al.* (2007), P adsorption to goethite may be prevented in the presence of soil humic acid

because the humic acid prevents access of P to sorption sites. In contrast, Borggaard *et al.* (2005) showed that P adsorption by synthetic aluminum oxide, ferrihydrite, and goethite was only slightly affected by the presence of humic substances. The lack of significant correlation between OM and EPC could be related to the low solid-to-solution ratio. The amount of soluble OM under the low solid-to-solution ratio might be not comparable to that of the other treatments in which the solid-to-solution ratio was 1:20.

Interestingly, four sediment characteristics (sand, silt, pH, Ca_{M3}) were not significantly correlated to EPC under any of the treatments, even when data from the in-stream deposits were excluded (Table 12 and 13). This did not confirm the common observation that these sediment properties likely control the EPC values. Low-surface area sand particles, usually composed of quartz, are not likely to retain P, therefore it was expected that EPC would increase with increment in the sand fraction of the sediments. Greater Ca content in the sediment was expected to prevent the dispersion of aggregated mineral particles and, consequently, minimize the release of colloid-bound P. Sediments with higher pH were expected to have greater EPC due to increasing negative charges on the surfaces of iron-oxides and ligand competition for adsorption sites between HCO_3^- and orthophosphate ions. Moreover, the lack of significant correlation between silt and EPC in this study did not confirm the results of Haggard *et al.* (1999) who found a significant and positive correlation between EPC and silt.

The reasons for the lack of significant correlation between EPC and these four sediment characteristics (sand, silt, pH, Ca_{M3}) are unclear, however, two hypotheses may be proposed. First, we speculate that the range of silt and sand concentrations in the sediment samples from Walnut Creek was not comparable to the ranges of other studies. Secondly, the

Ca_{M3} concentration and pH of the sediments may not have had a significant effect on adsorption conditions at equilibrium in the present study. In other words, the impact of the base solution properties and physicochemical treatments on equilibrium state should also be considered. As noted earlier, the base solution already contained 56 mg L^{-1} of Ca, perhaps minimizing the impact of Ca desorbed from the sediment samples during equilibration. For example, Lucci *et al*. (2010) showed that EPC values were significantly correlated with the concentration of Ca in the base solution, while Klotz (1991) found a significant correlation between EPC and stream water Ca. Moreover, the physicochemical treatments clearly affected equilibrium pH (Fig. 12). Still, further study is required to determine the specific dynamics of Ca and pH in the sediment-solution system used to determine EPC values.

Conclusions

The sink-source status for P mobility of twenty-five sediments in Walnut Creek was predicted for a variety of physicochemical treatments, where equilibrium phosphorus concentration (EPC) and phosphorus buffering capacity (PBC) were main parameters used in two approaches to predict P sink-source status. The physicochemical treatments (including variations in solid-to-solution ratio, redox potential, and shaking energy intensity) resulted in variation in the values of EPC and PBC. Consequently, predictions of the sink-source status of the sediments changed. In the first approach where the EPC values were compared to a standard value of dissolved P in the stream water, it was predicted that most of the twenty-five sediments would act as sources by releasing P to the stream water especially under an anoxic environment. The same conclusion was reached when the second approach was applied, in which calculated pore water P concentration was compared to the standard

dissolved P concentration in the stream water. Under all the treatments and with either the first or second approach, it was more likely that the in-stream deposits would act as sources than would the bank sediments or the floodplain soils. This observation was also supported by the higher Mehlich-3 extractable P and degree of P saturation in the in-stream deposits than that in the bank sediments and the floodplain soils. Moreover, this study showed that P content (total P, Mehlich-3 extractable P, or ammonium oxalate-extractable P) were the main sediment characteristics correlated to the EPC values.

CHAPTER 5

EFFECTS OF VARYING REDOX POTENTIAL ON PBC, EPC, AND P RELEASE IN WALNUT CREEK BANK SEDIMENTS

Introduction

Phosphorus (P) is an essential nutrient for plants. In general, P plays an important role in photosynthesis, respiration, and regulation of a number of enzymes (Hawkesford *et al.*, 2012). Although total P in soils is usually low, around 50 to 1,500 mg kg^{-1} (Havlin *et al.*, 1999), eroded soil materials in runoff from agricultural land are considered to be one of the factors contributing to elevated P levels in stream waters. Once deposited as sediment in a water body, the solid-phase P may function as a source to the overlying water column (Pettersson, 1998). When nitrogen is not limiting for phytoplankton growth in a stream, even a small increase in P might trigger eutrophication. This reflects the small stoichiometric ratio for P compare to other major nutrients necessary for algal growth. The classic example is 106C:16N:1P atomic ratio for phytoplankton in marine environments (Redfield, 1958). For freshwater stream environments, Stelzer and Lamberti (2001) did not find significant effects of N:P ratio (65:1, 17:1, 4:1) on total algal biovolume especially at day 9 of the experiment under high total nutrient concentration.

Besides its function as sources of P, eroded sediments may also act as P sinks when in contact with stream water along streambanks, in the stream bottom, or as suspended particles. Phosphate ions are readily adsorbed by Fe or Al oxyhydroxides in many sediments, although other adsorption sites associated with Ca and Mg carbonates in calcareous soil materials, manganese oxides, layer silicate clay minerals, or organic matter complexes are also possible

(Antelo *et al.*, 2007; Bar-Yosef *et al.*, 1988; Yao and Millero, 1996). Because the oxidation state of Fe can vary with redox potential, the stability of Fe oxides varies in aerobic and anaerobic environments, influencing P sorption characteristics of sediments (Pant and Reddy, 2001). In a freshwater stream, aerobic environments are likely where water flows freely without any barrier promoting the dissolution of atmospheric oxygen as the water moves. On the other hand, when water moves slowly or becomes stagnant (e.g. blocked by debris dams or beaver dams), dissolved oxygen enters more slowly. Further, anaerobic environments are promoted by the decomposition of sedimentary organic matter as well as aquatic microbial biomass (Briggs *et al.*, 2013; Burchsted *et al.*, 2010). In addition, anaerobic environments may develop in the hyporheic zone where anaerobic groundwater is discharged into stream sediments (Bianchin *et al.*, 2011).

This present study employed two experiments to investigate P adsorption by and release from bank sediments in Walnut Creek (a second-order stream in Jasper County, Iowa) at varying redox potentials. In the first experiment, an adsorption study was conducted to investigate the effects of varying redox potential on the values of phosphorus buffering capacity (PBC) and equilibrium phosphorus concentration (EPC), two useful sorption indices for evaluating whether sediments act as sinks or sources of P (Haggard *et al.*, 2007; Hongthanat *et al.*, 2011; Jarvie *et al.*, 2005). The second experiment was conducted to simulate P release from sediments to the water column under oxic and anoxic conditions. While the adsorption experiment measured sorption characteristics of the sediments under equilibrium conditions that might occur when sediment is resuspended during stream flow (e.g. Stutter *et al.*, 2010), the second experiment attempted to simulate P dynamics when groundwater enters a stream (e.g. Hoffmann *et al.*, 2009).

Materials and Methods

Sediment sampling and characterization

Sediment samples were collected to represent the major alluvial units in the Walnut Creek floodplain: the Camp Creek Member, the Roberts Creek Member, the Gunder Member, and Pre-Illinoian Till (Schilling *et al.*, 2004). The coordinates of the sampling site are 41° 33.382' N and 93° 15.887' W. Immediately after transport to the laboratory, a portion of each sample was subsampled and stored at 4°C, while another portion was air dried and sieved to pass a 2-mm screen. The samples stored in the cold room were prepared for the adsorption and desorption studies, and the <2-mm air-dried samples were used for sediment characterization.

Total nitrogen was determined by high-temperature dry combustion (Nelson and Sommers, 1996). Total organic matter was determined using a loss-on-ignition method (Konen *et al.*, 2002). Particle size distribution was determined gravimetrically (Kettler *et al.*, 2001), while pH was determined potentiometrically at a soil:water ratio of 1:1. Perchloric acid digestion was used to determine total P (Kuo, 1996), and concentrations were determined in the digest using the molybdate blue-ascorbic acid method (Watanabe and Olsen, 1965). Mehlich-3 solution (Mehlich, 1984) was used to extract exchangeable cations (Ca_{M3}, Mg_{M3}, K_{M3}, Na_{M3}), and their concentrations were determined using inductively coupled plasma-atomic emission spectrometry (ICP-AES). Mehlich-3 solution was also used to extract P (P_{M3}) and the concentrations were determined using the ascorbic acid-molybdate blue method (Watanabe and Olsen, 1965). Citrate-bicarbonate-dithionite extractable Fe (Fe_{CBD}) was determined by atomic absorption spectroscopy (Shang and Zelasny, 2008). Ammonium oxalate extractable Fe, Al, and Mn (Fe_{ox}, Al_{ox}, Mn_{ox}) were determined by ICP-

AES, and P (P_{ox}) in this extraction was determined using malachite green method (D'Angelo *et al.*, 2001).

Isotherm adsorption experiment

A batch adsorption experiment was used to assess the amount of phosphate adsorbed by the stream sediments (adsorbed solid phase P, abbreviated as Q) as a function of phosphate concentration in the solution (liquid phase P, commonly abbreviated as C) after equilibrium at a constant temperature. As a base solution, stream water from Walnut Creek was filtered through a 0.45-μm filter paper and then spiked with 0, 0.05, 0.10, 0.20, 0.40, and 0.80 mg P L^{-1}. The stream water had a pH of 8.0 (±0.10), electrical conductivity (EC) of 0.45 (±0.040) dS m^{-1}, and dissolved P of 0.050 (± 0.0087) mg L^{-1}.

The experiment was set up as a completely randomized design involving three treatments (without anaerobic incubation (A), with anaerobic incubation (AN), and with anaerobic incubation with addition of glucose (ANG)), each treatment was replicated three times. Incubation treatments were applied to each sediment type before the adsorption study. In the AN treatment, 30 mL of P-spiked base solution was added into a 50 mL centrifuge tube containing moist sediment which was equivalent to 1.5 g oven dried weight. The cap in the centrifuge tube was lined with a rubber septum to allow purging each sample with nitrogen (N_2). N_2-purging was conducted in the beginning of the incubation and repeated weekly. To minimize air infiltration, silicone glue was applied to the surface of the rubber septum and bottom part of the cap after the nitrogen purge. The AN samples were incubated for 30 days in a chamber filled with N_2. A similar anaerobic incubation process was used for the ANG treatment, except that glucose ($C_6H_{12}O_6$, Sigma) had been dissolved in the P spiked

base solution to attain a concentration of 0.25 g L^{-1}. Treatment A used similar amounts of soil sample and P-spiked base solution, however the sediments were not incubated for 30 days under an anaerobic environment.

An equilibrium state was set by shaking the samples at 200 excursions per minute for 24 hours. After the sediments settled, Eh and pH were measured by inserting probes into the tube so that the edge of probe was about 2 cm above the surface of settled sediment. Eh and pH were measured only for the spiked levels of 0.10 and 0.20 mg P L^{-1}. For A and AN treatments, Eh and pH were measured in a glove box which was saturated with N_2. Afterward, the tube was centrifuged at 4,300 x *g* for 15 minutes, followed by filtering the filtrate through a 0.45-μm filter paper. Equilibrium phosphate concentration in the solution (C) was determined using malachite green method (D'Angelo *et al.*, 2001). The equilibrium phosphorus concentration (EPC) and the phosphorus buffering capacity (PBC) were determined following the method described by Hongthanat *et al.* (2011) where P in the liquid phase (C) was plotted against P in the solid phase (Q), and a line was fit to the data using simple linear regression. An example for determining PBC and EPC in this study is shown in Fig, 16.

Quantifying P release from the sediments

While P adsorption was investigated by using batch equilibrium experiments, P release was quantified using a reactor which was purposely designed for this study (Fig. 17). In general, the main frame of the reactor was a glass canning jar with the lid modified to attach a small electric motor, inlet and outlet gas tubing, dialysis bag holder, and an access port. The electric motor was powered by 12 V DC power source, connected to a shaft which

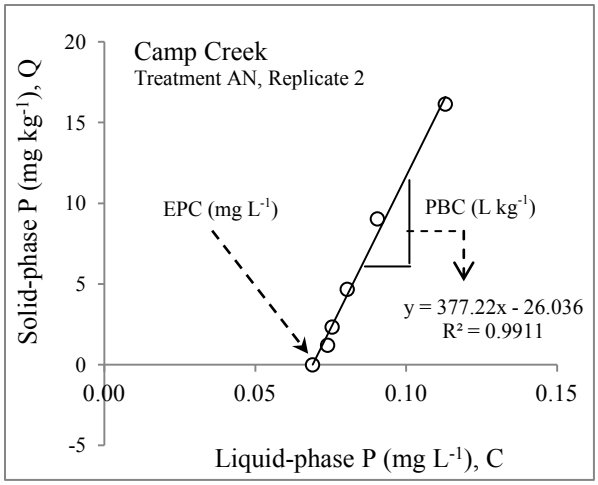

Figure 16. The liquid phase P (C) was plotted against P in the solid phase (Q) to determine phosphorus buffering capacity (PBC) and equilibrium phosphorus concentration (EPC) in the isotherm adsorption experiment. This figure shows an example for one of the anaerobic treatments of Camp Creek sediment.

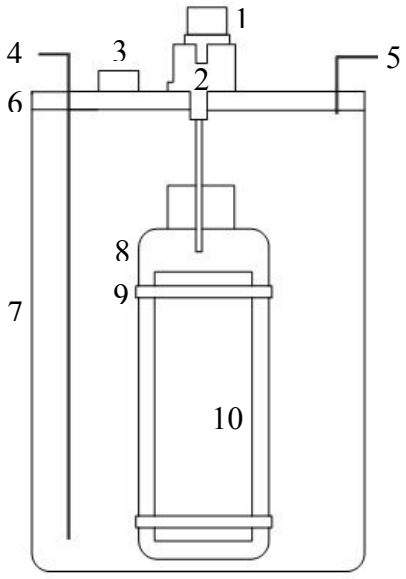

1. 12 V DC electric motor
2. Shaft to connect motor and dialysis bag holder
3. Sampling port
4. Air/N_2 inlet
5. Air outlet
6. Canning jar lid
7. Canning jar body
8. Dialysis bag holder
9. Dialysis bag clamp
10. 3500 MWCO dialysis tubing with sediment inside

Figure 17. Schematic design of reactor for quantifying P release from the sediments under oxic and anoxic environments.

rotated the dialysis tubing holder at 12 rpm for 8 hours a day. Since a metal may function as electron acceptor and promote Fe^{3+} reduction in the sediments (Martins *et al.*, 2014), the shaft and the dialysis tubing holder were designed to not contain any metal. The dialysis tubing had a 3,500 MWCO (Fisher). An anoxic environment was produced in the reactor by continuous nitrogen purging through the inlet tubing, and air from inside the reactor was expelled through the outlet tubing. In another treatment, an oxidizing environment was maintained by continuously pumping air through the inlet tubing. The access port was designed to fit a 10-mL pipet, pH probe, Eh probe, and thermometer; it could be opened easily and closed tightly after opening.

The experiment was set up on split-plot design, where sediment types and gas purging treatments were assigned as main plot and subplot, respectively. The experiment employed four sediments (Camp Creek, Roberts Creek, Gunder, and Pre Illinoian Till), two gas purging treatments (air and nitrogen purging), and three blocks. Overall, 24 reactors were used in this experiment. To arrange the reactors following split-plot design, a lab bench was divided into three blocks. Each block was divided into four plots, and each plot was randomly assigned to one of the four sediment types. Then each plot was divided into two subplots; one subplot was randomly assigned to a reactor purged with air and another subplot was assigned to a reactor purged with nitrogen.

The base solution used in this study was prepared in deionized water containing 1.3 *mM* $CaCl_2$, 0.1 *mM* $CaCO_3$, and 0.4 *mM* $MgCl_2 \cdot 6H_2O$. The electrical conductivity of the base solution was 0.45 dS/m, pH was 8.0, while dissolved organic C (DOC) and orthophosphate concentrations were below analytical detection limits. The initial volume of the base solution in each reactor was 600 mL, and the mass of moist sediment inside the

dialysis tubing was equivalent to 30 g of oven-dried mass. Solution samples were collected by using a 10-mL volumetric pipette on day 3, 6, 9, 12, and 24. Dissolved P and DOC were determined immediately after samples were collected. The P concentration was determined using the malachite green method, and DOC was measured by high-temperature combustion using a Shimadzu TOC 5050. Redox potential (Eh), pH, and temperature were measured at each sampling time.

Results and Discussion

Sediment properties

Selected chemical and physical properties of sediments used in this study were summarized in Table 14. There was a fairly narrow range of clay contents across the sediment, while the highest sand content was found in the Pre-Illinoian Till. The pH values were similar in the Camp Creek and Roberts Creek sediments (6.2 and 6.3, respectively), but higher in the Gunder material and in the till (7.4 and 8.1, respectively). The till was also calcareous. The lowest and highest extractable Fe_{CBD} was found on Gunder and till units , respectively. In Walnut Creek, the Gunder sediments normally occur below the water table, and this perhaps limiting the amount of Fe oxides present because of low redox potentials. In contrast, the high Fe_{CBD} in the till is also reflected by yellowish brown color in this sediment. Moreover, the younger sediments, Camp Creek and Roberts Creek, had relatively greater OM, total N, Fe_{ox}, and Al_{ox} than the Gunder and till sediments. The range of TP, P_{M3}, and P_{ox} was 473 to 588, 5 to 41, and 106 to 193 mg kg^{-1}, respectively. In all of these ranges, the lowest and highest values were in the till and Roberts Creek sediments, respectively.

Table 14. Selected sediment properties, where OM = organic matter, N= total N, TP = total P, $Fe_{ox}/Al_{ox}/Mn_{ox}/P_{ox}$ = ammonium oxalate extractable Fe/Al/Mn/P, Fe_{CBD} = citrate bicarbonate dithionite extractable Fe, $Ca_{M3}/Mg_{M3}/K_{M3}/Na_{M3}/P_{M3}$ = Mehlich-3 extractable Ca/Mg/K/Na/P.

Sediment properties	Camp Creek	Roberts Creek	Gunder	Till
pH (H_2O, 1:1)	6.2	6.3	7.4	8.1
Sand (%)	11	13	6	49
Silt (%)	64	60	72	30
Clay (%)	25	27	22	21
OM (%)	3.38	4.51	1.51	1.71
Total N (%)	0.14	0.14	0.06	0.03
Fe_{CBD} (mg kg^{-1})	6,825	5,862	3,813	10,124
Fe_{ox} (mg kg^{-1})	3,348	3,947	1,967	743
Al_{ox} (mg kg^{-1})	1,002	1,076	445	235
Mn_{ox} (mg kg^{-1})	702	1,263	154	166
P_{ox} (mg kg^{-1})	158	193	137	106
Ca_{M3} (cmol (+) kg^{-1})	9.88	14.92	10.68	33.75
Mg_{M3} (cmol (+) kg^{-1})	3.86	4.65	4.22	2.40
K_{M3} (cmol (+) kg^{-1})	0.26	0.37	0.30	0.26
Na_{M3} (cmol (+) kg^{-1})	0.30	0.39	0.24	0.25
P_{M3} (mg kg^{-1})	29	41	28	5
TP (mg kg^{-1})	491	588	484	473

Isotherm adsorption experiment

Redox potential (Eh) and pH at equilibrium

Figure 18 shows that anaerobic incubation significantly lowered redox potential at equilibrium, and the redox potential even lower when glucose was dissolved in the base solution prior to anaerobic incubation. Across the four sediment samples, the mean Eh values under AN (anaerobic incubation) and ANG (anaerobic incubation + glucose) treatments ranged from 339 to 360 mV and -17 to 19 mV, respectively. Three points should

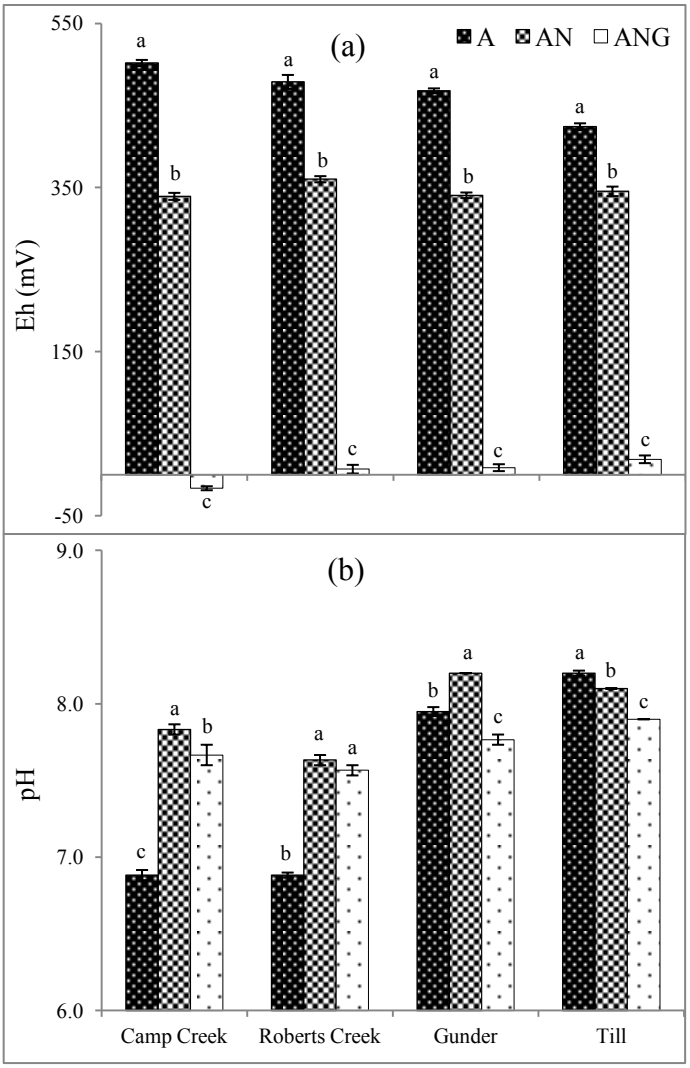

Figure 18. Effects of the treatments (A= without anaerobic incubation, AN=with anaerobic incubation, and ANG=with anaerobic incubation + glucose) on Eh (a) and pH (b) at equilibrium. Means with different letters within the same sediment are significantly different according to least significant different (LSD) test at $\alpha = 0.05$.

be considered regarding these Eh values. First, the Eh values under anaerobic incubation without addition of glucose were fairly close to 300 mV, a commonly recognized boundary between oxic and anoxic condition (Denic *et al.*, 2014). Second, the mean Eh values in the ANG treatment were significantly lower than those of the AN treatment, indicating the effect of a readily bioavailable carbon source, glucose, in promoting a more anaerobic environment. Third, the Eh values we report were measured about 2 cm above the settled sediment. The

Eh values might have been different if the electrode has been closer to the settled sediment or inserted into the settled sediment. For example, Hill and Robinson (2012) showed a sharp decrease in Eh at the sediment-water interface compared to that of an overlying water column.

The decrease of redox potential under the anaerobic incubation of this study was likely the result of three processes. First, during the early stage of anaerobic incubation, oxygen was depleted as aerobic microorganisms in the soil utilized available oxygen as an electron acceptor. Second, in the absence of oxygen, anaerobic microorganisms became more competitive due to their ability to use nitrate, Mn^{4+}, and Fe^{3+} as electron acceptors (Schlesinger and Bernhardt, 2013), further decreasing the redox potential. Finally, oxygen depletion was probably accelerated when nitrogen was periodically introduced to the reaction vessel. The first and second mechanisms were likely exaggerated by the abundance of glucose as an energy source and electron donor in the ANG treatment, resulting dramatic drop in the redox potential.

The four sediments exhibited different responses to the anaerobic incubation treatments with respect to the equilibrium pH (Fig. 18). For the Camp Creek, Roberts Creek, and Gunder sediments, the pH values were significantly higher after anaerobic incubation than without anaerobic incubation. On the other hand, pH of the AN treatment of the till was slightly lower than the pH of the till without anaerobic incubation. For the Camp Creek, Gunder, and till sediments, addition of glucose to the anaerobic incubation resulted in significantly lower pH than in the AN treatment with no glucose. In the Roberts Creek sediment, the addition of glucose did not change pH of the anaerobic treatments significantly. Protons are consumed in reduction processes (e.g. Essington, 2004) raising the pH of non-

alkaline soils. However, alkaline soils are usually buffered sufficiently to prevent dramatic changes in pH as reduction proceeds (Ponnamperuma, 1972).

PBC and EPC

Means of PBC and EPC values are summarized in Table 15, while plots of liquid phase P (C) against solid-phase P (Q) at equilibrium for all treatments are presented in Fig. 19. In comparison to treatment A (without anaerobic incubation), treatment AN (anaerobic incubation) significantly increased PBC values of the Camp Creek and Gunder sediments, while in the Roberts Creek deposit the increase was not statistically significant. Unlike other sediments, PBC values for the till dropped significantly from 970 L kg^{-1} (without anaerobic incubation) to 173 L kg^{-1} (with anaerobic incubation). Only the Gunder sediment showed a significant increase in EPC when samples were equilibrated under anaerobic conditions. When glucose was added to the anaerobic incubation (treatment ANG), all sediments had similar response: the PBC values were significantly lower than those without anaerobic incubation. The lower PBC values in the ANG treatment coincided with significantly higher EPC values than those in other treatments.

An increase in EPC values due to anaerobic incubation had been reported in previous studies (Brand-Klibanski *et al.*, 2007; Nair *et al.*, 1999; Pant and Reddy, 2001; Reddy *et al.*, 1998). Moreover, Pant and Reddy (2001) showed that anaerobic incubation also resulted in a decrease in the adsorption maximum capacity. In the present study, the increase in EPC and decrease in PBC was exhibited by all four sediments when treated with anaerobic incubation + glucose. It is likely that the deeply anoxic environment created with an abundant energy

Table 15. Effects of varying redox potential on phosphorus buffering capacity (PBC, in L kg^{-1}) and equilibrium phosphorus concentration (EPC, in mg L^{-1}). Treatment A is without anaerobic incubation, AN is with anaerobic incubation, ANG is with anaerobic incubation and addition of glucose.

Treatments	Camp Creek		Roberts Creek		Gunder		Till	
	PBC	EPC	PBC	EPC	PBC	EPC	PBC	EPC
A	188 b	0.036 b	326 a	0.030 b	132 b	0.029 c	970 a	0.011 b
AN	387 a	0.063 b	522 a	0.047 b	179 a	0.085 b	173 b	0.011 b
ANG	35 c	0.835 a	45 b	0.993 a	16 c	1.313 a	200 b	0.018 a

Note: means with the same letter within the same column are not significantly different according to least significant difference test at α=0.05

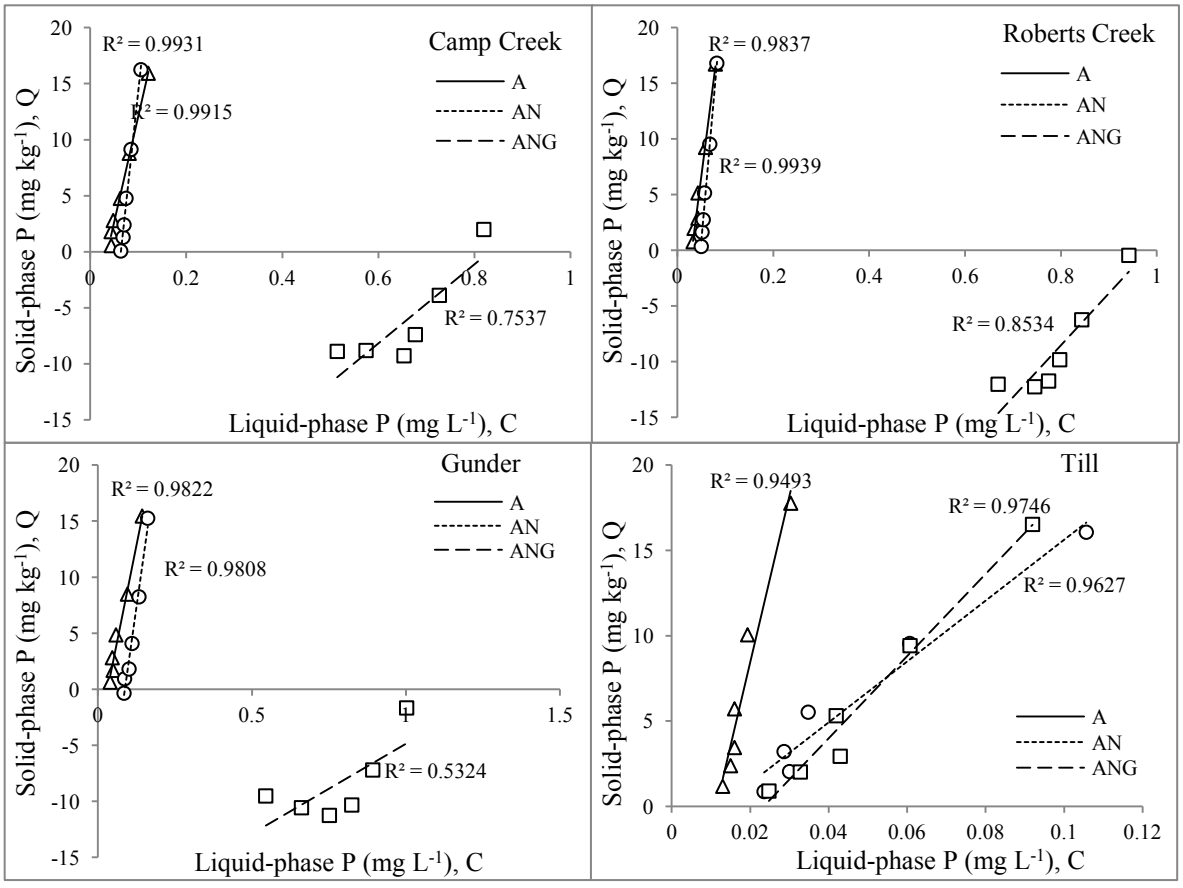

Figure 19. Simple linear regression in the isotherm adsorption experiment under different treatments (A= without anaerobic incubation (Δ symbol), AN=with anaerobic incubation (o symbol), and ANG=with anaerobic incubation + glucose (□ symbol)). Each of C and Q value plotted in the graph was the average of three replicates.

source was favorable to promote reduction of Fe^{3+} to Fe^{2+} and dissolution of Fe oxides, resulting in fewer sorption sites and the release of Fe-bound P. This was in line with significant drop of PBC values, which reflected a decrease in the capability of the solid phase to buffer increasing levels of P in the liquid phase.

As noted earlier, anaerobic incubation (without addition of glucose) led to higher PBC values than when no anaerobic incubation was applied, especially for the Camp Creek and Gunder sediments. This result may be comparable to the those of Reddy *et al.* (1998) and Nair *et al.* (1999), who demonstrated that the maximum P adsorption capacity increased with anaerobic incubation. Brand-Klibanski *et al.* (2007) suggested that the higher adsorption capacity of reduced soil could be linked to precipitation of mineral P particularly at higher P concentrations. In the present study, precipitation of mineral P under anaerobic conditions may have contributed to buffering the elevated level of liquid phase-P, especially at higher spiked P levels, reflected by higher PBC values. Nevertheless, different process must have occurred in the till where PBC significantly decreased with anaerobic incubation even without addition of glucose. As seen in Table 14, the till contained less ammonium oxalate-extractable Fe and Al but higher Mehlich-3 extractable Ca than other sediments. The relatively high PBC values in the till under treatment A (without anaerobic incubation) may result from P sorption by Fe/Al oxide as well as from precipitation of Ca-P minerals, considering higher redox potential and pH 8.2 at equilibrium state under this treatment. When subjected to reductive incubation, there was likely a decrease both in precipitation of Ca-P minerals and P sorption by Fe/Al oxide that was reflected by lower PBC values.

P release experiment

Redox potential (Eh)

Figure 20 shows the changes of redox potential (Eh), pH, dissolved organic carbon (DOC), and dissolved P in the solution for each sediment type on days 3, 6, 12, and 24. The differences in these parameter values between the air and nitrogen purge treatments are summarized in Table 16. In all sediment types, the nitrogen purge resulted in significantly lower Eh (± 300 mV) compared to the air purge (± 500 mV) during days 3 to 24. As noted earlier, an Eh of 300 mV can be considered as the boundary between oxic and anoxic conditions (Denic *et al.*, 2014). On that basis, we assumed that an anoxic condition had developed in the reactors purged with N_2. On the other hand, oxic conditions were likely maintained in the reactors that were continuously purged with air.

We note that there was a slight decrease of Eh on day 6 in all sediments both under nitrogen and air purging. The decrease may be related to a minor fluctuation of temperature that occurred on day 6. The temperature in the solution on day 6 was 23°C, a slight increase above the average of temperature of 22°C on days 3, 12, and 24. Since dissolved oxygen is in general negatively correlated with temperature (Helton *et al.*, 2012), we speculate that there was a decrease in dissolved oxygen in the reactors that day which in turn led to slightly lower Eh values.

pH

In contrast to Eh, nitrogen purging consistently resulted in significantly higher pH values than air purging throughout the incubation period. This finding was in line with a previous study in a controlled experiment by Wang *et al.* (2008) who found that water

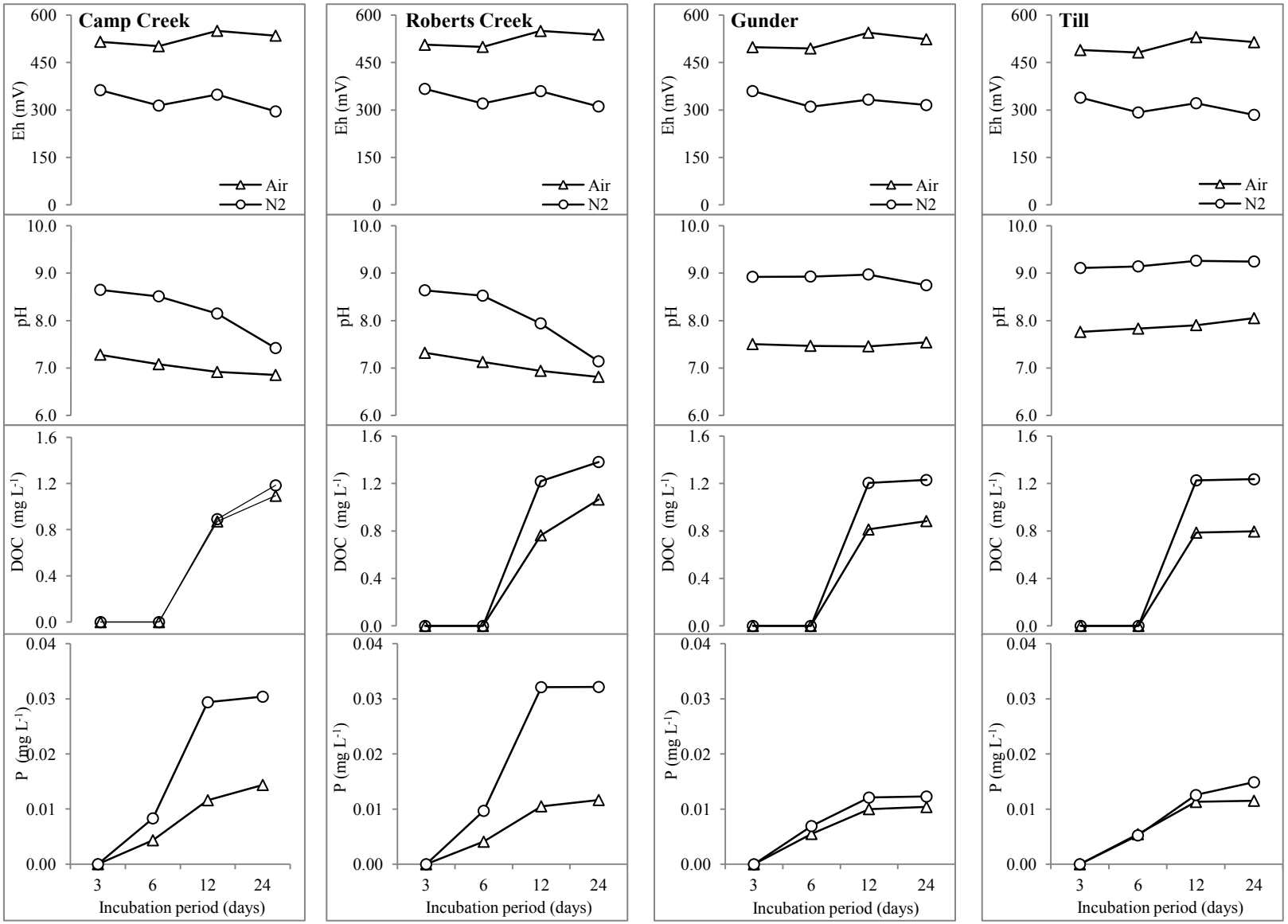

Figure 20. Dissolved P, dissolved organic carbon (DOC), pH, and redox potential (Eh) under oxic (air purging, -Δ-) and anoxic (N_2 purging, -o-) environment in the solution for each sediment during the 24 days of incubation.

Table 16. Differences between oxic conditions (with air purging) and anoxic conditions (with nitrogen purging) in redox potential (Eh), pH, dissolved organic carbon (DOC), and dissolved P in the solution for each sediment during 24 days of incubation. DOC and P concentrations are in mg L^{-1}, and Eh is in mV.

Parameters/ sediment types	Day 3		Day 6		Day 12		Day 24	
	Diff. †	*p*§	Diff. †	*p*§	Diff. †	*p*§	Diff. †	*p*§
Redox potential (Eh)								
Camp Creek	152.8	<0.0001	187.7	<0.0001	201.7	<0.0001	239.5	<0.0001
Roberts Creek	139.5	<0.0001	178.9	<0.0001	190.1	<0.0001	226.9	<0.0001
Gunder	138.9	<0.0001	183.9	<0.0001	211.4	<0.0001	208.1	<0.0001
Till	150.7	<0.0001	189.6	<0.0001	208.9	<0.0001	229.7	<0.0001
pH								
Camp Creek	-1.37	<0.0001	-1.43	<0.0001	-1.23	<0.0001	-0.57	<0.0001
Roberts Creek	-1.32	<0.0001	-1.40	<0.0001	-1.00	<0.0001	-0.33	0.0009
Gunder	-1.42	<0.0001	-1.46	<0.0001	-1.51	<0.0001	-1.20	<0.0001
Till	-1.35	<0.0001	-1.31	<0.0001	-1.36	<0.0001	-1.19	<0.0001
Dissolved organic carbon (DOC)								
Camp Creek	*n.a*	*n.a*	*n.a*	*n.a*	0.03	0.63	- 0.07	0.53
Roberts Creek	*n.a*	*n.a*	*n.a*	*n.a*	- 0.43	0.0002	- 0.33	0.01
Gunder	*n.a*	*n.a*	*n.a*	*n.a*	- 0.43	0.0002	- 0.33	0.01
Till	*n.a*	*n.a*	*n.a*	*n.a*	- 0.43	0.0002	- 0.47	<0.002
Dissolved P								
Camp Creek	*n.a*	*n.a*	-0.004	0.05	-0.018	<0.0001	-0.016	<0.0001
Roberts Creek	*n.a*	*n.a*	-0.005	<0.02	-0.022	<0.0001	-0.021	<0.0001
Gunder	*n.a*	*n.a*	-0.001	0.47	-0.002	0.06	-0.002	0.39
Till	*n.a*	*n.a*	0.000	0.85	-0.001	0.18	-0.004	0.13

Note † = difference of least squares means at α=0.05 (air purging – N_2 purging treatments), §=p- value, n.a = not available, values were not detected.

overlying sediment under anoxic conditions had higher pH values than that under oxic conditions. Interestingly, there was a different pattern of pH changes under oxic and anoxic environment among the sediment types. The pH under oxic conditions remained stable at ~7.5 in the Gunder reactors and ~7.9 in the till systems, and both increased to ~9.0 under

anoxic conditions. In the Camp Creek and Roberts Creek systems, the pH under oxic condition slightly decreased, from 7.3 on day 3 to 6.9 on day 24. Under anoxic conditions, the pH values were both ~8.6 on day 3, and then on day 24 the pH notably decreased to 7.4 and 7.1 in the Camp Creek and Roberts Creek systems, respectively.

Some variation in the pH of the solutions might be attributed directly to the gas purges. The industrial grade N_2 gas used in this study contained about 99.998% N, while the air presumably contained ~0.035% CO_2. Dissolution of CO_2 in the water of the systems purged with air probably increased the concentration of carbonic acid and led to a decrease in pH. Moreover, in initially non-alkaline aqueous systems, pH tends to increase as a result of reduction reactions, as noted earlier in the discussion of the adsorption experiment. Sediment properties are likely to have played an important role in regulating the pH in the solution. For example, the pattern of pH changes under anoxic condition differed in the Camp Creek and Roberts Creek systems *vs.* the Gunder and till systems, especially on days 12 and 24. The Gunder and till sediments were more alkaline than the Camp Creek and Roberts Creek sediments (the till was calcareous), leading to a higher pH buffering capacity.

Dissolved Organic Carbon (DOC)

In all the systems, DOC was detected starting on day 12. Except for the Camp Creek systems, anoxic conditions resulted in significantly higher DOC concentrations than did oxic conditions. However, even the highest mean DOC concentration in this study (1.4 mg L^{-1} for Camp Creek purged with nitrogen) was about four times lower than the average DOC concentration of 6 mg L^{-1} reported by Schilling and Jacobson (2014) in groundwater at a riparian well transect across Walnut Creek. Furthermore, DOC concentrations tended to

continue increasing on day 24 for the Camp Creek and Roberts Creek systems, while they tended to stabilize for the till and Gunder systems. This observation may be linked to the level of organic matter in the sediment. Camp Creek and Roberts Creek sediments had organic matter contents of 3.38% and 4.51%, respectively; the values were higher than those in the Gunder (1.51%) and the till (1.71%) sediments. With higher organic matter content, over a longer period of incubation there was a possibility that Camp Creek and Roberts Creek systems might exhibit even higher DOC concentrations as SOM was dissolved and microbial activity proceeded. However, further experimentation is still needed to test this hypothesis.

Dissolved P

There are four observations related to dissolved P concentration along the incubation period that can be noted in Fig. 20 and Table 16. First, dissolved P was detected in all the systems starting on day 6. The release of P in this study was relatively slow compared to other previous lab experiments employing sediment and water column. For example, P release was recorded in the first day of the experiment conducted by Lai and Lam (2008) as well as by Kim *et al.* (2003), and even during the first 10 minutes in a study by Li *et al.* (2013). Different sediment types as well as different methods employed in the experiment (e.g., solid-to-solution ratio, flow velocity, aerobic/anaerobic treatments) are likely to be the reasons for slower release of P in this study compared to other studies. In addition, the use of dialysis tubing in this study separated the sediment and the water, while in the study by Lai and Lam (2008), Kim *et al.* (2003) and Li *et al.* (2013) there was a direct contact in the interface between sediment and column water.

Secondly, dissolved P concentrations released from all the sediments both under oxic and anoxic condition increased from day 3 to day 12, then they tended to be stable from day 12 to day 24. Li *et al.* (2013) suggested that constant P concentrations in the water after a period of incubation indicated that an equilibrium state had been achieved. A similar mechanism is likely in the present study, where dissolved P concentrations remained stable starting on day 12. The stable dissolved P concentration varied among sediments and between the oxic and anoxic treatments, indicating that equilibrium P concentrations depend on factors that affect P sorption and desorption, e.g., EPC, PBC, and the physicochemical properties of the sediment and water.

Third, the highest dissolved P concentrations (~0.030 mg P L^{-1}) were found on days 12 and 24 under anoxic conditions in the Camp Creek and Roberts Creek systems. These values were two to three times the dissolved P concentrations under oxic conditions in all sediments as well as under anoxic conditions for the Gunder and till sediments. The dissolved P values in this study were comparable to those in a laboratory experiment reported by Jiang *et al.* (2008), but they were much lower than the dissolved P concentrations of 0.1 to 1.3 mg L^{-1} in groundwater sampled in a riparian well transect across Walnut Creek as reported by Schilling and Jacobson (2008a).

Last, after day 6, significant differences (at the p=0.05 level of significance) in dissolved P under oxic and anoxic condition were only found in the Roberts Creek and Camp Creek sediment systems. The negative value of the mean differences in Table 16 indicates that dissolved P under anoxic condition was higher than that under oxic condition, which is in line with other previous studies by Lai and Lam (2008), Kim *et al.* (2003) and Li *et al.* (2013). Besides the impact of decreasing Eh on the stability of P-binding Fe, Al, and Mn

oxides, higher pH under anoxic conditions might have contributed to the higher dissolved P concentrations. As suggested by Jin *et al.* (2006), higher pH values would increase the negative surface charge of Fe, Mn, and Al oxides, promoting the release of P from association with those solids phases. The potential for DOC to promote dissolution of P by anion exchange was unclear in this study. Under anoxic conditions, significantly higher DOC coincided with higher dissolved P in the Roberts Creek systems, but not in the Camp Creek systems. Perhaps there was a difference in the type of soluble organic compounds released by the two sediments, but this hypothesis needs to be tested in further experimental work.

Conclusions

The P sorption characteristics, represented by equilibrium phosphorus concentration (EPC) and phosphorus buffering capacity (PBC), varied among the Walnut Creek bank sediments (Camp Creek, Roberts Creek, Gunder, and Pre-Illinoian Till) that were collected from sites in this study. There was a significant increase in EPC when all sediment samples were subjected to decreasing redox potential (Eh), especially when an energy source for microbial activity was present. Phosphorus desorption from the samples was favored under low Eh. Oxic and anoxic conditions governed the Eh, pH, dissolved organic carbon, and release of P to the aqueous phase from some but all of the sediments. More dissolved P was released from the Camp Creek and Roberts Creek samples under anoxic conditions than from the other samples, suggesting that these sediments may function as internal P sources to the overlying water column in anoxic settings.

CHAPTER 6

PHOSPHORUS TRANSFORMATIONS IN WALNUT CREEK BANK SEDIMENTS AT VARYING REDOX POTENTIAL

Introduction

Phosphorus in stream water has become one of the central issues in the effort to prevent eutrophication and maintain the balance of organisms in the aquatic ecosystems. Industry, pasture, farming, and urban living are examples of human activities considered to be sources of P in the stream water (Alexander *et al.*, 2008; Arias *et al.*, 2013). One pathway for P to enter stream water is through streambank erosion (Palmer *et al.*, 2014; Zaimes *et al.*, 2008). In Iowa, streambank erosion is considered to be one of the main sources of suspended sediments in stream water (Schilling and Wolter, 2000). In Walnut Creek, Iowa, Palmer *et al.* (2014) reported that on average ~5,300 Mg of eroded sediment enter the stream water every year.

Along the creek, both streambanks and eroded sediments may be subjected to varying redox potentials. Flowing stream water in contact with the atmosphere is likely to be aerobic. Conversely, natural dams such as debris dams or beaver dams may block the flow of water, creating stagnant pools where eroded organic and inorganic materials may accumulate, creating anaerobic environments (Briggs *et al*., 2013). In addition, sediments could be subjected to low redox potential in the hyporheic zone where anaerobic groundwater discharges to stream water (Bianchin *et al.*, 2011). As suggested by Pettersson (1998), redox potential is one factor that controls variations in the release of sedimentary P to the overlying water column. Since solid-phase forms of P occur in specific organic and

inorganic P fractions (Hedley *et al.*, 1982; Tiessen and Moir, 2008; Zhang and Kovar, 2009), variations in redox potential might govern the redistribution of these fractions, which in turn would lead to changes in P concentrations in stream water.

Previous studies have revealed that changes in soil P fractions can be induced by land management. Long-term fertilizer application (Varinderpal-Singh *et al.*, 2007), application of biosolids (Sui *et al*., 1999a), and reforestation of farmlands (Schrijver *et al.*, 2012) are examples of cultivation practices that changed P fractions. Laboratory incubations have also been used to investigate P dynamics. Redistribution of P among its fractions in incubation studies have mostly been related to microbial activities triggered by the addition of energy sources to a soil system. For example, in a 9-month laboratory incubation of a soil treated with cellulose + N addition, Hedley *et al.* (1982) reported that labile *Pi* decreased due to immobilization. However, less attention has been addressed to changes among P fractions in streambank sediments at varying redox potential and their potential impacts on P in stream water. This present study was to investigate transformation of P fractions in Walnut Creek bank sediments at varying redox potential in a laboratory experiment.

Materials and Methods

Sediment sampling and characterization

Sediment samples were collected from alluvial banks of Walnut Creek in Jasper County, Iowa. The coordinates of the sampling site are 41° 33.382' N and 93° 15.887' W. Four sediment types were collected to represent four major stratigraphic units in Walnut Creek stream corridor (Schilling *et al.*, 2004). The first three alluvial units are the Camp Creek, Roberts Creek, and Gunder members of the De Forest Formation (Schilling *et al.*,

2006b). The De Forest Formation formed during the Holocene period over the last 11,000 years and occurs throughout Iowa. Baker *et al.* (1996) described in detail that the Gunder Member, the Roberts Creek Member, and the Camp Creek Member date from 11,000 to 4,000 yr BP, 4000 to 400 yr BP, and the last 380 yr, respectively. The fourth unit in Walnut Creek is Pre-Illinoian Till, a glacial deposit that dates to 2,000,000 to 500,000 yr BP.

Immediately after transport to laboratory, samples were air dried and sieved to pass a 2-mm screen for sediment characterization and P fractionation analysis. Total nitrogen was determined using high-temperature dry combustion (Nelson and Sommers, 1996). Total organic matter was determined using the loss-on-ignition method (Konen *et al.*, 2002). Particle size distribution was determined gravimetrically (Kettler *et al.*, 2001), while pH was determined at a soil to water ratio of 1:1. The perchloric acid digestion method (Kuo, 1996) was used to determine total P, and concentrations were determined in the digest by using the molybdate blue-ascorbic method (Watanabe and Olsen, 1965). Mehlich-3 solution (Mehlich, 1984) was used to extract exchangeable cations (Ca, Mg, K, Na), and the concentrations were determined using inductively coupled plasma-atomic emission spectrometry (ICP-AES). The Mehlich-3 solution was also used to extract P, and the P concentrations were determined using the molybdate blue-ascorbic method (Watanabe and Olsen, 1965). Citrate-bicarbonate-dithionite extractable Fe was determined by atomic absorption spectroscopy (Shang and Zelasny, 2008). Ammonium oxalate extractable Fe, Al, and Mn were determined by ICP-AES, and P in this extraction was determined using malachite green method (D'Angelo *et al.*, 2001).

Experimental setting

The experiment was set up for each sediment type in a completely randomized design using three treatments: without anaerobic incubation (A), anaerobic incubation (AN), and anaerobic incubation with addition of glucose (ANG). Each treatment was replicated three times. The incubation treatments were applied to each of the sediment samples before the fractionation analysis. In the AN treatment, 30 mL of deionized water were added to a 50-mL centrifuge tube containing 0.5 g air-dried sediment. The cap in the centrifuge tube was lined with a rubber septum to allow for purging by nitrogen (N_2). N_2 purging was conducted in the beginning of the incubation and repeated weekly. To minimize air infiltration, silicone glue was rubbed onto the surface of rubber septum and the bottom part of the cap after N_2 purging. The samples were incubated for 30 days in a chamber saturated with N_2. A similar anaerobic incubation process was applied for the ANG treatment, except that glucose ($C_6H_{12}O_6$, from Sigma) was dissolved in the water at a concentration of 0.083 g L^{-1}. Treatment A used similar amount of air dried sediment and deionized water, however the sediments were not incubated under an anaerobic environment and glucose was not dissolved in the water.

Sediment P fractionation

Methods of soil P fractionation in this study were generally based on sequential extraction by Tiessen and Moir (2008). The sequential extraction started with extraction with water and ended with concentrated H_2SO_4 (Fig. 21). Following this scheme, soil P fractions were classified into water extractable P (P_{H_2O}), labile P (P_{Lab}), slowly cycling P (P_{Slow}), stable P (P_{Stab}), and residue P (P_{Res}) (Schrijver *et al.*, 2012). The P_{H_2O} is the most labile P fraction

and can be released from the solid phase with water extraction. P_{Lab} is soil P that is extractable with 0.5 *M* $NaHCO_3$. The P_{Slow} fraction is extractable with 0.1 *M* NaOH and 1 *M* HCl, and it is thought to be associated with Fe and Al oxides, Ca, and organic compounds that are not readily available for plant uptake. The P_{Stab} fraction is more tightly bound to mineral and organic compounds than is slowly cycling P; it consists of P that can be extracted with concentrated HCl. Lastly, the P_{Res} is assumed to represent highly recalcitrant compounds in the soil; it was extracted in the last step with concentrated H_2SO_4.

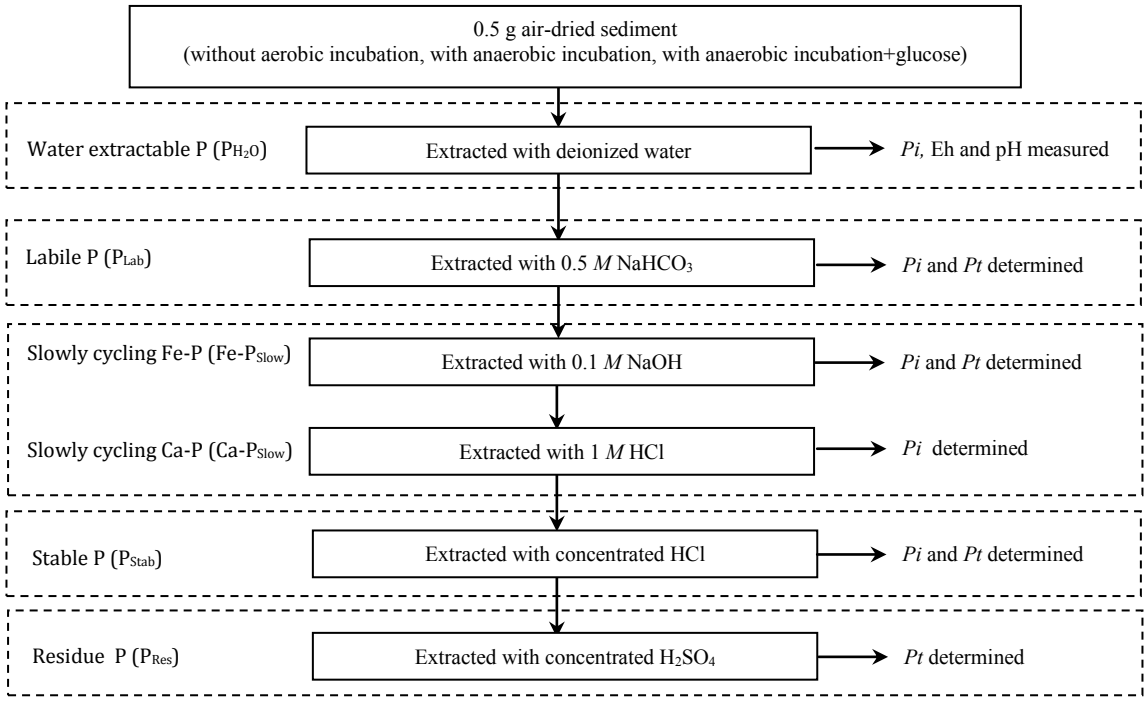

Figure 21. Sequential extraction for P fractionation analysis, adapted from Tiessen and Moir (2008).

It should be noted that a modification of the method of Tiessen and Moir (2008) was made in this study. The P_{H_2O} fraction was not determined using a resin strip, but it was measured directly from the filtrate after measuring Eh and pH. At the beginning of the

sequential extraction, all samples from all treatments were shaken in a reciprocal shaker at 200 excursions per minute for 16 hours. After the sediments settled, the Eh and pH of the solution were measured. For the AN and ANG treatments, the Eh and pH were measured in the N_2-filled glove box where the samples were equilibrated. Subsequently, the samples were centrifuged at 4,300 x *g* for 15 minutes and followed by filtering the solution through a 0.45-μm membrane filter. The filtrate was collected for determination of P_{H_2O}, and the sediments were prepared for the next step in the sequential extraction.

Similar shaking and centrifugation steps were conducted for the sequential extractions with 0.5 *M* $NaHCO_3$, 0.1 *M* NaOH, and 1 *M* HCl. In the last steps, extraction with concentrated HCl and concentrated H_2SO_4 were carried out in a water bath at 80°C and a digestion block at 360°C, respectively. Total P (*Pt*) in 0.5 *M* $NaHCO_3$, 0.1 *M* NaOH, and concentrated HCl were determined by digesting with ammonium persulfate in an autoclave at 121°C. Concentration of total P (*Pt*) and inorganic P (*Pi*) were determined using the molybdate blue-ascorbic acid method (Watanabe and Olsen, 1965), and organic P was calculated by subtracting *Pi* from *Pt*.

Results and Discussion

Sediment characteristics

Selected chemical and physical properties of the sediments were summarized in Table 17. Silt was dominant in the Camp Creek, Roberts Creek and Gunder deposits, while sand was dominant in the till. Clay content was somewhat similar in all sediment types. The till was characterized by the highest pH, Mehlich-3 extractable Ca, and citrate-bicarbonate-dithionite extractable Fe compared to the other sediments; it was also calcareous. The

highest values of total phosphorus, ammonium oxalate extractable P, and Mehlich-3 extractable P occurred in the Roberts Creek deposits. By contrast the lowest values for those characteristics were in the till. Moreover, the younger Camp Creek and Roberts Creek deposits had relatively greater organic matter contents, total N, and ammonium oxalate-extractable Al, Fe, and Mn than the older Gunder and the till deposits.

Table 17. Selected sediment characteristics.

Characteristics	Camp Creek	Robert Creeks	Gunder	Till
Particle size distribution				
Sand (%)	11	13	6	49
Silt (%)	64	60	72	30
Clay (%)	25	27	22	21
pH (H_2O, 1:1)	6.2	6.3	7.4	8.1
Organic matter content (%)	3.38	4.51	1.51	1.71
N total (%)	0.14	0.14	0.06	0.03
Total P (mg kg^{-1})	491	588	484	473
CBD extractable Fe (mg kg^{-1})	6,825	5,862	3,813	10,124
Ammonium oxalate extractable				
Fe (mg kg^{-1})	3,348	3,947	1,967	743
Al (mg kg^{-1})	1,002	1076	445	235
Mn (mg kg^{-1})	702	1263	154	166
P (mg kg^{-1})	158	193	137	106
Mehlich-3 extractable				
P (mg kg^{-1})	29	41	28	5
Ca (mg kg^{-1})	1,975	2,983	2,135	6,750
Mg (mg kg^{-1})	463	558	506	288
K (mg kg^{-1})	100	145	117	103
Na (mg kg^{-1})	70	89	55	57

Eh and pH

Figure 22 shows that in all sediment types, redox potential significantly decreased when sediments were incubated anaerobically (AN), and it was even lower when glucose was added to the anaerobic incubation (ANG). However, the magnitude of the decrease was not similar for each of sediment type. The Eh declined less in the older and more alkaline Gunder and till sediments than in the Camp Creek and the Roberts Creek sediments. In contrast to Eh, except for the till, there was significant increase in solution pH under the AN treatment and an even greater increase under the ANG treatment. In the till, pH remained stable at 7.2 either with or without anaerobic incubation. Then it significantly increased to 7.5 when glucose was added in the anaerobic incubation.

The decrease of redox potential due to anaerobic treatment (AN) in this study was associated with depletion of oxygen in an environment that was saturated with nitrogen. In the absence of oxygen, anaerobic microorganisms may become more dominant due to their ability to use nitrate, oxidized manganese, ferric iron, sulfate, organic compounds, or carbon dioxide as electron acceptors (Schlesinger and Bernhardt, 2013) under decreasing redox potential. This mechanism was likely exaggerated by the abundant energy sources from glucose as an electron donor in the treatment ANG, resulting in a dramatic drop of redox potential. With decreasing redox potential, protons are consumed in the reduction reaction (Essington, 2004), which may cause an increase in pH. The till, which was calcareous and more alkaline than the other sediment types, had a high pH buffering capacity, and therefore significant increase in pH was only found when glucose was added in the anaerobic incubation.

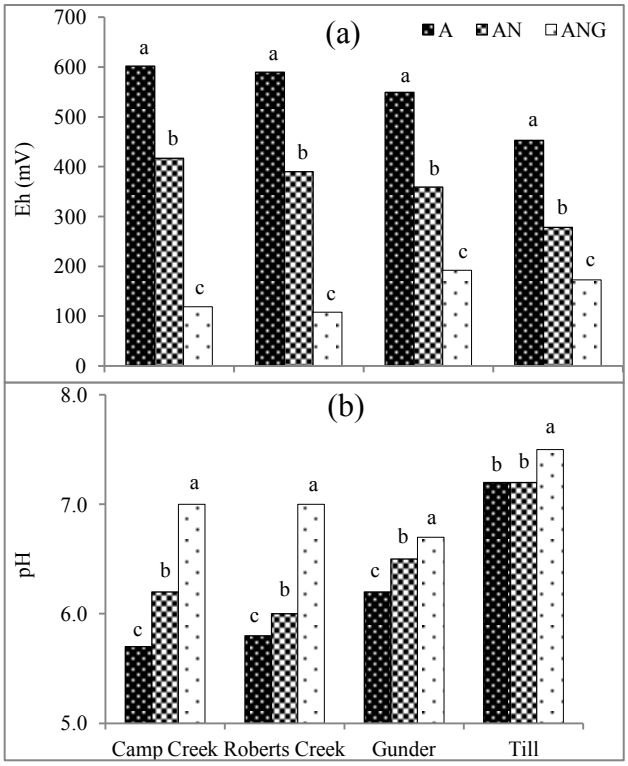

Figure 22. Effects of the treatments (A = without anaerobic incubation, AN = with anaerobic incubation, and ANG = with anaerobic incubation + glucose) on redox potential (Eh, (a)) and pH (1:60, (b)). Means with different letters in the same sediment type were significantly different according to the least significant difference (LSD) test at $\alpha = 0.05$.

Phosphorus fractions

Water extractable P (P_{H_2O})

The effects of the treatments on P_{H_2O} are presented in Fig. 23. In the Camp Creek sediment, there was no significant effect of varying redox potential on P_{H_2O}. In other words, changes in physicochemical properties triggered by the treatments were not sufficient to alter the equilibrium of P between solid and water for this type of sediment. By contrast, in the other sediment types P_{H_2O} significantly increased with anaerobic incubation (AN), but then it decreased when glucose was added to the anaerobic incubation (ANG). Especially in the low-OM Gunder and the till sediments, P_{H_2O} under ANG treatment was even significantly less

than in the A treatment (without anaerobic incubation). This result was comparable with a study by Du *et al.* (2011) who reported a depletion of P_{H_2O} after incubation of sediments treated with glucose for 72 hours.

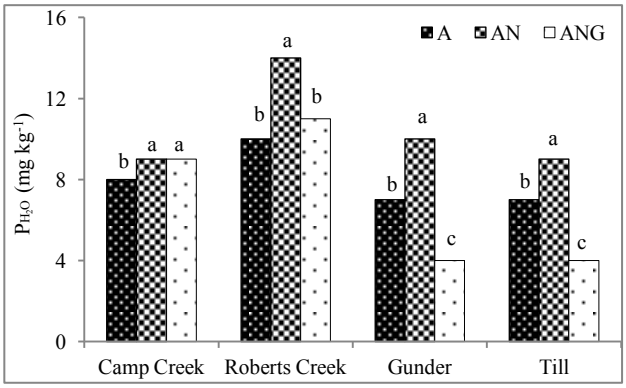

Figure 23. Effects of the treatments (A = without anaerobic incubation, AN = with anaerobic incubation, and ANG = with anaerobic incubation + glucose) on water extractable P (P_{H_2O}). Means with different letters in the same sediment type were significantly different according to least significant difference (LSD) test at $\alpha = 0.05$.

The release of P_{H_2O} from sediments as redox potential declines has been reported in previous studies (Kim *et al.*, 2003; Lai and Lam, 2008; Li *et al.*, 2013). Besides the decreasing Eh, increasing pH might promote the release of P from the oxide sorption sites (Jin *et al.*, 2006), which in turn contributed on the higher P_{H_2O} under AN treatment, especially in the Roberts Creek and Gunder sediments. However, a further increase in pH under the ANG treatment might have stimulated Ca-P precipitation, especially in the Roberts Creek, Gunder, and till sediments. Moreover, a further decrease in Eh with the abundant energy source of glucose might have nourished the growth of anaerobic microorganisms that immobilized some portion of P_{H_2O}. The precipitated Ca-P mineral and immobilized P might be counted as other P fractions or might have been lost during the filtration through the 0.45-

μm filter. Further study is needed to quantify precipitated and immobilized P that could be related to this process.

Labile P (P_{Lab})

Figure 24 shows organic and inorganic labile P (P_{Lab}) under the different treatments applied in this study. Except for the Gunder sediments, anaerobic incubation (AN) did not significantly change the concentration of inorganic P_{Lab}. However, a significant increase in inorganic P_{Lab} was found in all sediment types when glucose was added in the anaerobic incubation (ANG). A similar pattern was found for organic P_{Lab}, especially for the youngest and most organic matter-rich sediments, Camp Creek and Roberts Creek. Inorganic and organic P_{Lab} are held by weak chemical interactions at sorption sites and in organic compounds, however they were not extractable with water in the preceding extraction. When glucose was added to the anaerobic incubation (ANG), lowest Eh and highest pH values were the result, perhaps because more strongly bound P was transformed to weakly bound P, which was then extractable with 0.5 *M* $NaHCO_3$ and in turn increasing P_{Lab}.

As seen in Fig. 24, organic and inorganic P_{Lab} in the Camp Creek and the Roberts Creek sediments were higher than those in the Gunder and till sediments, indicating a greater potential of the Camp Creek and the Roberts Creek to contribute to inorganic P_{Lab} to the column water if the sediments are eroded to the Walnut Creek stream and subjected to decreasing redox potential. In contrast, organic P_{Lab} was not detected in the till and the Gunder sediments under all treatments. Relatively low organic matter contents in the Gunder (1.51%) and the till (1.71%) materials might generate a minimum amount of organic compounds extractable with 0.5 *M* $NaHCO_3$. In addition, Xu *et al.* (2013) suggested that the

decrease of organic P_{Lab} with increasing depth of sediments indicated a transformation of organic P_{Lab} fractions into nonlabile organic P pools during diagenesis. It is likely that a similar mechanism occurred in the Gunder and the till sediments which were older than the Camp Creek and the Roberts Creek sediments.

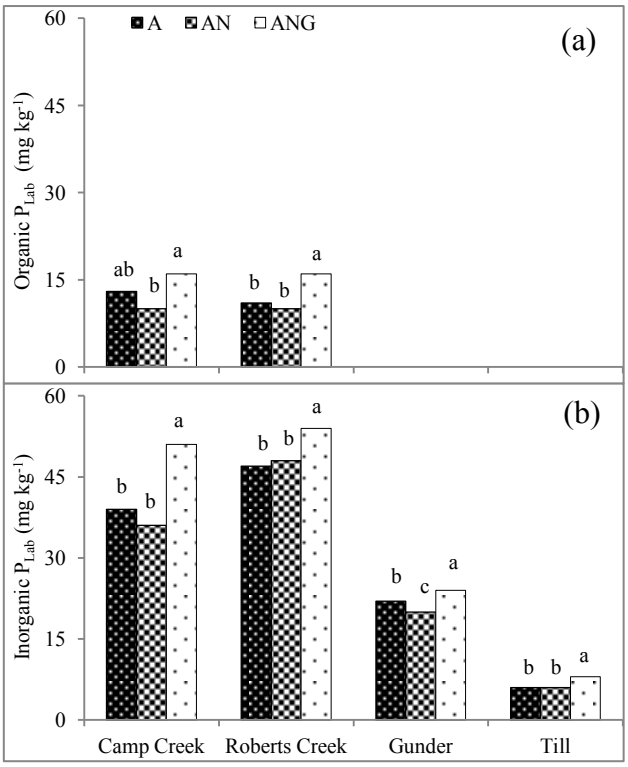

Figure 24. Effects of the treatments (A = without anaerobic incubation, AN = with anaerobic incubation, and ANG = with anaerobic incubation + glucose) on organic (a) and inorganic labile P (P_{Lab}, (b)). Means with different letters in the same sediment type were significantly different according to least significant difference (LSD) test at $\alpha = 0.05$.

Slowly cycling P (P_{Slow})

Figure 25 shows that except for the till, inorganic slowly cycling P that was associated with Fe (Fe-P_{slow}) significantly decreased when glucose was added in the anaerobic incubation (ANG treatment). In the Roberts Creek and the Gunder sediments, a significant decrease in Fe-P_{slow} also occurred in the AN treatment (anaerobic incubation

without glucose). As noted above, concentration of inorganic P_{Lab} increased at decreasing redox potential and increasing pH under the ANG treatment. Considering the decrease in Fe-P_{slow} under the same treatment, it could be speculated that some portion of Fe-P_{Slow} was transformed to inorganic P_{Lab}. This hypothesis is based on the study by Pettersson (1998), who suggested that P would be bound to Fe oxides more weakly under anaerobic conditions when Fe^{+3} has been reduced to Fe^{2+}.

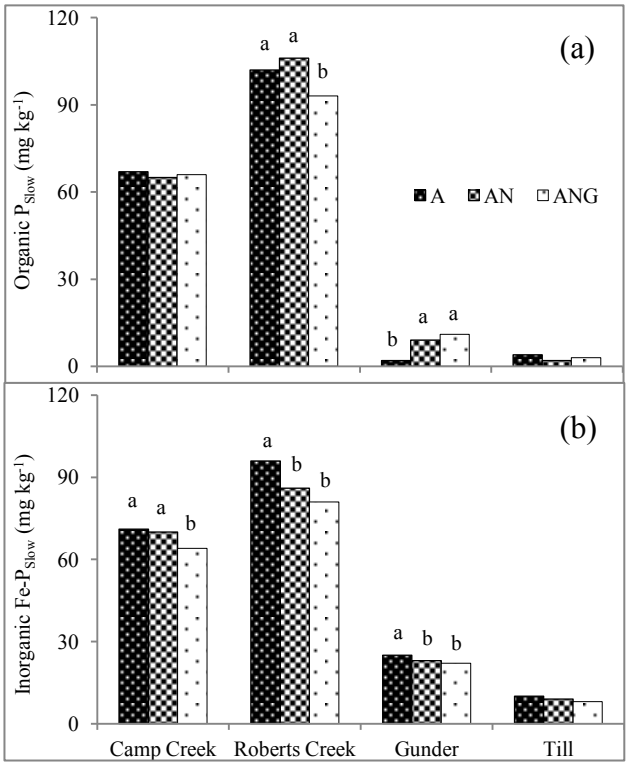

Figure 25. Effects of the treatments (A = without anaerobic incubation, AN = with anaerobic incubation, and ANG = with anaerobic incubation + glucose) on inorganic labile P associated with Fe (Fe-P_{Slow}, (a)) and organic P_{Slow} (b). Means with different letters in the same sediment type were significantly different according to least significant difference (LSD) test at $\alpha = 0.05$.

As seen in Fig. 25, there were no significant effects of varying redox potential on organic P_{Slow} in the Camp Creek and till sediments. However, a different response was

exhibited by the Roberts Creek and the Gunder deposits. Under anaerobic incubation with addition of glucose (ANG), the concentration of organic P_{Slow} significantly decreased in the Roberts Creek sediments but it significantly increased in the Gunder sediments. In Roberts Creek, the significant decrease in organic P_{Slow} could be linked to the significant increase in organic P_{Lab}, where some portions of the organic P_{Slow} fraction could have been transformed to the organic P_{Lab} under the ANG treatment. Nevertheless, factors associated with significant increase in organic P_{Slow} under decreasing redox potential in the Gunder sediments were unclear since there were no significant changes in other organic P fractions.

Figure 25 also shows that the Gunder and till sediments had less Fe-P_{Slow} and organic P_{Slow} than the Camp Creek and the Roberts Creek sediments. The concentration of Fe-P_{Slow} might be associated with the availability of adsorption sites on poorly crystalline Fe-oxides, as reflected by the ammonium oxalate-extractable Fe values (Kleinman and Sharpley, 2002; Rotterdam *et al*., 2012), as well as the pH of the sediment. The concentrations of Fe-P_{Slow} values and ammonium oxalate-extractable Fe values were ranked similarly: Roberts Creek > Camp Creek > Gunder> till. The lower Fe-P_{Slow} values in the Gunder and till sediments is likely due to fewer poorly crystalline, Fe-oxide adsorption sites on these two sediments. On the other hand, the higher ammonium oxalate-extractable Fe values and lower pH values of the Roberts Creek and Camp Creek sediments may have led to their higher Fe-P_{Slow} values.

For organic P_{Slow}, it should be pointed out that the extracting solution in this step (0.1 *M* NaOH) was alkaline and probably extracted a large portion of organic P associated with humic materials (Paing *et al.*, 1999). Consequently, it could be expected that higher organic matter contents would lead to higher organic P_{Slow} values. This hypothesis is consistent with

the similar rankings of organic P_{Slow} and organic matter in treatment A (without anaerobic incubation): Roberts Creek > Camp Creek > till > Gunder.

While Fe-P_{Slow} decreased under ANG treatment, variations in redox potential did not significantly affect the values of inorganic P_{Slow} associated with Ca (Ca-P_{Slow}) across all sediment types (Fig. 26). This indicated that physicochemical changes due to anaerobic incubation, with or without addition of glucose, were not sufficient to alter the concentration of Ca-P_{Slow}. While increasing pH associated with decreasing Eh might promote precipitation of Ca-P minerals or adsorption of P on the adsorption sites of Ca carbonates, thus potentially increasing Ca-P_{Slow}, there was no evidence of this process in the present study. Since inorganic Ca-P_{Slow} remained stable at varying redox potential, we infer that inorganic Ca-P_{Slow} is not likely to contribute to the more labile P fractions at decreasing redox potential.

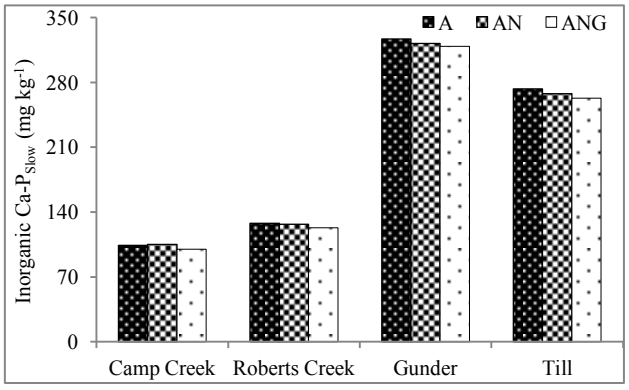

Figure 26. Effects of the treatments (A = without anaerobic incubation, AN = with anaerobic incubation, and ANG = with anaerobic incubation + glucose) on inorganic slowly cycling P associated with Ca (Ca-P_{Slow}). No significant differences among the means in the same sediment type were identified according to least significant difference (LSD) test at $\alpha = 0.05$.

Stable P (P_{Stab}) and Residue P (P_{Res})

Similar to inorganic Ca-P_{Slow}, there were no significant effects of varying redox potential on organic stable P (P_{Stab}), inorganic P_{Stab}, or residue P (P_{Res}), as seen in Fig. 27 and

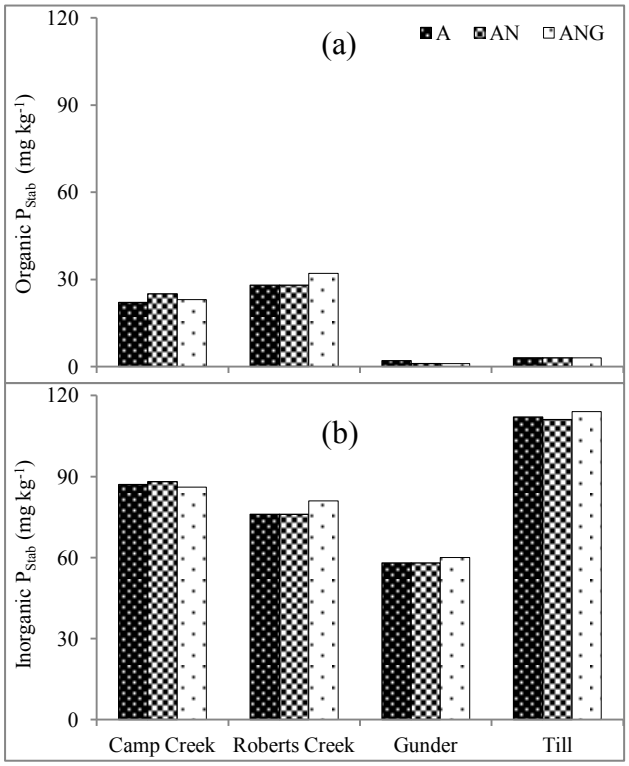

Figure 27. Effects of the treatments (A = without anaerobic incubation, AN = with anaerobic incubation, and ANG = with anaerobic incubation + glucose) on organic (a) and inorganic stable P (P_{Stab}, (b)). No significant differences among the means in the same sediment type were identified by least significant difference (LSD) test at $\alpha = 0.05$.

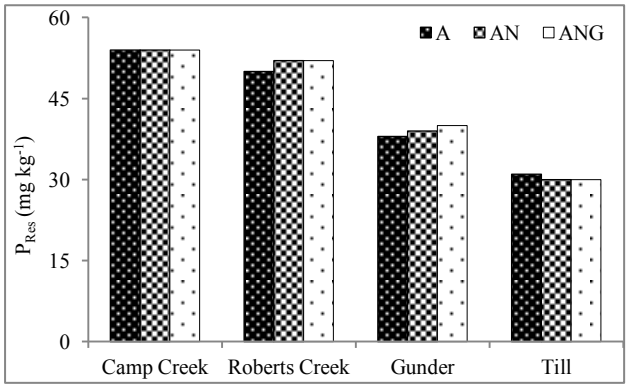

Figure 28. Effects of the treatments (A = without anaerobic incubation, AN = with anaerobic incubation, and ANG=with anaerobic incubation + glucose) on residue P (P_{Res}). No significant differences among the means in the same sediment type were identified by the least significant difference (LSD) test at $\alpha = 0.05$.

Fig. 28. In other words, concentrations of organic P_{Stab}, inorganic P_{Stab}, and P_{Res} in the sediments remained stable and were not affected by any physicochemical changes induced by the applied treatments.

Furthermore, organic P_{Stab} in the till and Gunder sediments ranged from 1-3 mg kg^{-1}, i.e., much lower than in the Camp Creek and Roberts Creek sediments which ranged from 22 to 32 mg kg^{-1}. The difference is likely to be related to the relatively low organic matter content of the Gunder (1.5%) and till (1.7%) sediments compared to the Camp Creek (3.4%) and Roberts Creek (4.5%) sediments. On the other hand, the inorganic P_{Stab} in the till was about 112 mg kg^{-1}, i.e., higher than that in the other sediment types, which ranged from 58 to 88 mg kg^{-1}. The predominant inorganic P_{Stab} in the till reflects the characteristics of this sediment: low organic matter, calcareous, and high CBD-extractable Fe (10,124 mg kg^{-1}). The P_{Res} values of the sediment types varied in a narrow range between 30 to 54 mg kg^{-1}, and it tended to decrease with increasing depth in the stratigraphy.

Sum of all individual P fractions (TP_{Sum})

As shown in Fig. 29, variations in redox potential did not significantly affect the sum of all individual P fractions (TP_{sum}) in the sediments. The result supported our previous hypothesis that an increase inorganic P_{Lab} under the ANG treatment was related to a decrease in Fe-P_{Slow}, such that TP_{sum} remained stable. We note that the TP_{sum} values were somewhat lower than the total P extracted with perchloric acid and nitric acid (TP). Several factors may be linked to this discrepancy. First, the sequential extraction may not accurately assess a specific P fraction because prior extractions in the sequence were incomplete (Wang *et al.*, 2010). Second, TP was determined in a single digestion step with perchloric acid and nitric

acid, so P was less likely to be lost during multiple steps of the sequential extraction. Third, organic P fractions might have been underestimated due to hydrolysis of organic P to inorganic P, especially with strong extractants (Blake *et al.*, 2003).

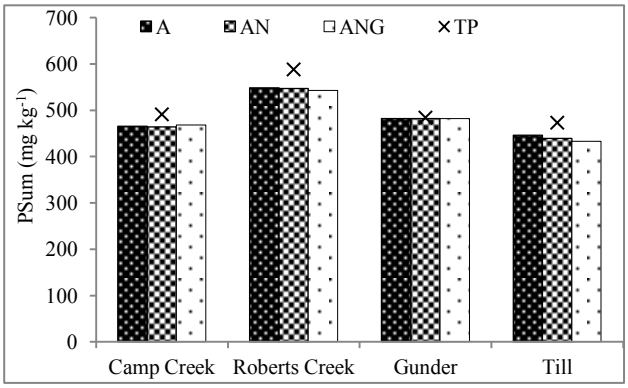

Figure 29. Effects of the treatments (A = without anaerobic incubation, AN = with anaerobic incubation, and ANG = with anaerobic incubation + glucose) on sum of all individual P fractions (TP_{sum}). No significant differences among the means in the same sediment type were identified by the least significant difference (LSD) test at $\alpha = 0.05$. Symbol X represents total P (TP) from the perchloric + nitric acid digestion in each of sediment type.

Conclusions

This study demonstrated that anaerobic incubation decreased redox potential (as assessed by Eh measurements) and increased pH in a sediment-solution system, especially when a readily bioavailable carbon source was present. Concomitantly, there was evidence that the forms of P in four bank sediments of Walnut Creek were redistributed. When the sediments were subjected to low redox potential, there was an increase in the concentration of inorganic labile P which was coincided with a decrease in slowly cycling P associated with Fe. Varying redox potential did not significantly change slowly cycling P associated with Ca, stable P, and residue P. Among the four bank sediments of Walnut Creek that were

collected from sites in this study, the younger sediments with more organic matter, i.e., the Camp Creek and Roberts Creek sediments, had greater labile and slowly cycling P associated with Fe, reflecting a greater potential to contribute to elevated levels of P in the stream water, especially if subjected to low redox potential in the stream.

CHAPTER 7

MALACHITE GREEN METHOD FOR DETERMINING P CONCENTRATION IN DIVERSE MATRICES

Introduction

Solid phase phosphorus (P) is distributed among different organic and inorganic pools in soils and sediments. The solid phase P can be classified into water extractable P (P_{H_2O}), labile P (P_{Lab}), slowly cycling P (P_{Slow}), stable P (P_{Stab}), and residue P (P_{Res}) using sequential extraction (Schrijver *et al.*, 2012; Tiessen and Moir, 2008). In terms of P dynamics in stream water and sediment systems, characterizing these fractions is an important step in recognizing the potential P load to the water column. The general approach for soil P fractionation is sequential extraction using specific extracting solutions. Soil is initially extracted with a "weak" extracting solution in the first step followed by "stronger" extracting solutions in subsequent steps. In the method developed by Tiessen and Moir (2008), P_{H_2O}, P_{Lab}, P_{Slow}, P_{Stab}, and P_{Res} are sequentially extracted with water, 0.5 *M* $NaHCO_3$, 0.1 *M* NaOH and 1 *M* HCl, concentrated HCl, and concentrated H_2SO_4, respectively. Inorganic P (*Pi*) and total P (*Pt*) are determined directly from the extracts, and organic P (*Po*) is then determined by subtracting *Pi* from *Pt*.

As in many laboratory P determinations, colorimetric analysis via ascorbic acid reduction (Watanabe and Olsen, 1965) is a very common method for determining P concentration in each extract during the sequential extraction. The molybdate blue-ascorbic acid (AA) method is based on the complexation of phosphate and molybdate ions to form a colored complex, and ascorbic acid is added as reducing agent to develop blue color. The

method is simple and very popular; however, it is time consuming, laborious (Huerta-Diaz *et al.*, 2005), generates significant chemical waste, and the reagents are not stable at room temperature for more than 24 hours. Another problem with the AA method is that the blue color develops very weakly to determine acidified ammonium oxalate extractable P (P_{ox}), a fraction of P associated with poorly crystalline sesquioxide minerals. In many studies (e.g., Bell *et al.* (2005), Dayton and Basta (2005), Yoo *et al.* (2006)), P_{ox} is commonly determined using inductively coupled plasma-atomic emission spectrometry (ICP-AES). The method is automated, and allows for either simultaneous or sequential analysis of multiple elements (Jarvis and Jarvis, 1992; Olesik, 1991; Rommers and Boumans, 1996). However, as in other automated techniques, expensive equipment (Huerta-Diaz *et al*., 2005) and skilled technical expertise are required for reliable ICP-AES determinations.

An alternative colorimetric method for determining P concentration in an extract is the malachite green (MG) method (Ohno and Zibilske, 1991; Subba Rao *et al.*, 1997). It is based on the complexation of malachite green with phosphate and molybdate ions (Ohno and Zibilske, 1991; Subba Rao *et al.*, 1997). Absorbance in the MG method can be measured with a 96-well micro plate reader (D'Angelo *et al*., 2001), making this method faster and less labor intensive. In addition, less chemical waste is generated than with the AA method (Jeannotte *et al.*, 2004). Moreover, MG method had been used by Pizzeghelloa *et al*. (2011) for measuring P_{ox} concentration in soils; therefore, it could be an alternative to ICP-AES determination. The purpose of this study was to compare the MG method to the AA method for determining P concentrations in extracts from a fractionation analysis and to the ICP-AES method for determining P concentrations in ammonium oxalate extracts.

Materials and Methods

Sediment sampling and characterization

Two experiments were conducted in this study. The first experiment compared the MG method to the AA method to determine P concentrations, while the second compared the colorimetric MG method to ICP-AES determinations of ammonium oxalate-extractable P (P_{ox}). Four sediments, representing major alluvial units in Walnut Creek, Iowa, (Camp Creek, Roberts Creek, Gunder, and Pre-Illinoian Till) were used in the first experiment. For the second experiment, thirty-one sediment samples (including twelve samples that were duplicates) from streambanks, in-stream deposits, and floodplain soils of Walnut Creek watershed were used. Sediment sampling and characterization were as described in Chapter 3.

Phosphorus fractionation

Methods of soil P fractionation in this study were based on sequential extraction by Tiessen and Moir (2008) as presented in Fig. 30. Following the scheme, 0.5 g of air-dried sediment were weighed into a 50-mL centrifuge tube. The sequential extraction started with water and ended with concentrated H_2SO_4 to extract P_{H_2O}, P_{Lab}, P_{Slow}, P_{Stab}, and P_{Res}. A modification from the reference fractionation method was made in this study for extracting P_{H_2O}. Instead of using an exchange resin strip, P_{H_2O} was determined directly in the extract after shaking in a reciprocal shaker at 200 oscillations per minute for 16 hours, centrifuging at 4,300 x *g* for 15 minutes, and filtering the solution through a 0.45-µ membrane filter. Similar shaking and centrifuging were conducted for sequential extraction with 0.5 *M* $NaHCO_3$, 0.1 *M* NaOH, and 1 *M* HCl. In the last steps, extraction with concentrated HCl and

concentrated H_2SO_4 were carried out in a water bath at 80°C and a digestion block at 360°C, respectively. Total P (*Pt*) concentrations in 0.5 *M* $NaHCO_3$, 0.1 *M* NaOH, and concentrated HCl were determined after the extracts were digested with ammonium persulfate in an autoclave at 121°C.

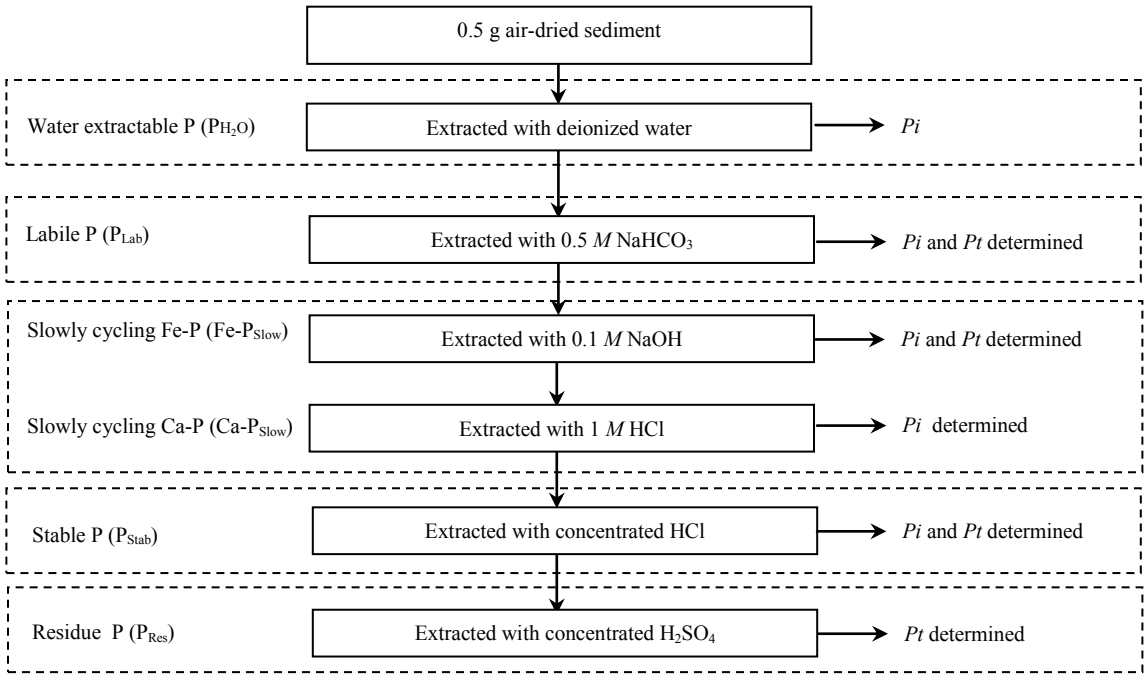

Figure 30. Sequential extractions for P fractionation analysis, adapted from Tiessen and Moir (2008).

Molybdate blue-ascorbic acid (AA) method

Two reagents were prepared for the AA method, A and B (Watanabe and Olsen, 1965). One liter of reagent A contained 6 g of ammonium molybdate, 0.1454 g of antimony potassium tartrate, and 70 mL of concentrated H_2SO_4. At the time samples were to be analyzed, reagent B was prepared by dissolving 0.528 g of ascorbic acid per 100 mL of reagent A. To determine P concentration in an extract, an aliquot of supernatant was transferred into a 25 mL volumetric flask, and 4 mL of deionized water and one drop of para-

nitrophenol were added. The pH was adjusted by adding a few drops of either NaOH or HCl until yellow color appeared. To develop the blue color, 4 mL of reagent B was added and volume was made by adding deionized water. After 30 minutes, absorbance was read at a wavelength (λ) of 880 nm, using a spectrophotometer (Spectronic 601, Milton Ray Inc.).

Malachite green (MG) method

Two reagents were prepared for the MG method (D'Angelo *et al*., 2001). Reagent 1 was 14.2 mmol L^{-1} ammonium molybdate in 3.1 *M* H_2SO_4. Reagent 2 was 3.5 g L^{-1} aqueous polyvinyl alcohol (PVA) and 0.35 g L^{-1} malachite green. Polyvinyl alcohol was used in Reagent 2 to stabilize the phosphomolybdate complex and to make the reagents stable at room temperature (Van Veldhoven and Mannaerts, 1987). To determine P concentration in an extract, an aliquot of supernatant was transferred into a 25 mL volumetric flask, pH was adjusted by adding the same amount of NaOH/HCl as used in the AA method (without the para-nitrophenol indicator), and then volume was made by adding deionized water. Therefore, the pH and dilution factor of the solution for both methods were similar.

To read absorbance, 200 μL of diluted supernatant were transferred with a single-channel electronic pipette (Rainin E4 XLS) into a designated well in a 96-well standard micro-plate. Then, 40 μL of reagent 1 were added with a multichannel pipette (Transferpette-8, BrandTech Scientific Inc.), followed by shaking for 30 minutes. Afterward, 40 μL of reagent 2 were added, followed by shaking for 60 minutes. Shaking was carried out at fixed speed of 100 rpm on Fisher Scientific Clinical Rotator Model 341. Absorbance was read using universal micro plate reader Model ELX 800 (BioTek Instruments, Inc.) at λ= 630 nm.

Ammonium oxalate extraction

Extracting solution (pH 3.0) was prepared by dissolving 24.9 g ammonium oxalate and 12.6 g oxalic acid in one liter of deionized water. To extract a sample, 1.00 g of air-dried sediment was weighed into a 50-mL centrifuge tube that had been wrapped in a foil. Then, 35 mL of the extracting solution were added. Samples were shaken on a reciprocal shaker (200 oscillations per minute) for 4 hours in the dark. After shaking, sediments were allowed to settle. Then, the supernatant was filtered through Whatman 40 filter paper into a 100 mL plastic bottle. Subsequently, 2 mL of the supernatant were transferred with a volumetric pipette into a 50 mL volumetric flask, and volume was made by adding deionized water (dilution factor was 25). The diluted extracts were submitted to the Soil and Plant Analysis Lab (SPAL), Department of Agronomy, Iowa State University for determination of P_{ox} concentration using inductively coupled plasma-atomic emission spectrometry (ICP-AES, Spectro Ciros EOP CCD) at λ=177.49 nm. For the MG method, only 1 mL of the extract was diluted to 50 mL because color did not develop at the higher concentration of extractant. The procedures to determine P_{ox} concentration with the MG method were similar to those in the P fractionation analysis; however, the pH of the diluted supernatant was not adjusted.

Experimental design and data analysis

In the first experiment, twenty-four samples (four sediment types, six sub samples per sediment type) were sequentially extracted following the scheme shown in Fig. 30. As a result, 24 sample supernatant solutions were collected from each extracting step. Using the AA method described earlier, absorbance from each extracting step was read once. For the MG method, 6 blocks (representing six sub-samples) were assigned to a 96-well standard

microplate, with each block containing four wells. Supernatant from a sub-sample of each sediment type was randomly assigned to one of the wells in the block. Therefore, each block accommodated four sediment types. Three 96-well standard microplates were utilized, and mean values from these three microplates were used to calculate P concentration. In addition, absorbance was read at 0, 0.5, 2, 6, 12, and 24 h after shaking to test the variation among measurement times.

For the second experiment, twenty-five sediment samples from the Walnut Creek watershed were used. Duplicate samples were designated for 6 samples (I-5a/b, B-17a/b, B-18a/b, B-19a/b, B-20a/b, and F-24a/b); therefore, in total there were 31 supernatant samples for analysis. For the MG method, mean values from two 98-well standard microplates were used to calculate concentration of ammonium oxalate-extractable P (P_{ox}). Then, the P_{ox} values determined by MG method were compared to those determined by ICP-AES. Statistical software package SAS 12.0 was used to perform statistical analysis for comparing MG to ICP-AES methods as well as MG to AA methods in the first experiment. The statistical analysis included simple regression analyses, paired *t*-test, and ANOVA.

Results and Discussion

Comparison of MG and AA methods during sequential extraction

The malachite green (MG) and molybdate blue- ascorbic acid (AA) colorimetric methods provided relatively similar P concentrations in most extracts (Fig. 31 to Fig. 34). However, a paired *t* test showed that the AA method resulted in higher P concentrations in the extracts of concentrated HCl *Pi* from Roberts Creek and Gunder sediments, as well as for 0.5 *M* $NaHCO_3$ *Pi*, 0.5 *M* $NaHCO_3$ *Pt,* and 0.1 *M* NaOH *Pi* for Till sediments (Table 18). The reasons for these differences are difficult to explain, since the differences were relatively

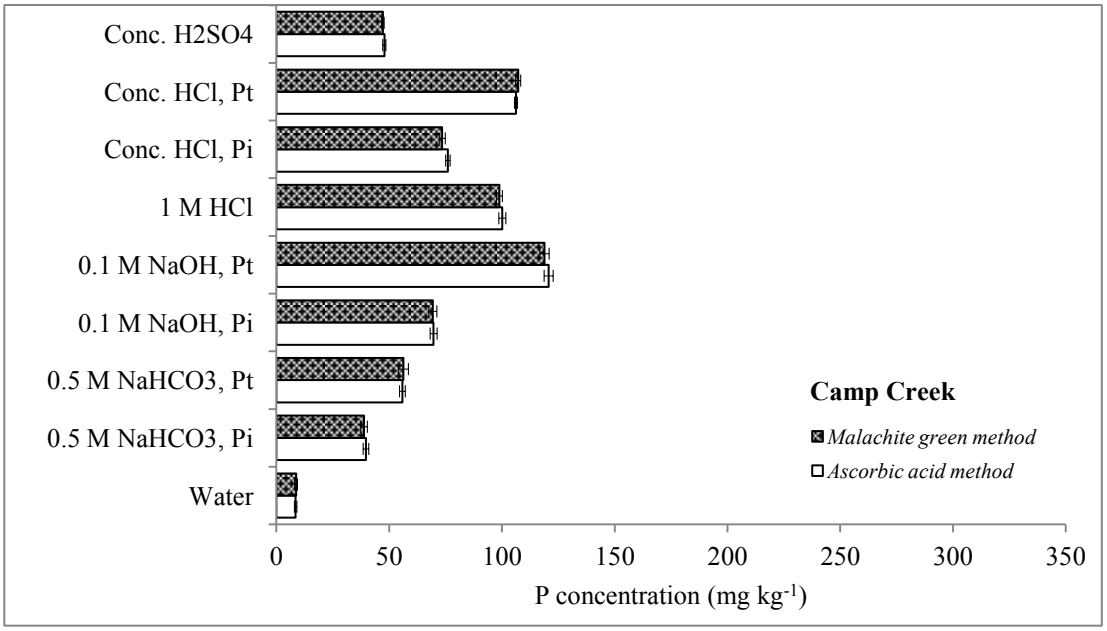

Figure 31. Phosphorus concentrations determined by the molybdate blue-ascorbic acid (AA) and malachite green (MG) colorimetric methods in the sequential extraction for Camp Creek. *Pi* and *Pt* are inorganic and total P, respectively. There were no significant differences between means within the same extract according to paired *t*-test at α=0.05.

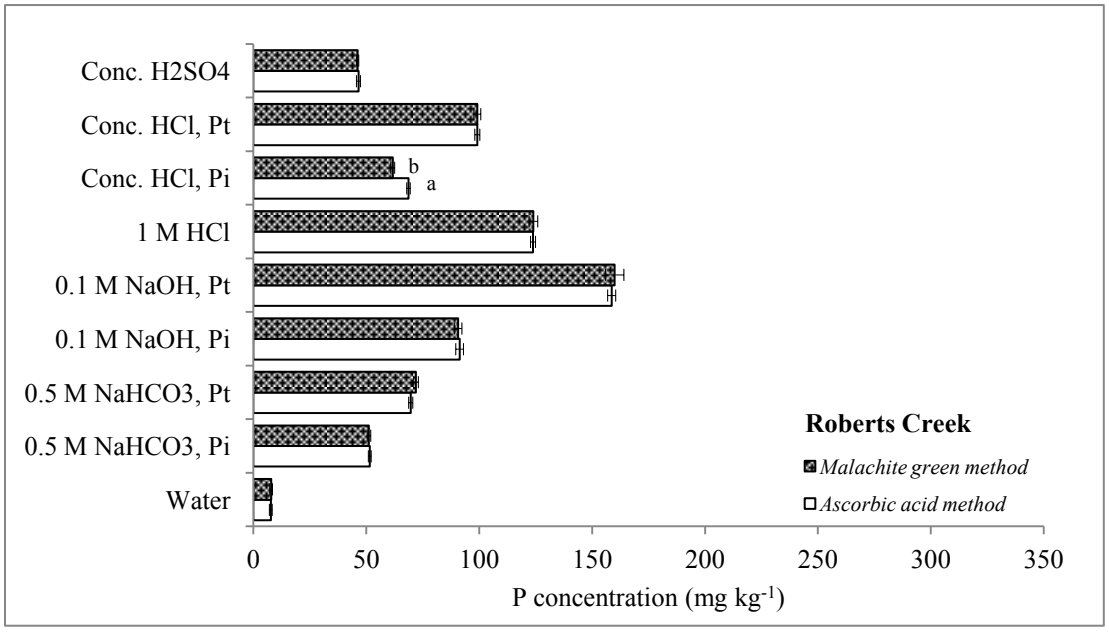

Figure 32. Phosphorus concentrations determined by the molybdate blue-ascorbic acid (AA) and malachite green (MG) colorimetric methods in the sequential extraction for Roberts Creek. *Pi* and *Pt* are inorganic and total P, respectively. Means with different letters in the same extract are significantly different according to paired *t*-test at α=0.05.

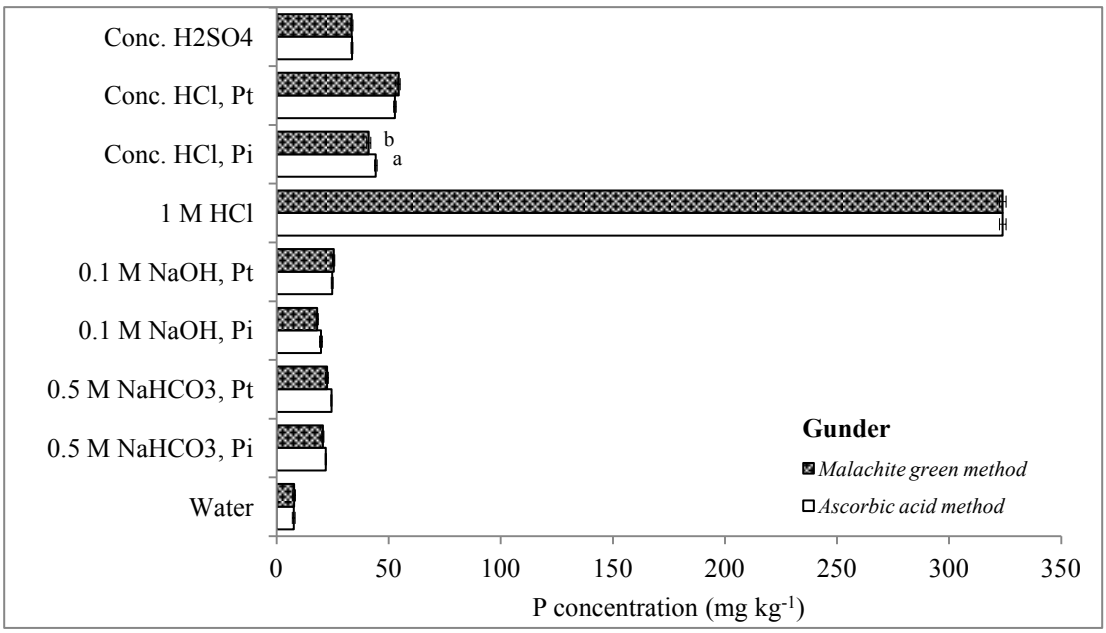

Figure 33. Phosphorus concentrations determined by the molybdate blue-ascorbic acid (AA) and malachite green (MG) colorimetric methods in the sequential extraction for Gunder. *Pi* and *Pt* are inorganic and total P, respectively. Means with different letters in the same extract are significantly different according to paired *t*-test at α=0.05.

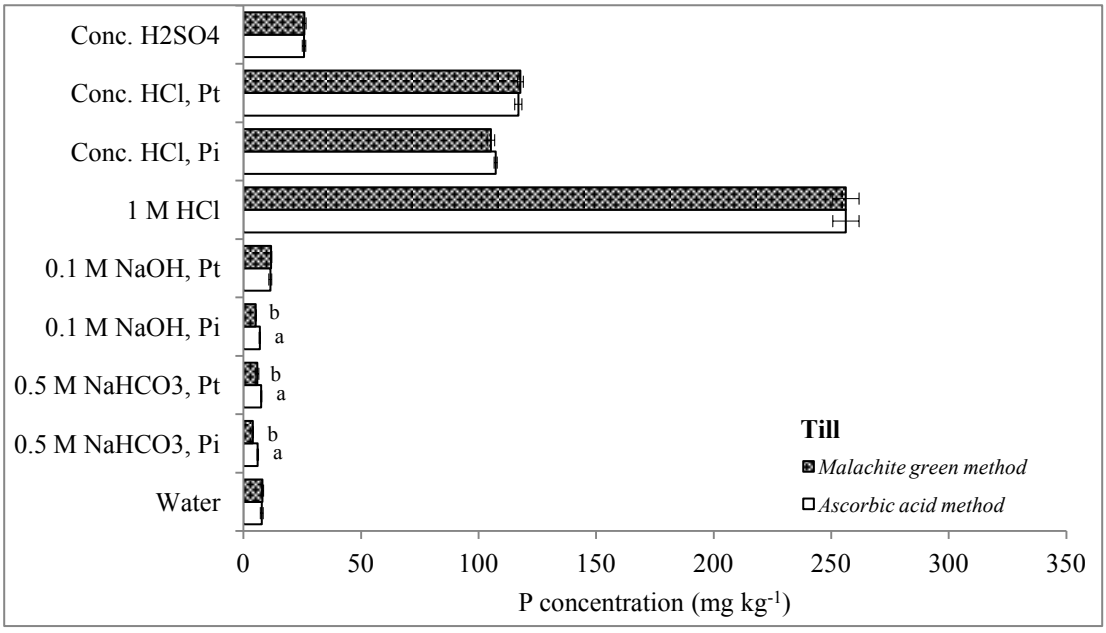

Figure 34. Phosphorus concentrations determined by the molybdate blue-ascorbic acid (AA) and malachite green (MG) colorimetric methods in the sequential extraction for Till. *Pi* and *Pt* are inorganic and total P, respectively. Means with different letters in the same extract are significantly different according to paired *t*-test at α=0.05.

Table 18. Paired *t* test for mean separation of P concentrations (mg kg^{-1}) in each extract from a sequential extraction as determined by molybdate blue-ascorbic acid (AA) and malachite green (MG) colorimetric methods. Four sediment materials were included.

Extracts	Different†	*t* value	*p*
Camp Creek			
Water	-0.167	-0.20	0.8455
0.5 *M* $NaHCO_3$, *Pi*	0.833	0.43	0.6729
0.5 *M* $NaHCO_3$, *Pt*	-0.500	-0.20	0.8458
0.1 *M* NaOH, *Pi*	0.333	0.14	0.8910
0.1 *M* NaOH, *Pt*	1.833	0.64	0.5366
1 *M* HCl	1.333	0.65	0.5294
Concentrated HCl, *Pi*	2.500	1.52	0.1603
Concentrated HCl, *Pt*	-1.000	-0.76	0.4637
Concentrated H_2SO_4	0.667	0.75	0.4702
Roberts Creek			
Water	-0.167	-0.19	0.8501
0.5 *M* $NaHCO_3$, *Pi*	0.333	0.33	0.7471
0.5 *M* $NaHCO_3$, *Pt*	-2.333	-1.69	0.1223
0.1 *M* NaOH, *Pi*	0.667	0.28	0.7868
0.1 *M* NaOH, *Pt*	-1.333	-0.30	0.7712
1 *M* HCl	-0.167	-0.07	0.9418
Concentrated HCl, *Pi*	7.000	6.01	0.0001**
Concentrated HCl, *Pt*	0.000	0.00	1.0000
Concentrated H_2SO_4	0.333	0.33	0.7471
Gunder			
Water			
0.5 *M* $NaHCO_3$, *Pi*	-0.167	-0.19	0.8501
0.5 *M* $NaHCO_3$, *Pt*	1.333	2.39	0.0379
0.1 *M* NaOH, *Pi*	2.000	3.04	0.0125
0.1 *M* NaOH, *Pt*	-0.667	-1.04	0.3229
1 *M* HCl	0.000	0.00	1.0000
Concentrated HCl, *Pi*	3.167	2.97	0.0141**
Concentrated HCl, *Pt*	-1.667	-1.93	0.0822
Concentrated H_2SO_4	0.167	0.22	0.8284
Till			
Water	-0.333	-0.43	0.6732
0.5 *M* $NaHCO_3$, *Pi*	2.167	5.40	0.0003**
0.5 *M* $NaHCO_3$, *Pt*	1.667	2.50	0.0314*
0.1 *M* NaOH, *Pi*	1.667	5.00	0.0005**
0.1 *M* NaOH, *Pt*	-0.333	-0.48	0.6400
1 *M* HCl	0.000	0.00	1.0000
Concentrated HCl, *Pi*	2.000	1.15	0.2767
Concentrated HCl, *Pt*	-0.833	-0.42	0.6843
Concentrated H_2SO_4	-0.167	-0.16	0.8727

† *P concentration determined by AA method – P concentration determined by MG method*

* = *significant at* α=0.05 , **= *significant at* α=0.01

small and did not consistently occur in all sediment types. However, the differences might be associated with matrix interference and the relatively low concentrations of P in the extracts.

For the first factor, D'Angelo *et al.* (2001) suggested that matrix interference might result in less accuracy with the MG method when HCl concentration is greater than 0.1 *M* and NaOH concentration exceeds 0.4 *M.* As noted earlier, in this study the dilution factor and pH adjustment of the concentrated HCl and 0.1 *M* NaOH extracts were similar for the MG and AA methods. For the concentrated HCl *Pi* extracts, the dilution might not be sufficient to prevent matrix interference in the MG method, causing lower values than those determined by the AA method, especially with Roberts Creek and Gunder sediments. Low P concentrations in the inorganic/total P_{Lab} and inorganic Fe-P_{Slow} extracts from the till sediments likely led to differences between the two methods. At low concentration of P in these extracts, a small change in the absorbance reading for the AA method might lead to a significant difference in the calculated concentration of P in the sediment. However, further research is needed to investigate these factors, using a wider concentration range of P from the various pools.

When data from the four sediment types were combined, P concentrations in all extracts determined by the MG method were strongly correlated ($p<0.0001$) with those determined by AA method (Fig. 35). This indicated a strong relationship between P_{ox} values determined by the AA and MG methods. Furthermore, agreement between the two methods was also investigated. Using simple linear regression, two methods *x* and *y* would agree if the equation for a fitted line is $y = x$ (slope=1 and intercept=0). As seen in Fig. 35, the intercepts in the graphs ranged from -0.83 to 6.80 mg kg^{-1}. The *t* test (Table 19) indicated that the intercepts were equal to 0 (α=0.01) for the extracts of water, 0.1 *M* NaOH *Pt,* 1 *M* HCl,

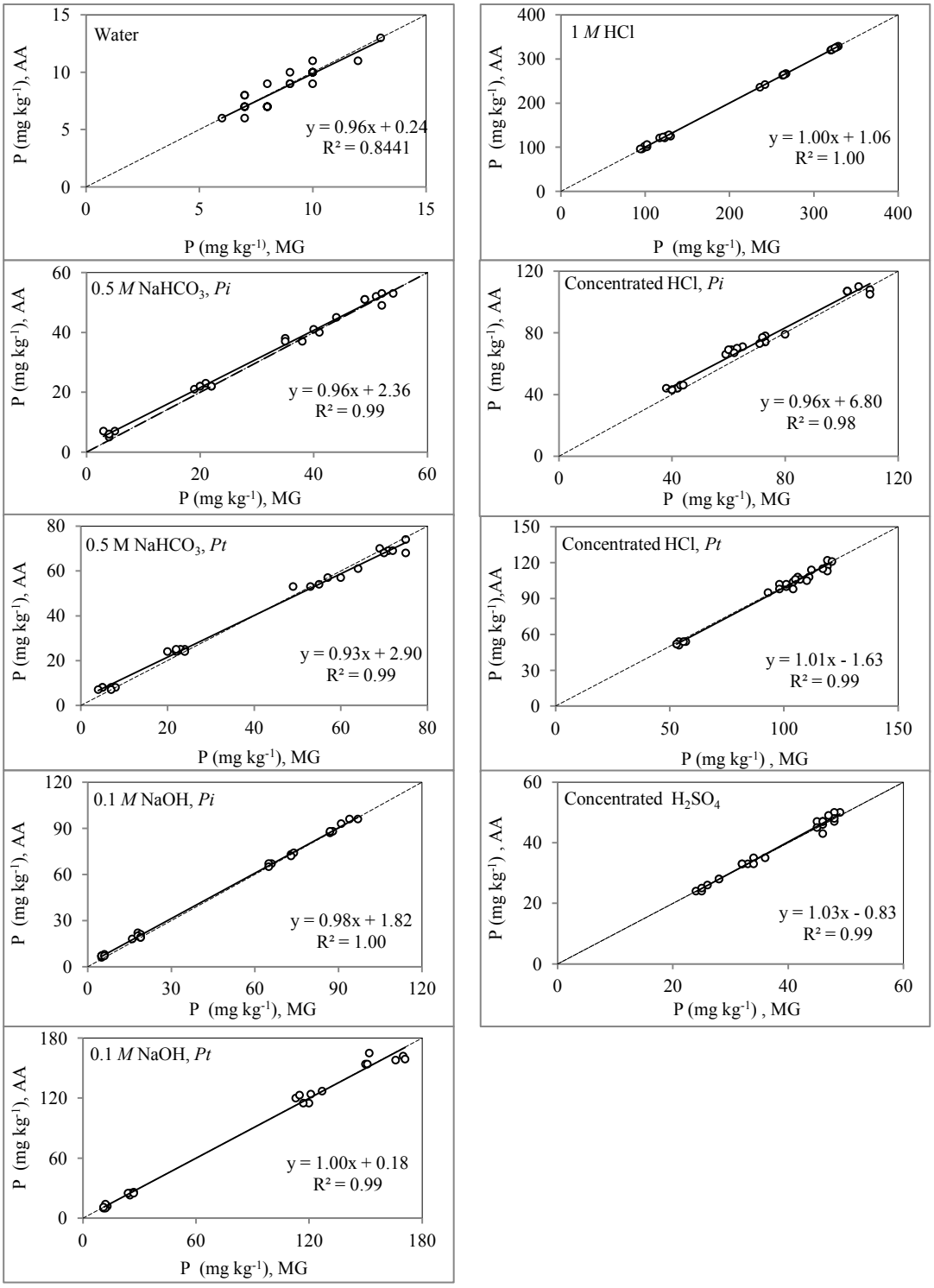

Figure 35. Simple regression between P in sediment (mg kg^{-1}) determined by malachite green method (MG, *x* axis) and molybdate blue-ascorbic acid method (AA, *y* axis) in the sequential extraction of P fractionation analysis. *Pi* and *Pt* are inorganic and total P, respectively. Dashed line represents equality line, straight line represents best fitted line. Data were combined for all sediment types (*n=24*).

Table 19. Simple linear regression between P in sediment (mg kg^{-1}) determined by molybdate blue-ascorbic acid (AA) and malachite green (MG) colorimetric methods. The AA and MG methods are dependent and independent variable, respectively. *Pi* and *Pt* are inorganic and total P, respectively. Data were combined for all sediment types (*n=24*).

Extracts	Intercept			Slope		
	Estimate	$t^{\dagger}$	$Pr>\|t\|^{\dagger}$	Estimate	$t^{\ddagger}$	$Pr>\|t\|^{\ddagger}$
Water	0.24	0.30	0.7670	0.96	-0.41	0.6836
0.5 *M* $NaHCO_3$, *Pi*	2.36	4.57	0.0002**	0.96	-2.72	0.0124*
0.5 *M* $NaHCO_3$, *Pt*	2.90	4.03	0.0006**	0.93	-4.51	0.0002**
0.1 *M* NaOH, *Pi*	1.82	4.98	<0.0001**	0.98	-2.53	0.0189*
0.1 *M* NaOH, *Pt*	0.18	0.10	0.9187	1.00	-0.22	0.8264
1 *M* HCl	1.06	1.20	0.2444	1.00	-0.96	0.3485
Concentrated HCl, *Pi*	6.8	3.39	0.0026**	0.96	-1.65	0.1133
Concentrated HCl, *Pt*	-1.63	-0.74	0.4691	1.01	0.35	0.7275
Concentrated H_2SO_4	-0.83	-0.81	0.4245	1.03	1.09	0.2890

† *t and Pr>|t| for* H_0 = *intercept is equal to 0*
‡ *t and Pr>|t| for* H_0 = *slope is equal to 1*
*=*significant at* α=0.05
**= significant at α=0.01

concentrated HCl *Pt,* and concentrated H_2SO_4. Moreover, the slopes ranged from 0.93 to 1.03. The *t* test in Table 19 indicated that the slopes were equal to 1 (α=0.01) for the extracts of water, 0.1 *M* NaOH *Pt*, 1 *M* HCl, concentrated HCl *Pi,* concentrated HCl *Pt,* and concentrated H_2SO_4. The slopes were not equal to 1 for 0.5 *M* $NaHCO_3$ *Pi* and 0.1 *M* NaOH *Pi* at α=0.05 and for 0.5 *M* $NaHCO_3$ *Pt* at α=0.01.

In all sediment types, both methodological comparison using a paired *t* test and simple linear regression revealed the agreement between the MG and AA methods for the extracts of water, 0.1 *M* NaOH *Pt*, 1 *M* HCl, concentrated HCl *Pt,* and concentrated H_2SO_4. In contrast, a discrepancy between two methods occurred for the extracts of 0.5 *M* $NaHCO_3$ *Pi,* 0.5 *M* $NaHCO_3$ *Pt,* 0.1 M NaOH *Pi,* and concentrated HCl *Pi.* However, the discrepancy depended on sediment type. A paired *t* test indicated that most of the discrepancies were

found with till sediments, whereas there was no discrepancy between the two methods with Camp Creek sediments. In addition, it could be argued that the magnitude of the discrepancies was low and probably in the range of errors for practical analysis in the lab.

Previous studies using a microplate reader or other systems showed the MG method as a satisfactory technique to determine P in matrices similar to those used in this study. The microplate system-MG method was used for determining P concentrations in water and 0.1 *M* NaOH by D'Angelo *et al.* (2001), while Jeannotte *et al.* (2004) used the system for 0.5 *M* $NaHCO_3$ extracts. Using a flow injection analysis system, the MG method has been proposed for determining P in river water (Motomizu and Oshima, 1987) and sea water (Susanto *et al.*, 1995). Pizzeghelloa *et al.* (2011) used a double beam UV–vis spectrophotometer for the MG method to determine P in water, concentrated HCl, and 0.5 *M* $NaHCO_3$ extracts. Ohno and Zibilske (1991) used a double-beam spectrophotometer and semimicro quartz cells for determining water-extractable P with the MG method. Subba Rao *et al.* (1997) also used a spectrophotometer to measure P in water and 0.5 *M* $NaHCO_3$ extracts with the MG method, where 25-mL volumetric flasks were employed to develop green color.

Furthermore, the MG and AA methods for determining P concentrations in water and 0.5 *M* $NaHCO_3$ extracts have been compared in previous studies. Using ten Indian soils with a wide range of properties, Subba Rao *et al.* (1997) suggested that the MG method had better precision and accuracy than the AA method for determining P in water and 0.5 *M* $NaHCO_3$ extracts. Greater sensitivity of the MG than AA methods for determining water-extractable P was also reported by Ohno and Zibilske (1991) for seven soils with varied organic matter content and pH. In 0.5 *M* $NaHCO_3$ extracts, Jeannotte *et al.* (2004) suggested that *Pi*

*c*oncentrations determined by the MG and AA methods were significantly correlated (r=0.998, p<0.05).

In comparison to previous studies, the correlation between the AA and MG methods for water-extractable P in this study agreed with the results of Subba Rao *et al.* (1997) and Ohno and Zibilske (1991). On the other hand, though strong correlation between P concentrations in 0.5 *M* $NaHCO_3$ determined by the MG and AA methods in this study agreed with Jeannotte *et al.* (2004) and Subba Rao *et al.* (1997), a slight discrepancy occurred with till sediments, which were calcareous, alkaline, and low in organic matter content. Unfortunately, few studies have compared the MG and AA methods for other matrices in the P fractionation analysis. The MG method was used for sequential extraction of P in river sediments by Wang *et al.* (2010); however, the authors used different methods for the sequential extraction and the MG method was not compared to AA method. Though slight differences may occur with some extracts, this study provided evidence that the MG method could be used as an alternative to the AA method for determining P concentration during sequential extraction of P. In addition, with the large number of extractions required for P fractionation, the microplate system in the MG method will generate less chemical waste, decrease labor, and provide rapid turnaround for measuring P concentration in each extract.

Effects of time on measured P concentration in MG method

Phosphorus concentration determined by the MG method in each extract varied with the length of time before measurement (t) and the sediment types (S) (Table 20). The effect of time before measurement was significant (α=0.01) for the extracts of concentrated acids

Table 20. ANOVA for investigating the effects of time before measurement on P concentration (mg L^{-1}) determined by the MG method in P fractionation analysis. *Pi* and *Pt* are inorganic and total P, respectively.

Source	df	Sum of Square	Mean Square	F Value	Pr>F
Water extractable P					
Sediment types (S) [§]	3	0.04273006	0.01424335	29.38	<.0001
Measurement times (*t*) [†]	5	0.00142300	0.00028460	0.59	0.7099
S x *t*	15	0.00001961	0.00000131	0.00	1.0000
Replicate [‡]	5	0.03900992	0.00780198	16.09	<.0001
$NaHCO_3$, Pi					
Sediment types (S) [§]	3	0.32945431	0.10981810	4323.32	<.0001
Measurement times (*t*) [†]	5	0.00012431	0.00002486	1.00	0.4203
S x *t*	15	0.00002369	0.00000158	0.06	1.0000
Replicate [‡]	5	0.00066322	0.00013264	5.34	0.0002
$NaHCO_3$, Pt					
Sediment types (S) [§]	3	1.10276806	0.36758935	3578.89	<.0001
Measurement times (*t*) [†]	5	0.00015722	0.00003144	0.31	0.9084
S x *t*	15	0.00000361	0.00000024	0.00	1.0000
Replicate [‡]	5	0.00485631	0.00097126	9.46	<.0001
0.1 M NaOH, Pi					
Sediment types (S) [§]	3	3.07861402	1.02620467	9605.82	<.0001
Measurement times (*t*) [†]	5	0.00052512	0.00010502	0.98	0.4313
S x *t*	15	0.00037135	0.00002476	0.23	0.9987
Replicate [‡]	5	0.00895553	0.00179111	16.77	<.0001
0.1 M NaOH, Pt					
Sediment types (S) [§]	3	3.10370063	1.03456688	4158.30	<.0001
Measurement times (*t*) [†]	5	3.10370063	0.00003136	0.13	0.9863
S x *t*	15	0.00077649	0.00005177	0.21	0.9993
Replicate [‡]	5	0.00970698	0.00194140	7.80	<.0001
1 M HCl					
Sediment types (S) [§]	3	0.55706322	0.1868774	7410.04	<0.0001
Measurement times (*t*) [†]	5	0.00008139	0.00001628	0.65	0.6624
S x *t*	15	0.00004361	0.00000291	0.12	1.0000
Replicate [‡]	5	0.00158456	0.00031691	12.65	<0.0001
Concentrated HCl, Pi					
Sediment types (S) [§]	3	0.05615161	0.01871720	3842.95	<.0001
Measurement times (*t*) [†]	5	0.00023956	0.00004791	9.84	<.0001
S x *t*	15	0.00002039	0.00000136	0.28	0.9964
Replicate [‡]	5	0.00028156	0.00005631	11.56	<.0001
Concentrated HCl, Pt [‡]					
Sediment types (S) [§]	3	0.08655208	0.02885069	6641.66	<.0001
Measurement times (*t*) [†]	5	0.00007312	0.00001462	3.37	0.0071
S x *t*	15	0.00000280	0.00000019	0.04	1.0000
Replicate [‡]	5	0.00041228	0.00008246	18.98	<.0001
Concentrated H_2SO_4					
Sediment types (S) [§]	3	0.02834785	0.00944928	4000.52	<.0001
Measurement times (*t*) [†]	5	0.00016153	0.00003231	13.68	<.0001
S x *t*	15	0.00001177	0.00000078	0.33	0.9908
Replicate [‡]	5	0.00043087	0.00008617	36.48	<.0001

[§]Sediment types (S) were Camp Creek, Roberts Creek, Gunder and Till

[†] Measurement times (*t*) were 0, 0.5, 2, 6, 12, and 24 hours after microplate shaking in a clinical rotator.

[‡]Six replicates in each sediment type

(HCl *Pi,* HCl *Pt,* and H_2SO_4). In the other extracts, there were no significant difference among the P concentrations when they were measured at *t*=0 h to *t*=24 h after shaking in the clinical rotator. Since the interaction between main factors (S x *t*) in all extracts was not significant, mean P concentrations averaged over *S* were employed for mean comparison at *t*=0 h to *t*=24 h (Table 21). The mean comparison provided evidence that a significant increase in concentrated HCl-extractable *Pi* and *Pt* started at *t*=6 h and *t*=12 h, respectively. For the concentrated H_2SO_4 extracts, there was a significant decrease in measured P concentration at *t*=2 h. The reasons for the decrease were unclear, since measured values at the other times remained stable. Considering these discrepancies, it is recommended to read the absorbance no longer than 30 minutes after shaking.

Table 21. Concentration of P in each extract at different measurement times, averaged over sediment types. Means followed by different letters in the same row are significantly different at α=0.05. *Pi* is inorganic P, *Pt* is total P.

Extracts	P concentration (mg L^{-1}) at *t* (hour) measurement time§					
	t=0.0	*t*=0.5	*t*=2.0	*t*=6.0	*t*=12.0	*t*=24.0
Water	0.149	0.150	0.152	0.155	0.156	0.158
0.5 *M* $NaHCO_3$, *Pi*	0.079	0.079	0.079	0.080	0.080	0.081
0.5 *M* $NaHCO_3$, *Pt*	0.130	0.130	0.130	0.130	0.130	0.133
0.1 *M* NaOH, *Pi*	0.192	0.191	0.191	0.193	0.194	0.196
0.1 *M* NaOH, *Pt*	0.185	0.185	0.186	0.186	0.186	0.183
1 *M* HCl	0.135	0.135	0.135	0.136	0.136	0.137
Concentrated HCl, *Pi*	0.066 b	0.066 b	0.067 b	0.069 a	0.069 a	0.069 a
Concentrated HCl, *Pt*	0.088 b	0.087 b	0.087 b	0.088 ab	0.089 a	0.089 a
Concentrated H_2SO_4	0.061 a	0.061 a	0.058 b	0.061 a	0.061 a	0.061 a

§*Measurement time after shaking on Fisher Scientific Clinical Rotator.*

MG and ICP-AES methods for determining ammonium oxalate extractable P (P_{ox})

Three aspects could be inferred from comparisons of the MG and ICP-AES methods in determining concentrations of P_{ox} (Table 22). First, P_{ox} could be determined by the MG method in all samples, while ICP-AES method did not detect P_{ox} in twelve samples. Secondly, P_{ox} values ranged from 60 to 823 mg kg^{-1} for the MG method. In comparison, the range of P_{ox} values from the ICP-AES determination was from 54 to 680 kg^{-1}, excluding samples that were below detection limit. Third, the MG method consistently resulted in higher P_{ox} values than the ICP-AES method in all samples. Considering only the detectable P_{ox} values for two methods (n=19), mean difference between the MG and ICP-AES methods was 127 mg kg^{-1} (SE=62.0, p = 0.0485).

The P_{ox} values measured by ICP-AES were plotted against those obtained by MG method (Fig. 36). As with the t test to estimate mean differences, the twelve samples that were below detection limit under ICP-AES method were excluded. Results indicated that P_{ox} values determined by the ICP-AES method were strongly correlated with those determined by the MG method. The linear regression model was [ICP-AES] = -(102 ± 21.3) + (0.93 ± 0.05) [MG], and it was significant at α=0.01. The negative intercept indicates a better capability of the MG method for measuring P_{ox} at a low concentration than the ICP-AES method. Moreover, the relatively large intercept indicates a large discrepancy between two methods. The slope (0.93± 0.05) was equal to 1 at α=0.01. Therefore, it could be predicted that the discrepancy would exist in either low or high P_{ox} concentration.

The systematic differences between the two methods in this study were likely linked to dilution factor and detection limit of the methods. The dilution factor for the MG and ICP-AES methods was 50 and 25, respectively. It was difficult to get similar dilution factor for

Table 22. Ammonium oxalate extractable P (P_{ox}) concentration (mg kg^{-1}) determined by inductively coupled plasma (ICP) spectroscopy and the malachite green colorimetric method (MG) in soil and sediment samples from the Walnut Creek watershed in central Iowa.

Group	Sample Code	Description	P_{ox} (mg kg^{-1})		
			ICP-AES	MG	Difference‡
Banks	B-2	Camp Creek (1)	BDL †	127	*n.a*
	B-3	Roberts Creek (1)	467	479	-12
	B-7	Till (1)	BDL †	124	*n.a*
	B-17a	Camp Creek (2)	BDL †	160	*n.a*
	B-17b	Camp Creek (2)	BDL †	157	*n.a*
	B-18a	Roberts Creek (2)	54	191	-137
	B-18b	Roberts Creek (2)	86	194	-108
	B-19a	Gunder (1)	BDL †	145	*n.a*
	B-19b	Gunder (1)	BDL †	130	*n.a*
	B-20a	Till (2)	BDL †	100	*n.a*
	B-20b	Till (2)	BDL †	111	*n.a*
	B-21	Camp Creek (3)	67	188	-121
	B-22	Roberts Creek (3)	BDL †	129	*n.a*
In-stream deposit	I-4	Stream bottom sediment (1)	315	499	-184
	I-5a	Slump, debris dam	BDL †	55	*n.a*
	I-5b	Slump, debris dam	BDL †	65	*n.a*
	I-6	Stream bed sediments, debris dam	510	655	-145
	I-8	Sand bar	196	351	-155
	I-11	Stream bottom sediment (2)	482	648	-166
	I-12	Slump (1)	167	329	-162
	I-13	Bar	680	823	-143
	I-23	Slump (2)	102	297	-195
	I-24a	Stream bottom sediment (3)	127	281	-154
	I-24b	Stream bottom sediment (3)	112	270	-158
	I-25	Beaver dam	206	353	-147
Floodplain	F-1	Pasture	83	160	-77
	F-9	Forest (1)	83	170	-87
	F-10	Forest (2)	196	292	-96
	F-14	Corn Field, tillage	75	129	-54
	F-15	Soybean field	BDL †	119	*n.a*
	F-16	Corn Field, no tillage	54	161	-107

† *Below detection limit*.
‡ *P concentration determined by ICP-AES method – P concentration determined by MG method*
n.a = not available, P_{ox} values was undetected with ICP-AES

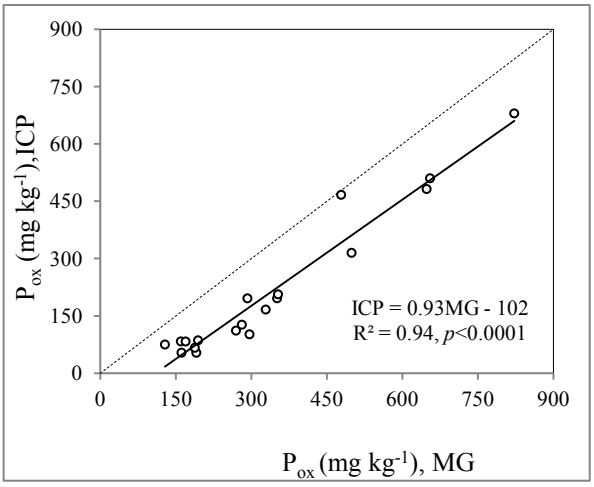

Figure 36. Comparison of inductively coupled plasma-atomic emission spectrometry (ICP-AES, *y* axis) and ICP-AES and the malachite green colorimetric method (MG, *x* axis) in determining P_{ox} concentrations (mg kg^{-1}). Dashed line represents equality line, straight line represents best fit line. Data are only for P_{ox} values detectable with both methods (n=19).

the two methods in this study. The dilution factor could not be greater than 25 for ICP-AES method, since P concentrations in 12 samples were already below the detection limit. On the other hand, the dilution factor could not be less than 50 for MG method, because the green color would not develop. The difference in the dilution factor might have caused both a discrepancy in calculating P_{ox} concentration and matrix interference. For the detection limit of the methods, D'Angelo *et al*. (2001) suggested 0.006 mg P L^{-1} for the MG method in various matrices (water, 1 *M* KCl, 0.1 *M* NaOH, 0.01 *M* $CaCl_2$, and 0.1 *M* HCl). This value is lower than the detection limit for ICP-AES method at $\lambda \pm 178$ nm, reported as 0.018 mg P L^{-1} (Tyler, 1992) and 0.050 mg P L^{-1} (Nakahara, 1985). In another study, Wennrich *et al.* (1995) suggested detection limits of 0.015, 0.080, and 0.150 mg P L^{-1} in water, 25% methanol, and 25% ethanol, respectively. According to Marina and López (2001), poor sensitivity in the ICP-AES method makes it difficult to attain a low detection limit. With a

lower detection limit, the MG method had better sensitivity and accuracy in measuring P at low concentrations.

Comparisons of P determination by ICP-AES and colorimetric methods (i.e. ascorbic acid-molybdate blue) have been reported in previous studies. Sikora *et al.* (2005) reported that Mehlich-3 extractable P (P_{M3}) concentrations determined by ICP-AES method were similar to those by colorimetric methods for 1,118 soils in Kentucky. In other studies, however, the ICP-AES method has been commonly reported to produce in higher values for P concentration than the colorimetric method. For example, Pittman *et al.* (2005), using 6,400 soil samples, found that P_{M3} concentration obtained by the ICP-AES method was 9.1 mg kg^{-1} greater than those determined by colorimetric method. Higher P_{M3} concentrations with the ICP-AES method were also reported by Mallarino (2003) for 59 Iowan soils, with concentrations 12 mg kg^{-1} greater than those determined by the colorimetric method. Using 10 selected samples of Quebec soils, Sen Tran *et al.* (1990) suggested that P_{M3} concentrations determined with ICP-AES were, on average, 5.7 mg kg^{-1} greater than those determined with the colorimetric method. Though the differences between the ICP-AES and colorimetric methods generally depend on soil properties, the range of P concentrations, and the type of soil test extractants (Ivanov *et al.*, 2012), a study by Hart and Cornish (2009) revealed that the ICP-AES method also resulted in significantly higher concentrations of 0.5 *M* $NaHCO_3$ (pH=8.5) extractable P than the colorimetric method in 714 soil samples from New South Wales, Australia. According to Ivanov *et al.* (2012), higher P concentrations from ICP-AES determinations compared to a colorimetric method was due to the organic P (*Po*) in the extract. The colorimetric method measures inorganic orthophosphate, while the ICP-AES method measures both *Po* and orthophosphate. This is so because the plasma in an ICP

atomizes both *Po* and orthophosphate and hence P atoms from both sources contribute the emission intensity.

The lower values of P_{ox} determined with the ICP-AES method compared to the colorimetric MG method in this study contradict the previous studies. The disagreement suggests that there was an analytical problem that might be related to three factors in the ICP-AES method used in this study. Potential analytical issues include: (1) matrix interference, (2) selection of the analytical wavelength, and (3) differential viscosity or density between the standards and the samples. Matrix interference could come from the oxalate itself. It is possible that the relatively high concentration of oxalate ions in the extract could cool the plasma and reduce emission intensity of the analyte. Alternatively, matrix interference could have occurred in the form of molecular compound formation, ionization, or solute vaporization, potentially suppressing the signal of the analyte. Second, the P_{ox} values determined by ICP-AES might be higher if the wavelength selected had been set in the more sensitive near ultra-violet region, for example at $\lambda = 213.62$ nm. Third, standards and samples might not have been perfectly matched since there were some small amounts of nitric acid in the stock solutions of P, Fe, and Al. This might lead to a difference of viscosity and density between the sample solutions and the standards that could, in turn, influence the efficiency of the transport of fluid to the nebulizer. A more complete and deliberate calibration of the ICP-AES method used in this study is needed to explore the possible analytical problems above; however, this was beyond the scope of the present study.

Though in this study the MG method generated greater P_{ox} values than the ICP-AES method, the MG method could be useful for determining P_{ox}. First, the MG method is relatively simple and inexpensive compared to ICP-AES method. Second, the MG method is

more sensitive at low P_{ox} concentration. The accuracy in measuring P_{ox} concentration is essential for calculating degree of P saturation (DPS), one of the indicators to predict P loss from sediments/soils (Hooda *et al*., 2000; Kleinman and Sharpley, 2002; Ohno *et al*., 2007). Low precision of ICP-AES method (Huerta-Diaz *et al.*, 2005) might lead to an underestimate of DPS values that in turn produce inaccuracy in predicting environmental risks associated with P loss from soils/sediments. However, further research is required to investigate the use of the MG method for quantifying P_{ox} in soils and sediments with a wider range of properties.

Conclusions

The two experiments in this study suggest that the MG method is a reliable technique for measuring P concentrations in diverse matrices. For assessing the sequential extraction of P during fractionation analysis, the MG and AA methods resulted in similar P concentration in water, 0.1 *M* NaOH *Pt*, 1 *M* HCl, concentrated HCl *Pt,* and concentrated H_2SO_4 extracts. A slight discrepancy between the MG and AA methods occurred for 0.5 *M* $NaHCO_3$ (*Pi* and *Pt*), 0.1 *M* NaOH (*Pi*), and concentrated HCl (*Pi*) extracts, and the discrepancy depended on sediment type. For determining concentrations of ammonium oxalate extractable P (P_{ox}), the MG method resulted in significantly higher values than those obtained by inductively coupled plasma-atomic emission spectrometry (ICP-AES) method. Despite the discrepancy for some extracts in the sequential extraction and greater P_{ox} values, the microplate system-MG method could be valuable because of its simplicity, sensitivity, and rapidity compared to the AA or ICP-AES methods.

CHAPTER 8

GENERAL CONCLUSIONS

Phosphorus (P) is a major non-point source pollutant of surface waters. Elevated levels of P in streams can cause eutrophication and, in turn, create imbalance in the aquatic ecosystem. High P levels in stream water are often associated with P movement through erosion and surface run off from agricultural land and pastures. This study explored P dynamics in Walnut Creek, Jasper County, Iowa. The alluvial cross section of the Walnut Creek watershed is composed of a sequence of sediments that contribute differentially to the amounts and forms of P entering the stream. Experiments focused on the distribution and transformations of solid phase P in the sediments, P sink/source status of the sediments under varying physicochemical conditions, P release from the sediments to the column water under varying redox potential, and comparison of methods for determining P concentration in diverse matrices.

This study has demonstrated that P forms vary greatly among sediments from the bank, in-stream deposits, and the floodplain of Walnut Creek watershed. Results verified the hypothesis that sediments may contribute differentially to the amounts and forms of P if the sediments are eroded and enter the stream. The inorganic P (*Pi*) bound to Fe was the dominant *Pi* fraction in most of the sediments, reflecting its potential for contributing to dissolved P in the stream water, especially under anaerobic conditions due to the possible disruption of the bond when insoluble Fe(III) is reduced to soluble Fe(II). Organic P (*Po*) comprised about half of the total P in the floodplain sediments, indicating greater potential for the floodplain sediments to contribute *Po* to the stream.

Interestingly, the in-stream deposits had the highest concentrations of total P, Mehlich-3 extractable P, and ammonium oxalate-extractable P, reflecting a potential major contributor to P leaving the watershed from bed sediment re-suspension during high-flow events. This was supported by the output from a model to predict P sink/source status of the sediments, using input data of equilibrium phosphorus concentration (EPC) and phosphorus buffering capacity (PBC). The model predicted that under all physicochemical treatments (by varying redox potential, shaking energy intensity, and solid-to-solution ratio), it was more likely that the in-stream deposits would act as P sources than would the bank sediments or the floodplain soils. In addition, better correlation between P forms and other sediment properties were found when data from the in-stream deposits were excluded from the analysis. This indicates a unique character of the in-stream deposits that was different from that of the bank and the floodplain; likely, it was due to the processes of P adsorption/desorption, P mineralization/immobilization, and P precipitation/dissolution during transport, mixing, and deposition of the sediments along the creek.

The EPC values of sediments varied widely in the Walnut Creek watershed, and the values increased under low redox potential, reflecting the potential of sediments to be sources of P for the stream water when subjected to an anaerobic environment. The increase of EPC values under an anaerobic environment was likely associated with the decrease of Eh and increase of pH due to anoxic conditions created by the anaerobic incubation treatment. In another experiment with samples only from the four major alluvial units of Walnut Creek banks (the Camp Creek, the Roberts Creek, the Gunder, and the Pre-Illinoian Till), the anoxic environment and its effects on Eh/pH were exaggerated with addition of bioavailable carbon in the anaerobic incubation. As a consequence, PBC values decreased significantly,

indicating less ability of the bank sediments to buffer the effects of increasing P in the stream water.

There was also evidence that anaerobic conditions and addition of bioavailable carbon resulted in a redistribution of the forms of P in the bank sediments. The redistribution was especially evident for labile *Pi* and slowly cycling Fe-bound *Pi*. When the bank sediments were subjected to low redox potential, there was an increase in the concentration of labile *Pi* which coincided with a decrease in slowly cycling Fe-bound *Pi*. Among the four bank sediments of Walnut Creek, the younger sediments with more organic matter, i.e., the Camp Creek and Roberts Creek sediments, had greater labile and slowly cycling P associated with Fe, suggesting a greater potential to contribute to elevated levels of P in the stream water, especially if subjected to low redox potential in the stream. This was supported with the results from the experiment to investigate P release under oxic-anoxic conditions. Under anoxic conditions, Camp Creek and Roberts Creek sediments exhibited the highest dissolved P concentrations in the overlying water column.

In a separate laboratory study, the malachite green (MG) and molybdate blue-ascorbic acid (AA) colorimetric methods produced similar results when P concentrations were determined in matrices of water, 0.1 *M* NaOH (total P, abbreviated as *Pt*), 1 *M* HCl, concentrated HCl (*Pt*), and concentrated H_2SO_4. However, a slight discrepancy between the MG and AA methods occurred for 0.5 *M* $NaHCO_3$ (*Pi* and *Pt*), 0.1 *M* NaOH (*Pi*), and concentrated HCl (*Pi*) extracts; it should be noted that the discrepancy depended on sediment type. In addition, P concentrations in ammonium oxalate extracts determined by the MG were significantly higher than those determined by inductively coupled plasma-atomic emission spectrometry (ICP-AES).

In general, this study provided information about the dynamics of P in the Walnut Creek watershed, especially as related to P forms and their transformation at varying redox potential, P sink/source status of the sediments at varying physicochemical conditions, and P release from the sediments to the overlying column water under oxic/anoxic conditions. The findings will be useful for robust modeling predictions of the fate of P in Walnut Creek, as well as other Midwestern streams. This study also demonstrated that despite some discrepancies with the AA and ICP-AES methods, the MG colorimetric method is a reliable technique for determining P concentrations in diverse matrices of P fractionation analysis, as well as in ammonium oxalate extracts.

REFERENCES

Alexander, R.B., R.A. Smith, G.E. Schwarz, E.W. Boyer, J.V. Nolan, and J.W. Brakebill. 2008. Differences in phosphorus and nitrogen delivery to the Gulf of Mexico from the Mississippi River Basin. Environmental Science and Technology 42:822-830.

Alleoni, L.R.F., A.R. Fernandes, and M.d. Campos. 2014. Degree of phosphorus saturation of an Oxisol amended with biosolids in a long-term field experiment. Environmental Science and Pollution Research 21:5511-5520.

Antelo, J., F. Arce, M. Avena, S. Fiol, R. López, and F. Macías. 2007. Adsorption of a soil humic acid at the surface of goethite and its competitive interaction with phosphate. Geoderma 138:12-19.

Arai, Y., and D.L. Sparks. 2001. ATR–FTIR spectroscopic investigation on phosphate adsorption mechanisms at the ferrihydrite–water Interface. Journal of Colloid and Interface Science 241:317-326.

Arias, M.E., M.T. Brown, and J.J. Sansalone. 2013. Characterization of storm water–suspended sediments and phosphorus in an urban catchment in Florida. Journal of Environmental Engineering 139:277-288.

Baker, R.G., E.A.B. III, D.P. Schwert, D.G. Horton, C.A. Chumbley, L.A. Gonzalez, and M.K. Reagan. 1996. Holocene paleoenvironments of Northeast Iowa. Ecological Monograph 66:203-234.

Bar-Yosef, B., U. Kafkafi, R. Rosenberg, and G. Sposito. 1988. Phosphorus adsorption by kaolinite and montmorilonite: I. Effect of time, ionic strength, and pH. Soil Science Society of America Journal 52:1580-1585.

Baykov, A.A., O.A. Evtushenko, and A.M. Avaeva. 1988. A malachite green procedure for orthophosphate determination and its use in alkaline phosphatase-based enzyme immunoassay. Analytical Biochemistry 171:266-270.

Beauchemin, S., and R.R. Simard. 1999. Soil phosphorus saturation degree: Review of some indices and their suitability for P management in Québec, Canada. Canadian Journal of Soil Science 79:615-625.

Bechmann, M.E., P.J.A. Kleinman, A.N. Sharpley, and L.S. Saporito. 2005. Freeze–thaw effects on phosphorus loss in runoff from manured and catch-cropped soils. Journal of Environmental Quality 34:2301-2309.

Bell, A.A.W., J.S. Bailey, R.V. Smith, and M.M. Allen. 2005. Development of an alternative to the Olsen bicarbonate-extraction test for determining plant-available phosphorus in basaltic soils. Soil Use and Management 21:330 - 336.

Bianchi, T.S., S.F. DiMarco, J.H.C. Jr, R.D. Hetland, P. Chapman, J.W. Day, and M.A. Allison. 2010. The science of hypoxia in the Northern Gulf of Mexico: a review. Science of the Total Environment 408:1471–1484.

Bianchin, M.S., L. Smith, and R.D. Beckie. 2011. Defining the hyporheic zone in a large tidally influenced river. Journal of Hydrology 406:16–29.

Blake, L., A.E. Johnston, P.R. Poulton, and K.W.T. Goulding. 2003. Changes in soil phosphorus fractions following positive and negative phosphorus balances for long periods. Plant and Soil 254:245–261.

Borggaard, O.K., B. Raben-Lange, A.L. Gimsing, and B.W. Strobel. 2005. Influence of humic substances on phosphate adsorption by aluminium and iron oxides. Geoderma 127:270–279.

Brand-Klibanski, S., M.I. Litaor, and M. Shenker. 2007. Overestimation of phosphorus adsorption capacity in reduced soils: An artifact of typical batch adsorption experiments. Soil Science Society of America Journal 71:1128-1136.

Breeuwsma, A., J.G.A. Reijerink, and O.F. Schoumans. 1995. Impact of manure on accumulation and leaching of phosphate in areas of intensive livestock farming., p. 239-249, *In* K. Steele, ed. Animal waste and the land–water interface. Lewis Publication, Boca Raton, Florida.

Briggs, M.A., L.K. Lautz, D.K. Hare, and R. González-Pinzón. 2013. Relating hyporheic fluxes, residence times, and redox-sensitive biogeochemical processes upstream of beaver dams. Freshwater Science 32:622-641.

Burchsted, D., M. Daniels, R. Thorson, and J. Vokoun. 2010. The river discontinuum: Applying beaver modifications to baseline conditions for restoration of forested headwaters. BioScience 60:910-922.

Casson, J.P., D.R. Bennett, S.C. Nolan, B.M. Olson, and G.R. Ontkean. 2006. Degree of phosphorus saturation thresholds in manure-amended soils of Alberta. Journal of Environmental Quality 35:2212–2221.

CCME. 2004. Canadian water quality guidelines for the protection of aquatic life: Phosphorus: Canadian Guidance Framework for the Management of Freshwater Systems. In: Canadian environmental quality guidelines, 2004. Canadian Council of Ministers of the Environment, Winnipeg.

Cleveland, C.C., and D. Liptzin. 2007. C:N:P stoichiometry in soil: is there a ‘‘Redfield ratio’’ for the microbial biomass? Biogeochemistry 85:235–252.

Correll, D.L. 1998. The role of phosphorus in the eutrophication of receiving waters: a review. Journal of Environmental Quality 27:261-266.

Cross, W.F., J.P. Benstead, P.C. Frost, and S.A. Thomas. 2005. Ecological stoichiometry in freshwater benthic systems: recent progress and perspectives. Freshwater Biology 50:1895-1912.

D’Angelo, E., J. Crutchfield, and M. Vandiviere. 2001. Rapid, sensitive, microscale determination of phosphate in water and soil. Journal of Environmental Quality 30:2206-2209.

Dalal, R.C. 1977. Soil organic phosphorus. Advances in Agronomy 29:85-117.

Dayton, E.A., and N.T. Basta. 2005. A method for determining the phosphorus sorption capacity and amorphous aluminum of aluminum-based drinking water treatment residuals. Journal of Environmental Quality 34:1112–1118.

Dayton, E.A., S.D. Whitacre, and C.H. Holloman. 2014. Demonstrating the relationship between soil phosphorus measures and phosphorus solubility: Implications for Ohio phosphorus risk assessment tools. Journal of Great Lakes Research 40:473–478.

Deng, Y., and J.B. Dixon. 2002. Soil organic matter and organic–mineral interactions, p. 69-107, *In* J. B. Dixon and D. G. Schulze, eds. Soil Mineralogy with Environmental Applications. Soil Science Society of America, Madison, WI, USA.

Denic, M., K. Stoeckl, B. Gum, and J. Geist. 2014. Physicochemical assessment of *Unio crassus* habitat quality in a small upland stream and implications for conservation. Hydrobiologia 735:111-122.

Devau, N., E.L. Cadre, P. Hinsinger, B. Jaillard, and F. Gérard. 2009. Soil pH controls the environmental availability of phosphorus: Experimental and mechanistic modelling approaches. Applied Geochemistry 24:2163–2174.

Du, S.T., J.L. Shentu, B.F. Luo, I.H. Shamsi, X.Y. Lin, Y.S. Zhang, and C.W. Jin. 2011. Facilitation of phosphorus adsorption onto sediment by aquatic plant debris. Journal of Hazardous Materials 191:212-218.

Essington, M.E. 2004. Soil and water chemistry: an integrative approach. CRC Press, Boca Raton.

Fang, F., P.L. Brezonik, D.J. Mulla, and L.K. Hatch. 2002. Estimating runoff phosphorus losses from calcareous soils in the Minnesota River basin. Journal of Environmental Quality 31:1918–1929.

Favaretto, N., L.D. Norton, C.T. Johnston, J. Bigham, and M. Sperrin. 2012. Nitrogen and phosphorus leaching as affected by gypsum amendment and exchangeable calcium and magnesium. Soil Science Society of America Journal 76:575-585.

Frossard, E., P. Demaria, S. Sinaj, and M. Schärer. 2014. A flow-through reactor to asses potential phosphate release from agricultural soils. Geoderma 219-220:125-135.

Gadde, R.R., and H.A. Laitinen. 1974. Studies of heavy metal adsorption by hydrous iron and manganese oxides Analytical Chemistry 46:2022-2026.

Gikonyo, E.W., A.R. Zaharah, M.M. Hanafi, and A.R. Anuar. 2011. Degree of phosphorus saturation and soil phosphorus thresholds in an Ultisol amended with Triple Superphosphate and Phosphate Rocks. The Scientific World Journal 11:1421–1441.

Glaesner, N., E. Donner, J. Magid, G.H. Rubaek, H. Zhang, and E. Lombi. 2012. Characterization of leached phosphorus from soil, manure, and manure-amended soil by physical and chemical fractionation and diffusive gradients in thin films (DGT. Environmental Science and Technology 46:10564-10571.

Haggard, B.E., E.H. Stanley, and R. Hyler. 1999. Sediment-phosphorus relationships in three Northcentral Oklahoma streams. Transactions of the ASAE 42:1709-1714.

Haggard, B.E., D.R. Smith, and K.R. Brye. 2007. Variations in stream water and sediment phosphorus among select Ozark catchments. Journal of Environmental Quality 36:1725-1734.

Hart, M.R., and P.S. Cornish. 2009. Comparison of bicarbonate-extractable soil phosphorus measured by ICP-AES and colourimetry in soils of south-eastern New South Wales. Australian Journal of Soil Research 47:742-746.

Havlin, J.L., J.D. Beaton, S.L. Tisdale, and W.L. Nelson. 1999. Soil fertility and fertilizers : an introduction to nutrient management Prentice Hall, Upper Saddle River, NJ.

Hawkesford, M., W.H. M., T. Kichey, H. Lambers, J. Schjoerring, I.S. Møller, and P. White. 2012. Functions of macronutrients, *In* P. Marschner, ed. Marschner's Mineral Nutrition of Higher Plants, 3rd ed. Elsevier Ltd.

He, Z., T.S. Griffin, and C.W. Honeycutt. 2004. Evaluation of soil phosphorus transformations by sequential fractionation and phosphatase activity. Soil Science 169:515-527.

Heathwaite, A.L., and R.M. Dils. 2000. Characterising phosphorus loss in surface and subsurface hydrological pathways. The Science of the Total Environment 251/252:523-538.

Heckrath, G., P.C. Brookes, P.R. Poulton, and K.W.T. Goulding. 1995. Phosphorus leaching from soils containing different phosphorus concentrations in the Broadbalk experiment. Journal of Environmental Quality 24:904-910.

Hedley, M.J., J.W.B. Stewart, and B.S. Chauhan. 1982. Changes in inorganic and organic soil phosphorus fractions induced by cultivation practices and by laboratory incubations. Soil Science Society of America Journal 46:970-976.

Helton, A.M., G.C. Poole, R.A. Payn, C. Izurieta, and J.A. Stanford. 2012. Scaling flow path processes to fluvial landscapes: An integrated field and model assessment of temperature and dissolved oxygen dynamics in a river-floodplain-aquifer system. Journal of Geophysical Research 117.

Hill, C.R., and J.S. Robinson. 2012. Phosphorus flux from wetland ditch sediments. Science of the Total Environment 437:315–322.

Hoffmann, C.C., C. Kjaergaard, J. Uusi-Kämppä, H.C.B. Hansen, and B. Kronvang. 2009. Phosphorus retention in riparian buffers: Review of their efficiency. Journal of Environmental Quality 38:1942-1955.

Holford, I.C.R. 1997. Soil phosphorus: its measurement, and its uptake by plants. Australian Journal of Soil Research 35:227-239.

Hong, J.K., and I. Yamane. 1980. Inositol phosphate and inositol humic acid and fulvic acid fractions extracted by three methods. Soil Science and Plant Nutrition 26:491-496.

Hongthanat, N., J. Kovar, and M. Thompson. 2011. Sorption indices to estimate risk of soil phosphorus loss in the Rathbun Lake watershed, Iowa. Soil Science 176:237-244.

Hooda, P.S., A.R. Rendell, A.C. Edwards, P.J.A. Withers, M.N. Aitken, and V.W. Truesdale. 2000. Relating soil phosphorus indices to potential phosphorus release to water. Journal of Environmental Quality 29:1166–1171.

Huanxin, W., B.J. Presley, and D.J. Velinsky. 1997. Distribution and sources of phosphorus in tidal river sediments in the Washington, DC, area. Environmental Geology 30:224-230.

Hubbard, L., D.W. Kolpin, S.J. Kalkhoff, and D.M. Robertson. 2011. Nutrient and sediment concentrations and corresponding loads during the historic June 2008 flooding in Eastern Iowa. Journal of Environmental Quality 40:166–175.

Huerta-Diaz, M.A., A. Tovar-Sánchez, G. Filippelli, J. Latimer, and S.A. Sañudo-Wilhelmy. 2005. A combined CDB-MAGIC method for the determination of phosphorus associated with sedimentary iron oxyhydroxides. Applied Geochemistry 20:2108-2115.

Ige, D.V., O.O. Akinremi, and D.N. Flaten. 2005. Environmental index for estimating the risk of phosphorus loss in calcareous soils of Manitoba. Journal of Environmental Quality 1944–1951:1944-1951.

Itaya, K., and M. Ui. 1966. A new micromethod for the colorimetric determination of inorganic phosphate. Clinica Chimica Acta 14:361-366.

Ivanov, K., P. Zaprjanova, M. Petkova, V. Stefanova, V. Kmetov, D. Georgieva, and V. Angelova. 2012. Comparison of inductively coupled plasma mass spectrometry and colorimetric determination of total and extractable phosphorus in soils. Spectrochimica Acta Part B 71-72:117-122.

Jacobson, L.M., M.B. David, and L.E. Drinkwater. 2011. A spatial analysis of phosphorus in the Mississippi River Basin. Journal of Environmental Quality 40:931-941.

Jaisi, D.P., R.K. Kukkadapu, D.D. Eberl, and H. Dong. 2005. Control of Fe(III) site occupancy on the rate and extent of microbial reduction of Fe(III) in nontronite. Geochimica 69:5429-5440.

Jarvie, H.P., M.D. Ju¨rgens, R.J. Williams, C. Neal, J.J.L. Davies, C. Barrett, and J. White. 2005. Role of river bed sediments as sources and sinks of phosphorus across two major eutrophic UK river basins: the Hampshire Avon and Herefordshire Wye. Journal of Hydrology 304:51-74.

Jarvis, I., and K.E. Jarvis. 1992. Inductively coupled plasma-atomic emission spectrometry in exploration geochemistry Journal of Geochemical Exploration 44:139-200.

Jeannotte, R., D.W. Sommerville, C. Hamel, and J.K. Whalen. 2004. A microplate assay to measure soil microbial biomass phosphorus. Biology and Fertililty of Soils 40:201-205.

Jiang, X., X. Jin, Y. Yao, L. Li, and F. Wu. 2008. Effects of biological activity, light, temperature and oxygen on phosphorus release processes at the sediment and water interface of Taihu Lake, China. Water Research 42:2251–2259.

Jin, X., S. Wang, Y. Pang, and F.C. Wu. 2006. Phosphorus fractions and the effect of pH on the phosphorus release of the sediments from different trophic areas in Taihu Lake, China. Environmental Pollution 139:288-295.

Kang, J., A. Amoozegar, D. Hesterberg, and D.L. Osmond. 2011. Phosphorus leaching in a sandy soil as affected by organic and inorganic fertilizer sources. Geoderma 161:194-201.

Kettler, T.A., J.W. Doran, and T.L. Gilbert. 2001. Simplified method for soil particle-size determination to accompany soil-quality analyses. Soil Science Society of America Journal 65:849-852.

Kim, L.-H., E. Choi, and M. K.Stenstrom. 2003. Sediment characteristics, phosphorus types and phosphorus release rates between river and lake sediments. Chemosphere 50:53-61.

Kirkby, C.A., J.A. Kirkegaard, A.E. Richardson, L.J. Wade, C. Blanchard, and G. Batten. 2011. Stable soil organic matter: A comparison of C:N:P:S ratios in Australian and other world soils. Geoderma 163:197-208.

Kisand, A. 2005. Distribution of sediment phosphorus fractions in hypertrophic strongly stratified Lake Verevi. Hydrobiologia 547:33-39.

Kleinman, P.J.A., and A.N. Sharpley. 2002. Estimating soil phosphorus sorption saturation from Mehlich-3 data. Communications in Soil Science and Plant Analysis 33:1825-1839.

Klotz, R.L. 1991. Temporal relation between soluble reactive phosphorus and factors in stream water and sediments in Hoxie Gorge Creek, New York. Canadian Journal of Fisheries and Aquatic Sciences 48:84-90.

Konen, M.E., P.M. Jacobs, C.L. Burras, B.J. Talaga, and J.A. Mason. 2002. Equations for predicting soil organic carbon using Loss-on-Ignition for North Central U.S. soils. Soil Science Society of America Journal 66:1878–1881.

Koski-Vähälä, J., and H. Hartikainen. 2001. Assessment of the risk of phosphorus loading due to resuspended sediment. Journal of Environmental Quality 30:960–966.

Kuo, S. 1996. Phosphorus, p. 869-919, *In* D. L. Sparks, ed. Methods of Soil Analysis. Part 3. Chemical Methods. . Soil Science Society of America, Madison, WI.

Laboski, C.A.M., and J.A. Lamb. 2004. Impact of manure application on soil phosphorus sorption characteristics and subsequent water quality implications. Soil Science 169:440–448.

Lai, D.Y.F., and K.C. Lam. 2008. Phosphorus retention and release by sediments in the eutrophic Mai Po Marshes, Hong Kong. Marine Pollution Bulletin 57:349-356.

Leinweber, P., E. Lünsmann, and K.U. Eckhardt. 1997. Phosphorus sorption capacities and saturation of soils in two regions with different livestock densities in northwest Germany. Soil Use and Management 13:82-89.

Lerch, R.N., C. Baffaut, N.R. Kitchen, and E.J. Sadler. 2015. Long-term agroecosystem research in the Central Mississippi River Basin: Dissolved nitrogen and phosphorus transport in a high-runoff-potential watershed. Journal of Environmental Quality 44:44–57.

Li, H., L. Liu, M. Li, and X. Zhang. 2013. Effects of pH, temperature, dissolved oxygen, and flow rate on phosphorus release processes at the sediment and water interface in storm sewer. Journal of Analytical Methods in Chemistry 2013:1-7.

Lucci, G.M., R.W. McDowell, and L.M. Condron. 2010. Evaluation of base solutions to determine equilibrium phosphorus concentrations (EPC_0) in stream sediments. International Agrophysics 24:157-163.

Malarino, A.P. 2003. Field calibration for corn of the Mehlich-3 soil phosphorus test with colorimetric and inductively coupled plasma emission spectroscopy determination methods. Soil Science Society of America Journal 68:1928-1934.

Manzoni, S., J.A. Trofymow, R.B. Jackson, and A. Porporato. 2010. Stoichiometric controls on carbon, nitrogen and phosphorus dynamics in decomposing litter. Ecological Monograph 80:89-106.

Marina, M.A., and M.C.B. López. 2001. Determination of phosphorus in raw materials for ceramics: comparison between X-ray fluorescence spectrometry and inductively coupled plasma-atomic emission spectrometry. Analytica Chimica Acta 432 157–163.

Martins, G., L. Peixoto, A.G. Brito, and R. Nogueira. 2014. Phosphorus–iron interaction in sediments: can an electrode minimize phosphorus release from sediments? Reviews in Environmental Science and Bio/Technology 13:265–275.

McDowell, R.W., and A.N. Sharpley. 2001a. A comparison of fluvial sediment phosphorus (P) chemistry in relation to location and potential to influence stream P concentrations. Aquatic Geochemistry 7:255–265.

McDowell, R.W., and A.N. Sharpley. 2001b. Phosphorus losses in subsurface flow before and after manure application to intensively farmed land. The Science of the Total Environment 278:113-125.

Mehlich, A. 1984. Mehlich 3 soil test extractant: A modification of Mehlich 2 extractant. Communications in Soil Science and Plant Analysis 15 1409-1416.

Motomizu, S., and M. Oshima. 1987. Spectrophotometric determination of phosphorus as orthophosphate based on solvent extraction of the ion associate of molybdophosphate with malachite green using flow injection. Analyst 112:295-300.

Nair, V.D., R.R. Villapando, and D.A. Graetz. 1999. Phosphorus retention capacity of the spodic horizon under varying environmental conditions. Journal of Environmental Quality 28:1308-1313.

Nair, V.D., K.M. Portier, D.A. Graetz, and M.L. Walker. 2004. An environmental threshold for degree of phosphorus saturation in sandy soils. Journal of Environmental Quality 33:107-113.

Nakahara, T. 1985. Determination of phosphorus in steels and copper metals by vacuum ultraviolet atomic emission spectrometry with inductively coupled plasma. Spectrochimica Acta 408:293-300.

Nelson, D.W., and L.E. Sommers. 1996. Total carbon, organic carbon and organic matter, p. 539-577, *In* D. L. Sparks, ed. Methods of Soil Analysis. Part 3. Chemical Methods. Book Ser. 5. Soil Sci. Soc. Am., Madison, WI.

Ohno, T., and L.M. Zibilske. 1991. Determination of low concentrations of phosphorus in soil extracts using malachite green. Soil Science Society of America Journal 55:892-895.

Ohno, T., B.R. Hoskins, and M.S. Erich. 2007. Soil organic matter effects on plant available and water soluble phosphorus. Biology and Fertililty of Soils 43:683-690.

Olesik, J.W. 1991. Elemental analysis using ICP-OES and ICP/MS. Analytical Chemistry 63:12A-21A.

Paing, J., E. Gomez, and B. Picot. 1999. Humic substances interactions with sedimentary phosphorus. Analusis 27:436-438.

Palmer, J.A., K.E. Schilling, T.M. Isenhart, R.C. Schultz, and M.D. Tomer. 2014. Streambank erosion rates and loads within a single watershed: bridging the gap between temporal and spatial scales. Geomorphology 209:66-78.

Pant, H.K., and K.R. Reddy. 2001. Phosphorus sorption characteristics of estuarine sediments under different redox conditions. Journal of Environmental Quality 30:1474-1480.

Pautler, M.C., and J.T. Sims. 2000. Relationships between soil test phosphorus, soluble phosphorus and phosphorus saturation in Delaware soils. Soil Science Society of America Journal 64:765–773.

Pettersson, K. 1998. Mechanisms for internal loading of phosphorus in lakes. Hydrobiologia 373/374:21-25.

Phiri, S., E. Barrios, I.M. Rao, and B.R. Singh. 2001. Changes in soil organic matter and phosphorus fractions under planted fallows and a crop rotation system on a Colombian volcanic-ash soil. Plant and Soil 231:211-223.

Pittman, J.J., H. Zhang, J.L. Schroder, and M.E. Payton. 2005. Differences of phosphorus in Mehlich 3 extracts determined by colorimetric and spectroscopic methods. Communications in Soil Science and Plant Analysis 36:1641-1659.

Pizzeghelloa, D., A. Berti, S. Nardib, and F. Moraria. 2011. Phosphorus forms and P-sorption properties in three alkaline soils after long-term mineral and manure applications in north-eastern Italy. Agriculture, Ecosystems and Environment 141:58-66.

Ponnamperuma, F.N. 1972. The chemistry of submerged soils. Advance Agronomy 24:29-96.

Pöthig, R., H. Behrendt, D. Opitz, and G. Furrer. 2010. A universal method to assess the potential of phosphorus loss from soil to aquatic ecosystems. Environmental Science and Pollution Research 17:497-504.

Pratt, C., A. Shilton, S. Pratt, R.G. Haverkamp, and I. Elmetri. 2007. Effects of redox potential and pH changes on phosphorus retention by melter slag filters treating wastewater. Environmental Science and Technology 41:6585-6590.

Pribyl, D.W. 2010. A critical review of the conventional SOC to SOM conversion factor. Geoderma 156:75-83.

Ptacnik, R., T. Andersen, and T. Tamminen. 2010. Performance of the Redfield ratio and a family of nutrient limitation indicators as thresholds for phytoplankton N vs. P limitation. Ecosystems 13:1201-1214.

Quintero, C.E., G.N. Boschetti, and R.A. Benavidez. 1999. Phosphorus retention in some soils of the Argentinean Mesopotamia. Communications in Soil Science and Plant Analysis 30:1449-1461.

Rabalais, N.N., R.E. Turner, and D. Scavia. 2002. Beyond science into policy: Gulf of Mexico hypoxia and the Mississippi River. BioScience 52:129-142.

Reddy, K.R., G.A.O. Connor, and P.M. Gale. 1998. Phosphorus sorption capacities of wetland soils and stream sediments impacted by dairy effluent. Journal of Environmental Quality 27:438-447.

Redfield, A.C.A.S. 1958. The biological control of chemical factors in the environment. American Scientist 46:205-221.

Renneson, M., C. Vandenberghe, J. Dufey, J.M. Marcoen, L. Bock, and G. Colinet. 2015. Degree of phosphorus saturation in agricultural loamy soils with a near-neutral pH. European Journal of Soil Science 66:33-41.

Rommers, P., and P. Boumans. 1996. ICP-AES versus (LA-)IPC-MS: Competition or a happy marriage? – A view supported by current data. Fresenius' Journal of Analytical Chemistry 355:763-770.

Rotterdam, A.M.D.v., D.W. Busssink, E.J.M. Temminghoff, and W.H.v. Riemsdijk. 2012. Predicting the potential of soils to supply phosphorus by integrating soil chemical processes and standard soil tests. Geoderma 189-190:617-626.

Royer, T.V., M.B. David, and L.E. Gentry. 2006. Timing of riverine export of nitrate and phosphorus from agricultural watersheds in Illinois: implications for reducing nutrient loading to the Mississippi river. Environmental Science and Technology 40:4126-4131.

Schilling, K.E., and C.F. Wolter. 2000. Application of GPS and GIS to map channel features in Walnut Creek, Iowa. Journal of The American Water Resources Association 36:1423-1434.

Schilling, K.E., and P. Jacobson. 2008a. Groundwater nutrient concentrations near an incised midwestern stream: Effects of floodplain lithology and land management. Biogeochemistry 87:199–216.

Schilling, K.E., and P. Jacobson. 2008b. Nutrient concentration patterns near an incised stream: effects of floodplain lithology and land management. Biogeochemistry 87:199-216.

Schilling, K.E., and P. Jacobson. 2014. Effectiveness of natural riparian buffers to reduce subsurface nutrient losses to incised streams. Catena:140-148.

Schilling, K.E., Y.K. Zhang, and P. Drobney. 2004. Water table fluctuations near an incised stream, Walnut Creek, Iowa. Journal of Hydrology 286:236-248.

Schilling, K.E., Z. Li, and Y.K. Zhang. 2006a. Groundwater-surface water interaction in the riparian zone of an incised stream, Walnut Creek, Iowa. Journal of Hydrology 327:140-150.

Schilling, K.E., T. Hubbard, J. Luzier, and J. Spooner. 2006b. Walnut Creek watershed restoration and water quality monitoring project: final report. Iowa Department of Natural Resources, Iowa City, IA.

Schilling, K.E., T.M. Isenhart, J.A. Palmer, C.F. Wolter, and J. Spooner. 2011. Impacts of land-cover change on suspended sediment transport in two agricultural watersheds. Journal of The American Water Resources Association 47:672-686.

Schilling, K.E., J.A. Palmer, E.A.B. III, P. Jacobson, R.C. Schultz, and T.M. Isenhart. 2009. Vertical distribution of total carbon, nitrogen, and phosphorus in riparian soils of Walnut Creek, southern Iowa. Catena 77:266-273.

Schlesinger, W.H., and E.S. Bernhardt. 2013. Biogeochemistry: An analysis of global change. 3 ed. Academic Press.

Schrijver, A.D., P.D. Frenne, J. Staelens, L. Baeten, K. Verheyen, L. Vesterdal, K. Hansen, L. Augusto, and D.L. Achat. 2012. Four decades of post-agricultural forest development have caused major redistributions of soil phosphorus fractions. Oecologia 169:221-234.

Sen Tran, T., M. Giroux, J. Guilbeault, and P. Audesse. 1990. Evaluation of Mehlich 3 extractant to estimate the available P in Quebec soils. Communications in Soil Science and Plant Analysis 21:1-28.

Shang, C., and L.W. Zelasny. 2008. Selective dissolution techniques for mineral analysis of soils and sediments, p. 33-80, *In* A. L. Ulery and L. R. Dress, eds. Methods of Soil Analysis Part 5—Mineralogical Methods. Soil Science Society of America, Madison, Wisconsin, USA.

Sharpley, A.N., T. Daniel, T. Sims, J. Lemunyon, R. Stevens, and R. Parry. 2003. Agricultural Phosphorus and Eutrophication, 2nd ed. U.S. Department of Agriculture, Agricultural Research Service, ARS-149, 44pp.

Sikora, F.J., P.S. Howe, L.E. Hill, D.C. Reid, and D.E. Harover. 2005. Comparison of colorimetric and ICP determination of phosphorus in Mehlich3 soil extracts. Communications in Soil Science and Plant Analysis 36:875-887.

Sims, J.T., R.R. Simard, and B.C. Joern. 1998. Phosphorus loss in agricultural drainage: historical perspective and current research. Journal of Environmental Quality 27:277-293.

Sims, J.T., R.O. Maguire, A.B. Leytem, K.L. Gartley, and M.C. Pautler. 2002. Evaluation of Mehlich 3 as an agri-environmental soil phosphorus test for the Mid-Atlantic United States of America. Soil Science Society of America Journal 66:2016–2032.

Sinaj, S., C. Stamm, G.S. Toor, L.M. Condron, T. Hendry, H.J. Di, K.C. Cameron, and E. Frossard. 2002. Phosphorus exchangeability and leaching losses from two grassland soils. Journal of Environmental Quality 31:319-330.

Smolders, A.J.P., E.C.H.E.T. Lucassen, R. Bobbink, J.G.M. Roelofs, and L.P.M. Lamers. 2010. How nitrate leaching from agricultural lands provokes phosphate eutrophication in groundwater fed wetlands: the sulphur bridge. Biogeochemistry 98:1-7.

Soil Survey Staff, N.R.C.S., United States Department of Agriculture. Web Soil Survey. Available at http://websoilsurvey.nrcs.usda.gov/. Accessed 05/16/2016.

Stelzer, R.S., and G.A. Lamberti. 2001. Effects of N: P ratio and total nutrient concentration on stream periphyton community structure, biomass, and elemental composition. Limnology and Oceanography 46:356–367.

Stumm, W., and J.J. Morgan. 1970. Aquatic chemistry: An introduction emphasizing chemical equilibria in natural waters Willey-Interscience, New York.

Stutter, M.I., B.O.L. Demars, and S.J. Langan. 2010. River phosphorus cycling: Separating biotic and abiotic uptake during short-term changes in sewage effluent loading. Water Research 44:4425-4436.

Subba Rao, A., K. Sammi Reddy, and P.N. Takkar. 1997. Malachite green method compared to ascorbic acid for estimating small amounts of phosphorus in water, 0.01 M calcium chloride, and Olsen soil extracts. Communications in Soil Science and Plant Analysis 28:589-601.

Sui, Y., and M.L. Thompson. 2000. Phosphorus sorption, desorption, and buffering capacity in a biosolids-amended Mollisol. Soil Science Society of America Journal 64:161-169.

Sui, Y., M.L. Thompson, and C. Shang. 1999a. Fractionation of phosphorus in a Mollisol amended with biosolids. Soil Science Society of America Journal 63:1174-1180.

Sui, Y., M.L. Thompson, and C.W. Mize. 1999b. Redistribution of biosolids-derived total phosphorus applied to a Mollisol. Journal of Environmental Quality 28:1068-1074.

Susanto, J.P., M. Oshima, S. Motomizu, H. Mikasa, and Y. Hori. 1995. Determination of micro amounts of phosphorus with malachite green using a filtration-dissolution preconcentration method and flow injection-spectrophotometric detection. Analyst 120:187-190.

Sylvan, J.B., Q. Dortch, D.M. Nelson, A.F.M. Brown, W. Morrison, and J.W. Ammerman. 2006. Phosphorus limits phytoplankton growth on the Louisiana shelf during the period of hypoxia formation. Environmental Science and Technology 40:7548-7553.

Taylor, A.W., and H.M. Kunishi. 1971. Phosphate equilibria on stream sediment and soil in a watershed draining an agricultural region. Journal of Agricultural and Food Chemistry 19:827-831.

Tiessen, H., and J.O. Moir. 2008. Characterization of available P by sequential extraction, p. 293-306, *In* M. R. Carter, ed. Soil sampling and analysis, 2nd edn ed. Canadian Society of Soil Sceince, New York.

Tufekcioglu, M., R.C. Schultz, G.N. Zaimes, T.M. Isenhart, and A. Tufekcioglu. 2012. Riparian grazing impacts on streambank erosion and phosphorus loss via surface runoff. Journal of The American Water Resources Association 49:103-113.

Turner, B.L., and P.M. Haygarth. 2000. Phosphorus forms and concentrations in leachate under four grassland soil types. Soil Science Society of America Journal 64:1090-1099.

Tyler, G. 1992. AA or ICP-which do you choose? . Chemistry in Australia 159(4):150-152.

Upreti, K., S.R. Joshi, J. McGrath, and D.P. Jaisi. 2015. Factors controlling phosphorus mobilization in a coastal plain tributary to the Chesapeake Bay. Soil Science Society of America Journal 79:826-837.

USEPA. 1986. Quality criteria for water (EPA 440/5-86-001). United States-Environmental Protection Agency, Washington, DC.

Vadas, P.A., and J.T. Sims. 1998. Redox status, poultry litter, and phosphorus solubility in Atlantic Coastal Plain soils. Soil Science Society of America Journal 62:1025-1034.

Van Moorleghem, C., L. Six, F. Degryse, E. Smolders, and R. Merckx. 2011. Effects of organic P forms and P present in inorganic colloids on the determination of dissolved P in environmental samples by the diffuse gradient in thin films technique, ion chromatography, and colorimetry. Analytical Chemistry 83:5317-5323.

Van Veldhoven, P.P., and G.P. Mannaerts. 1987. Inorganic and organic phosphate measurements in the nanomolar range. Analytical Biochemistry 161:45-48.

Varinderpal-Singh, N.S. Dhillon, B.S. Brar, and Raj-Kumar. 2007. Relative contribution of different sized soil separates to inorganic P fractions in a Typic Ustochrept of N-W India. Nutrient Cycling in Agroecosystems 79:161-168.

Wang, S., X. Jin, Q. Bua, L. Jiao, and F. Wu. 2008. Effects of dissolved oxygen supply level on phosphorus release from lake sediments. Colloids and Surfaces A: Physicochemical and Engineering Aspects 316:245-252.

Wang, Z., C. Lin, M. He, X. Quan, and Z. Yang. 2010. Phosphorus content and fractionation of phosphate in the surface sediments of the Dalio river system in China. Environmental Earth Science 59:1349-1357.

Watanabe, F.S., and S.R. Olsen. 1965. Test of an ascorbic acid method for determining phosphorus in water and $NaHCO_3$ extracts from soil. Soil Science Society Proceeding:677-678.

Wennrich, R., A. Mroczek, K. Dittrich, and G. Werner. 1995. Determination of nonmetals using ICP-AES-techniques. Fresenius' Journal of Analytical Chemistry 352:461-469.

Williams, C.H., and A. Steinbergs. 1958. Sulphur and phosphorus in some eastern Australian soils. Australian Journal of Agricultural Research:483-491.

Wilson, C.G., R.A. Kuhnle, D.D. Bosch, J.L. Steiner, P.J. Starks, M.D. Tomer, and G.V. Wilson. 2008. Quantifying relative contributions from sediment sources in Conservation Effects Assessment Project watersheds. Journal of Soil and Water Conservation 63:523-532.

Xu, D., S. Ding, B. Li, X. Bai, C. Fan, and C. Zhang. 2013. Speciation of organic phosphorus in a sediment profile of Lake Taihu I: Chemical forms and their transformation. Journal of Environmental Sciences 25:637-644.

Xue, Q., L. Lu, Y. Zhou, L. Qi, P. Dai, X. Liu, C. Sun, and X. Lin. 2014. Deriving sorption indices for the prediction of potential phosphorus loss from calcareous soils. Environmental Science and Pollution Research 21:1564-1571.

Yan, X., D. Wanga, H. Zhang, G. Zhanga, and Z. Weid. 2013. Organic amendments affect phosphorus sorption characteristics in a paddy soil. Agriculture, Ecosystems and Environment 175:47-53.

Yao, W., and F.J. Millero. 1996. Adsorption of phosphate on manganese dioxide in seawater. Environmental Science and Technology 30:536-541.

Yoo, J.-H., H.-M. Roa, W.-J. Choib, S.-H. Yoo, and K.-H. Han. 2006. Phosphorus adsorption and removal by sediments of a constructed marsh in Korea. Ecological Engineering 27:109-117.

You, S.J., S. Thakali, and H.E. Allen. 2006. Characteristics of soil organic matter (SOM) extracted using base with subsequent pH lowering and sequential pH extraction. Environment International 36:101-105.

Zaimes, G.N., R.C. Schultz, and T.M. Isenhart. 2008. Total phosphorus cocentrations and compaction in riparian area under different land-uses of Iowa. Agriculture, Ecosystems and Environment 127:22-30.

Zhang, H., and J.L. Kovar. 2009. Fractionation of soil phosphorus, *In* J. L. Kovar and G. M. Pierzynski, eds. Methods of Phosphorus Analysis for Soils, Sediments, Residuals, and Water:Second Edition, Vol. 408. Southern Cooperative Series Bulletin.

Zhang, H.C., Z.H. Chao, Q.R. Shen, and M.H. Wong. 2003. Effect of phosphate fertilizer application on phosphorus (P) losses from paddy soils in Taihu Lake Region I. Effect phosphate fertilizer rate on P losses from paddy soil. Chemosphere 50:695-701.

Zhou, M., and Y. Li. 2001. Phosphorus-sorption characteristics of calcareous soils and limestone from the Southern Everglades and adjacent farmlands. Soil Science Society of America Journal 65:1404-1412.

Zhou, X., and G. Arthur. 1992. Improved procedures for the determination of lipid phosphorus by malachite green. Journal of Lipid Research 33:1233-1236.

APPENDIX A

NOMENCLATURE

A	Treatment without anaerobic incubation
AA	Molybdate blue-ascorbic acid method
Al_{ox}	Ammonium oxalate extractable Al
Al-*Pi*	Al bound inorganic P
AN	Treatment with anaerobic incubation
ANG	Treatment with anaerobic incubation + glucose
BDL	Below Detection Limit
C	Liquid-phase P
Ca_{M3}	Mehlich-3 extractable Ca
Ca-*Pi*	Ca bound inorganic P
C_{pw}	Pore water P concentration
DOC	Dissolved Organic Carbon
DPS	Degree of Phosphorus Saturation
EPC	Equilibrium Phosphorus Concentration
Fe_{CBD}	Citrate-bicarbonate-dithionite extractable Fe
Fe_{ox}	Ammonium oxalate extractable Fe
Fe-*Pi*	Fe bound inorganic P
HA-*Po*	Organic P associated with humic acid
ICP-AES	Inductively Coupled Plasma-Atomic Emission Spectrometry
K_{M3}	Mehlich-3 extractable K

Lab-*Po*	Labile organic P
LS	Treatment of low solid-to-solution ratio
HE	Treatment of high shaking energy
MG	Malachite green method
Mg_{M3}	Mehlich-3 extractable Mg
MLab-*Po*	Moderately labile organic P
Mn_{ox}	Ammonium oxalate extractable Mn
Na_{M3}	Mehlich-3 extractable Na
NLab-*Po*	Nonlabile organic P
OM	Organic matter
OX	Treatment of oxic environment
PBC	Phosphorus Buffering Capacity
P_{H_2O}	Water extractable P
Pi	Inorganic P
Pi_{sum}	Sum of all individual inorganic P fractions
P_{Lab}	Labile P
P_{M3}	Mehlich-3 extractable P
Po	Organic P
Po_{sum}	Sum of all individual organic P fractions
P_{ox}	Ammonium oxalate extractable P
P_{Res}	Residue P
PSD	Particle size distribution
P_{Slow}	Slowly cycling P

P_{Stab}	Stable P
Pt	Total P in a P fraction
Q	Solid-phase P
RS-*Pi*	Reductant soluble inorganic P
SL-*Pi*	Soluble and loosely bound inorganic P
TP	Total P determined by perchloric+nitric acid digestion
TP_{sum}	Sum of all individual P fractions

APPENDIX B

SUPPORTING MATERIALS

Appendix B1. Coordinates of the sampling sites.

Group	Code	Description	Coordinate position
Banks	B-2	Camp Creek (1)	41° 36.355’ N, 93° 18.372’ W
	B-3	Roberts Creek (1)	41° 36.355’ N, 93° 18.372’ W
	B-7	Till (1)	41° 35.705’ N, 93° 17.389’ W
	B-17	Camp Creek (2)	41° 33.382' N, 93° 15.887' W
	B-18	Roberts Creek (2)	41° 33.382' N, 93° 15.887' W
	B-19	Gunder (1)	41° 33.382' N, 93° 15.887' W
	B-20	Till (2)	41° 33.382' N, 93° 15.887' W
	B-21	Camp Creek (3)	41° 32.763’ N, 93° 15.578’ W
	B-22	Roberts Creek (3)	41° 32.763’ N, 93° 15.578’ W
In-stream	I-4	Stream bottom sediment (1)	41° 36.355’ N, 93° 18.372’ W
deposit	I-5	Slump, debris dam	41° 35.807’ N, 93° 17.522’ W
	I-6	Stream bed sediments, debris dam	41° 35.807’ N, 93° 17.522’ W
	I-8	Sand bar	41° 35.705’ N, 93° 17.389’ W
	I-11	Stream bottom sediment (2)	41° 32.519’ N, 93° 15.481’ W
	I-12	Slump (1)	41° 32.519’ N, 93° 15.481’ W
	I-13	Bar	41° 32.519’ N, 93° 15.481’ W
	I-23	Slump (2)	41° 32.763’ N, 93° 15.578’ W
	I-24	Stream bottom sediment (3)	41° 32.763’ N, 93° 15.578’ W
	I-25	Beaver dam	41° 35.732’ N, 93° 17.436’ W
Floodplain	F-1	Pasture	41° 36.355’ N, 93° 18.372’ W
	F-9	Forest (1)	41° 35.705’ N, 93° 17.389’ W
	F-10	Forest (2)	41° 32.519’ N, 93° 15.481’ W
	F-14	Corn Field, tillage	41° 35.705’ N, 93° 17.389’ W
	F-15	Soybean field	41° 32.519’ N, 93° 15.481’ W
	F-16	Corn Field, no tillage	41° 36.525’ N, 93° 17.464’ W

Appendix B2. Stratigraphy of Walnut Creek bank for the sampling sites of B-17, B-18, B-19, and B-20.

B-17. Camp Creek Member
B-18. Roberts Creek Member
B-19. Gunder Member
B.20. Pre-Illinoian Till

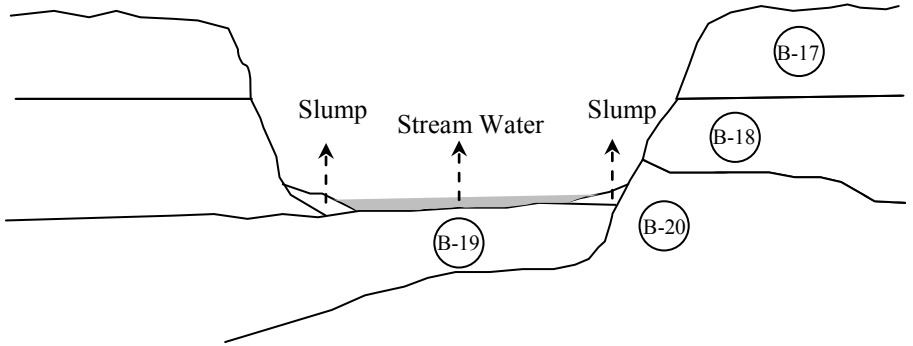

Appendix B3. Inorganic P fractions (data for Fig. 8). Nomenclatures (SL-*Pi,* Al-*Pi,* Fe-*Pi,* RS-*Pi,* Ca-*Pi,* P_{isum}, P_{sum}) refer to Appendix A.

Group	Code	Description	SL- *Pi*	Al-*Pi*	Fe- *Pi*	RS-*Pi*	Ca-*Pi*	Pi_{sum}	% Pi_{sum} to P_{sum}
			---------- mg kg^{-1} ----------						
Banks	B-2	Camp Creek (1)	5	29	88	47	36	205	42.9
	B-3	Roberts Creek (1)	7	65	121	72	142	407	52.1
	B-7	Till (1)	7	29	55	58	159	308	75.3
	B-17	Camp Creek (2)	6	16	102	48	66	238	55.7
	B-18	Roberts Creek (2)	5	24	140	53	84	306	60.6
	B-19	Gunder (1)	5	11	37	26	288	367	89.7
	B-20	Till (2)	6	0	1	69	269	345	83.1
	B-21	Camp Creek (3)	5	44	114	73	70	306	59.2
	B-22	Roberts Creek (3)	11	33	90	70	81	285	55.2
In-stream deposit	I-4	Stream bottom sediment (1)	11	68	151	95	198	523	86.6
	I-5	Slump, debris dam	4	4	31	7	79	125	35.0
	I-6	Stream bed sediments, debris dam	5	47	278	223	184	737	75.9
	I-8	Sand bar	7	56	257	85	75	480	79.7
	I-11	Stream bottom sediment (2)	6	80	571	48	151	856	90.3
	I-12	Slump (1)	8	65	167	62	75	377	68.4
	I-13	Bar	6	99	422	32	115	674	85.9
	I-23	Slump (3)	5	54	180	218	118	575	84.3
	I-24	Stream bottom sediment (3)	6	38	217	34	100	395	62.4
	I-25	Beaver dam	7	54	243	65	101	470	76.2
Floodplain	F-1	Pasture	5	19	97	58	37	216	41.9
	F-9	Forest (1)	7	49	99	47	39	241	43.5
	F-10	Forest (2)	6	55	148	83	62	354	52.7
	F-14	Corn Field, tillage	7	25	104	52	39	227	49.0
	F-15	Soybean field	6	22	91	75	27	221	47.2
	F-16	Corn Field, no tillage	9	49	112	61	26	257	50.8

Appendix B4. Organic P fractions (data for Fig. 9). Nomenclatures (Lab-*Po,* MLab-*Po,* FA-*Po,* HA-*Po,* NLab-*Po,* Po_{sum}, P_{sum}) refer to Appendix A.

Group	Code	Description	Lab-*Po*	MLab-*Po*	FA-*Po*	HA-*Po*	NLab-*Po*	Po_{sum}	% Po_{sum} to P_{sum}
			---------- mg kg^{-1} ----------						
Banks	B-2	Camp Creek (1)	37	2	78	73	83	273	57.1
	B-3	Roberts Creek (1)	33	4	127	105	106	375	47.9
	B-7	Till (1)	6	6	14	2	73	101	24.7
	B-17	Camp Creek (2)	18	5	63	54	49	189	44.3
	B-18	Roberts Creek (2)	17	3	64	71	44	199	39.4
	B-19	Gunder (1)	2	0	8	5	27	42	10.3
	B-20	Till (2)	2	2	9	5	52	70	16.9
	B-21	Camp Creek (3)	30	5	55	49	72	211	40.8
	B-22	Roberts Creek (3)	31	8	57	62	73	231	44.8
In-stream deposit	I-4	Stream bottom sediment (1)	4	5	18	7	47	81	13.4
	I-5	Slump, debris dam	27	8	58	71	68	232	65.0
	I-6	Stream bed sediments, debris dam	12	4	35	20	163	234	24.1
	I-8	Sand bar	13	3	33	27	46	122	20.3
	I-11	Stream bottom sediment (2)	8	7	22	14	41	92	9.7
	I-12	Slump (1)	22	5	45	43	59	174	31.6
	I-13	Bar	8	4	27	27	45	111	14.1
	I-23	Slump (3)	9	7	17	25	49	107	15.7
	I-24	Stream bottom sediment (3)	25	12	117	7	77	238	37.6
	I-25	Beaver dam	8	5	54	39	41	147	23.8
Floodplain	F-1	Pasture	38	2	90	84	86	300	58.1
	F-9	Forest (1)	47	9	87	85	85	313	56.5
	F-10	Forest (2)	38	5	96	92	87	318	47.3
	F-14	Corn Field, tillage	19	6	71	74	66	236	51.0
	F-15	Soybean field	22	6	85	68	66	247	52.8
	F-16	Corn Field, no tillage	25	3	82	77	62	249	49.2

Appendix B5. pH and Eh at equilibrium in the adsorption study (data for Fig. 12). Nomenclatures of the treatments (OX, AN, HE, LS) refer to Appendix A.

Group	Code	Description	pH				Eh (mV)			
			OX	AN	HE	LS	OX	AN	HE	LS
Banks	B-2	Camp Creek (1)	6.9	7.4	6.9	7.8	553	411	528	491
	B-3	Roberts Creek (1)	6.9	7.4	6.9	7.7	549	401	531	489
	B-7	Till (1)	7.7	8.1	7.7	8.2	506	382	554	570
	B-17	Camp Creek (2)	7.0	7.9	7.0	7.7	556	378	567	486
	B-18	Roberts Creek (2)	6.9	7.8	6.9	7.6	555	381	570	488
	B-19	Gunder (1)	7.8	8.1	7.9	8.2	472	355	487	464
	B-20	Till (2)	7.9	8.1	7.9	8.3	479	347	496	467
	B-21	Camp Creek (3)	7.0	7.9	7.1	7.8	509	363	530	481
	B-22	Roberts Creek (3)	6.9	7.8	6.9	7.7	518	364	535	483
In-stream deposit	I-4	Stream bottom sediment (1)	7.3	7.7	7.4	8.0	524	395	551	489
	I-5	Slump, debris dam	6.5	6.8	6.4	7.5	567	430	491	478
	I-6	Stream bed sediments, debris dam	7.6	7.8	7.7	8.1	502	387	510	485
	I-8	Sand bar	7.4	8.1	7.5	8.0	503	381	539	564
	I-11	Stream bottom sediment (2)	7.1	7.9	7.2	7.8	509	384	538	560
	I-12	Slump (1)	7.2	8.0	7.3	8.0	503	383	537	559
	I-13	Bar	7.2	8.0	7.2	7.8	558	378	579	517
	I-23	Slump (3)	7.3	8.0	7.3	8.0	502	344	525	474
	I-24	Stream bottom sediment (3)	6.3	7.3	6.4	7.5	321	130	301	463
	I-25	Beaver dam	7.8	8.0	7.6	8.1	368	-132	597	558
Floodplain	F-1	Pasture	6.9	7.5	6.8	7.7	559	397	544	495
	F-9	Forest (1)	6.9	7.9	6.8	7.7	537	390	538	563
	F-10	Forest (2)	6.8	7.9	7.0	7.7	530	386	555	564
	F-14	Corn Field, tillage	7.1	8.0	7.0	7.7	561	383	578	500
	F-15	Soybean field	7.1	8.0	7.1	7.8	558	376	572	494
	F-16	Corn Field, no tillage	6.9	7.9	7.0	7.7	563	374	573	491

Appendix B6. Liquid-phase P (C, in mg L^{-1}) and solid-phase P (Q, in mg kg^{-1}) in the isotherm adsorption study under the treatment of OX (data for Table 11). Nomenclatures of the treatment (OX) refer to Appendix A, sample codes refer to Appendix B1.

Spiked P Level (mg L^{-1})	B-2		B-3		B-7		B-17		B-18		B-19		B-20	
	C	Q	C	Q	C	Q	C	Q	C	Q	C	Q	C	Q
0.00	0.043	-0.526	0.146	-2.576	0.002	0.269	0.041	0.548	0.032	0.725	0.037	0.612	0.013	1.100
0.05	0.048	0.445	0.142	-1.424	0.003	0.450	0.046	1.762	0.036	1.962	0.041	1.859	0.015	2.381
0.10	0.051	1.598	0.158	-0.543	0.004	1.794	0.048	2.880	0.037	3.088	0.046	2.923	0.016	3.532
0.20	0.059	3.632	0.182	1.170	0.005	3.967	0.063	5.021	0.040	5.497	0.038	5.541	0.016	5.980
0.40	0.074	8.064	0.222	5.096	0.007	8.131	0.082	9.270	0.053	9.857	0.073	9.429	0.019	10.555
0.80	0.134	15.376	0.312	11.797	0.019	17.105	0.125	16.014	0.079	16.900	0.139	15.705	0.030	17.904
Spiked P Level (mg L^{-1})	B-21		B-22		I-4		I-5		I-6		I-8		I-11	
	C	Q	C	Q	C	Q	C	Q	C	Q	C	Q	C	Q
0.00	0.059	0.170	0.042	0.494	0.041	-0.371	0.007	0.169	0.032	-0.190	0.039	-0.327	0.003	0.382
0.05	0.067	1.144	0.048	1.528	0.048	0.496	0.008	0.338	0.038	0.691	0.045	0.530	0.005	1.347
0.10	0.068	2.084	0.048	2.486	0.054	1.698	0.008	1.703	0.044	1.892	0.053	1.629	0.006	2.648
0.20	0.074	4.237	0.057	4.587	0.076	3.458	0.010	3.835	0.054	3.903	0.059	3.642	0.009	4.804
0.40	0.092	8.287	0.068	8.763	0.086	7.640	0.015	7.926	0.066	7.943	0.074	7.425	0.009	9.093
0.80	0.135	16.068	0.101	16.755	0.143	15.051	0.018	17.007	0.095	15.831	0.130	14.500	0.016	17.505
Spiked P Level (mg L^{-1})	I-12		I-13		I-23		I-24		I-25		F-1		F-9	
	C	Q	C	Q	C	Q	C	Q	C	Q	C	Q	C	Q
0.00	0.172	-3.017	0.104	-0.661	0.142	-1.503	0.007	1.199	0.049	-0.105	0.038	-0.425	0.038	-0.425
0.05	0.202	-2.623	0.104	0.667	0.160	-0.700	0.010	2.286	0.061	1.305	0.044	0.524	0.044	0.524
0.10	0.205	-1.356	0.120	1.413	0.162	0.206	0.010	3.238	0.064	2.570	0.047	1.680	0.047	1.680
0.20	0.225	0.475	0.127	3.536	0.144	2.852	0.012	5.488	0.072	4.411	0.052	3.772	0.052	3.772
0.40	0.287	3.547	0.127	7.921	0.209	5.953	0.012	9.906	0.076	8.634	0.073	8.089	0.073	8.089
0.80	0.357	10.745	0.146	15.855	0.258	13.638	0.016	18.489	0.083	15.739	0.142	15.253	0.142	15.253
Spiked P Level (mg L^{-1})	F-10		F-14		F-15		F-16							
	C	Q	C	Q	C	Q	C	Q						
0.00	0.108	-1.235	0.014	1.152	0.012	1.187	0.052	0.393						
0.05	0.116	-0.625	0.025	2.247	0.017	2.403	0.096	0.822						
0.10	0.121	0.250	0.039	3.037	0.019	3.432	0.142	0.971						
0.20	0.152	1.375	0.026	5.545	0.024	5.587	0.149	3.079						
0.40	0.174	4.141	0.048	9.509	0.041	9.609	0.201	6.419						
0.80	0.218	9.603	0.074	17.263	0.053	17.656	0.327	12.197						

Appendix B7. Liquid-phase P (C, in mg L^{-1}) and solid-phase P (Q, in mg kg^{-1}) in the isotherm adsorption study under the treatment of AN (data for Table 11). Nomenclatures of the treatment (AN) refer to Appendix A, sample codes refer to Appendix B1.

Spiked P Level (mg L^{-1})	B-2		B-3		B-7		B-17		B-18		B-19		B-20	
	C	Q	C	Q	C	Q	C	Q	C	Q	C	Q	C	Q
0.00	0.103	-1.843	0.287	-5.626	0.027	0.245	0.047	-0.105	0.038	0.085	0.055	-0.050	0.026	0.546
0.05	0.108	-1.013	0.257	-4.043	0.038	1.605	0.050	1.143	0.044	1.274	0.055	1.143	0.026	1.726
0.10	0.119	-0.064	0.311	-3.927	0.038	2.916	0.050	2.199	0.050	2.205	0.065	1.976	0.028	2.721
0.20	0.126	2.213	0.335	-1.953	0.050	5.116	0.064	4.322	0.051	4.588	0.082	3.897	0.033	4.871
0.40	0.121	7.013	0.347	2.508	0.047	9.415	0.077	8.363	0.054	8.845	0.081	8.113	0.044	8.884
0.80	0.168	13.850	0.406	9.113	0.083	16.993	0.095	16.456	0.069	16.979	0.139	14.910	0.090	15.889
Spiked P Level (mg L^{-1})	B-21		B-22		I-4		I-5		I-6		I-8		I-11	
	C	Q	C	Q	C	Q	C	Q	C	Q	C	Q	C	Q
0.00	0.091	-0.763	0.074	-0.426	0.091	-0.763	0.074	-0.426	0.091	-0.763	0.301	-5.242	0.137	-1.958
0.05	0.095	0.335	0.080	0.637	0.095	0.335	0.080	0.637	0.095	0.335	0.343	-4.492	0.113	0.094
0.10	0.099	1.294	0.083	1.624	0.099	1.294	0.083	1.624	0.099	1.294	0.350	-3.328	0.162	0.436
0.20	0.096	3.610	0.081	3.931	0.096	3.610	0.081	3.931	0.096	3.610	0.359	-1.060	0.215	1.821
0.40	0.100	7.720	0.086	8.014	0.100	7.720	0.086	8.014	0.100	7.720	0.389	2.566	0.246	5.441
0.80	0.126	15.139	0.110	15.504	0.126	15.139	0.110	15.504	0.126	15.139	0.432	10.012	0.311	12.447
Spiked P Level (mg L^{-1})	I-12		I-13		I-23		I-24		I-25		F-1		F-9	
	C	Q	C	Q	C	Q	C	Q	C	Q	C	Q	C	Q
0.00	0.418	-7.598	0.200	-3.160	0.157	-2.093	0.042	0.224	0.153	-2.184	0.122	-2.234	0.095	-1.115
0.05	0.467	-6.990	0.214	-2.127	0.172	-1.187	0.044	1.352	0.175	-0.991	0.135	-1.549	0.091	0.545
0.10	0.460	-5.527	0.203	-0.869	0.149	0.306	0.047	2.337	0.194	-0.045	0.137	-0.425	0.091	1.870
0.20	0.483	-3.543	0.218	1.234	0.172	2.102	0.048	4.581	0.210	1.642	0.143	1.872	0.098	4.148
0.40	0.504	0.285	0.228	5.337	0.202	5.681	0.051	8.716	0.219	5.748	0.166	6.110	0.114	8.082
0.80	0.584	6.998	0.249	13.330	0.242	12.831	0.065	16.354	0.253	12.349	0.193	13.318	0.138	15.916
Spiked P Level (mg L^{-1})	F-10		F-14		F-15		F-16							
	C	Q	C	Q	C	Q	C	Q						
0.00	0.270	-4.631	0.050	-0.155	0.055	-0.271	0.186	-2.878						
0.05	0.265	-2.951	0.063	0.890	0.052	1.098	0.213	-2.109						
0.10	0.277	-1.864	0.073	1.728	0.059	2.018	0.235	-1.502						
0.20	0.298	0.150	0.078	4.034	0.076	4.089	0.296	-0.315						
0.40	0.324	3.894	0.101	7.886	0.086	8.194	0.343	3.027						
0.80	0.372	11.270	0.107	16.191	0.133	15.731	0.440	9.532						

Appendix B8. Liquid-phase P (C, in mg L^{-1}) and solid-phase P (Q, in mg kg^{-1}) in the isotherm adsorption study under the treatment of HE (data for Table 11). Nomenclatures of the treatment (HE) refer to Appendix A, sample codes refer to Appendix B1.

Spiked P Level (mg L^{-1})	B-2		B-3		B-7		B-17		B-18		B-19		B-20	
	C	Q	C	Q	C	Q	C	Q	C	Q	C	Q	C	Q
0.00	0.048	-0.747	0.167	-3.115	0.010	0.025	0.047	0.488	0.035	0.725	0.038	0.460	0.014	0.547
0.05	0.052	-0.125	0.172	-2.514	0.010	0.716	0.060	1.528	0.038	1.973	0.050	1.322	0.020	1.770
0.10	0.057	0.612	0.178	-1.793	0.011	1.545	0.054	2.862	0.049	2.962	0.043	2.353	0.023	3.127
0.20	0.062	2.754	0.191	0.164	0.019	3.602	0.059	5.055	0.048	5.257	0.056	4.471	0.035	4.480
0.40	0.089	6.512	0.238	3.500	0.044	7.418	0.082	8.931	0.051	9.491	0.070	7.726	0.061	8.165
0.80	0.134	14.136	0.304	10.653	0.056	15.663	0.129	16.648	0.074	17.652	0.112	15.383	0.070	15.946

Spiked P Level (mg L^{-1})	B-21		B-22		I-4		I-5		I-6		I-8		I-11	
	C	Q	C	Q	C	Q	C	Q	C	Q	C	Q	C	Q
0.00	0.057	0.075	0.040	0.413	0.091	-1.541	0.010	0.015	0.066	-1.049	0.071	-1.136	0.012	0.040
0.05	0.065	1.026	0.047	1.389	0.094	-1.263	0.014	0.642	0.066	-0.706	0.086	-1.098	0.018	0.265
0.10	0.065	1.913	0.050	2.205	0.098	-0.035	0.014	1.479	0.070	0.525	0.097	-0.010	0.030	1.333
0.20	0.069	4.190	0.060	4.376	0.103	2.165	0.017	3.628	0.080	2.615	0.104	2.122	0.035	3.517
0.40	0.084	7.418	0.069	7.707	0.128	6.049	0.026	7.731	0.089	6.830	0.113	6.353	0.041	7.811
0.80	0.120	15.248	0.101	15.639	0.174	14.031	0.041	15.906	0.135	14.833	0.170	14.117	0.056	16.469

Spiked P Level (mg L^{-1})	I-12		I-13		I-23		I-24		I-25		F-1		F-9	
	C	Q	C	Q	C	Q	C	Q	C	Q	C	Q	C	Q
0.00	0.186	-3.425	0.161	-1.796	0.110	-0.990	0.014	0.885	0.071	-0.578	0.060	-0.977	0.043	-0.646
0.05	0.213	-3.625	0.165	-0.573	0.122	-0.131	0.016	1.908	0.075	0.694	0.067	-0.420	0.048	-0.030
0.10	0.214	-2.359	0.171	0.497	0.138	0.443	0.017	2.713	0.078	2.039	0.079	0.170	0.051	0.741
0.20	0.253	-0.833	0.176	2.672	0.127	3.023	0.017	4.867	0.085	3.493	0.080	2.378	0.060	2.783
0.40	0.310	2.407	0.192	6.648	0.155	5.954	0.018	8.189	0.096	7.469	0.115	5.994	0.107	6.145
0.80	0.406	9.402	0.217	14.718	0.196	13.723	0.021	16.115	0.098	15.381	0.165	13.503	0.119	14.409

Spiked P Level (mg L^{-1})	F-10		F-14		F-15		F-16	
	C	Q	C	Q	C	Q	C	Q
0.00	0.156	-2.845	0.045	0.522	0.047	0.474	0.155	-1.697
0.05	0.164	-2.663	0.048	1.744	0.054	1.626	0.170	-0.684
0.10	0.173	-1.541	0.062	2.671	0.060	2.727	0.229	-0.648
0.20	0.194	0.334	0.069	4.816	0.068	4.844	0.228	1.669
0.40	0.235	3.913	0.089	8.691	0.078	8.922	0.307	4.399
0.80	0.330	10.939	0.122	16.642	0.145	16.169	0.351	12.163

Appendix B9. Liquid-phase P (C, in mg L^{-1}) and solid-phase P (Q, in mg kg^{-1}) in the isotherm adsorption study under the treatment of LS (data for Table 11). Nomenclatures of the treatment (LS) refer to Appendix A, sample codes refer to Appendix B1.

Spiked P Level (mg L^{-1})	B-2		B-3		B-7		B-17		B-18		B-19		B-20	
	C	Q	C	Q	C	Q	C	Q	C	Q	C	Q	C	Q
0.00	0.031	-1.399	0.070	-8.978	0.036	1.463	0.041	-1.769	0.042	-1.898	0.051	1.488	0.026	3.508
0.05	0.045	5.983	0.093	-3.603	0.097	5.659	0.073	5.104	0.065	6.876	0.078	5.759	0.085	8.274
0.10	0.066	11.506	0.119	0.616	0.137	10.772	0.095	11.036	0.076	14.944	0.112	10.186	0.114	15.377
0.20	0.117	23.506	0.179	10.325	0.207	16.751	0.147	23.042	0.120	28.771	0.184	18.605	0.237	10.731
0.40	0.248	38.603	0.309	26.071	0.369	26.688	0.291	37.981	0.212	54.460	0.353	28.841	0.412	18.705
0.80	0.565	55.362	0.617	44.540	0.737	26.324	0.632	61.421	0.469	94.441	0.683	42.940	0.786	16.524
Spiked P Level (mg L^{-1})	B-21		B-22		I-4		I-5		I-6		I-8		I-11	
	C	Q	C	Q	C	Q	C	Q	C	Q	C	Q	C	Q
0.00	0.067	-1.660	0.050	1.752	0.022	-0.357	0.015	5.690	0.027	-1.375	0.044	-4.742	0.007	2.675
0.05	0.089	3.438	0.073	6.768	0.052	-2.491	0.040	17.419	0.045	-1.110	0.056	-3.150	0.010	5.999
0.10	0.122	8.343	0.097	13.329	0.087	6.308	0.058	27.132	0.068	10.048	0.077	8.427	0.015	21.053
0.20	0.171	21.817	0.144	26.470	0.137	14.177	0.096	39.821	0.114	18.593	0.121	17.127	0.026	36.369
0.40	0.297	40.601	0.257	48.276	0.254	31.840	0.197	62.442	0.207	41.719	0.235	35.592	0.069	69.258
0.80	0.614	56.503	0.549	68.358	0.579	54.687	0.446	87.802	0.492	70.350	0.526	64.070	0.258	118.878
Spiked P Level (mg L^{-1})	I-12		I-13		I-23		I-24		I-25		F-1		F-9	
	C	Q	C	Q	C	Q	C	Q	C	Q	C	Q	C	Q
0.00	0.069	-9.521	0.136	-20.823	0.120	-12.282	0.011	9.524	0.072	-5.669	0.026	-0.503	0.023	0.083
0.05	0.083	-8.553	0.188	-17.416	0.185	-15.983	0.012	18.707	0.127	-0.188	0.049	5.143	0.042	6.465
0.10	0.128	-1.712	0.182	-5.891	0.211	-9.640	0.019	28.346	0.146	9.381	0.059	12.570	0.056	13.172
0.20	0.168	7.918	0.221	8.352	0.283	-0.703	0.024	50.653	0.188	20.789	0.121	21.780	0.121	21.888
0.40	0.315	20.144	0.321	32.484	0.427	14.948	0.056	88.276	0.291	43.244	0.249	37.952	0.245	38.692
0.80	0.659	39.027	0.539	78.030	0.778	24.569	0.068	161.820	0.479	77.559	0.550	58.190	0.515	64.438
Spiked P Level (mg L^{-1})	F-10		F-14		F-15		F-16							
	C	Q	C	Q	C	Q	C	Q						
0.00	0.040	-3.879	0.059	-5.218	0.040	-1.601	0.103	-13.981						
0.05	0.067	-5.328	0.094	1.070	0.075	4.853	0.197	-19.393						
0.10	0.081	7.470	0.083	13.789	0.097	10.780	0.146	1.113						
0.20	0.127	15.960	0.164	19.399	0.164	19.668	0.216	9.238						
0.40	0.260	30.874	0.298	36.913	0.281	40.058	0.417	13.410						
0.80	0.588	51.994	0.641	59.481	0.643	58.941	0.702	47.113						

Appendix B10. Pore water P concentration (C_{pw}), data for Fig. 14. Nomenclature of the treatments (OX, AN, LS) refer to Appendix A.

Group	Code	Description	C_{pw} (mg L^{-1})		
			OX	AN	LS
Bank	B-2	Camp Creek (1)	0.029	0.021	0.018
	B-7	Till (1)	0.007	0.023	0.076
	B-17	Camp Creek (2)	0.033	0.019	0.025
	B-18	Roberts Creek (2)	0.015	0.009	0.013
	B-19	Gunder (1)	0.037	0.029	0.039
	B-20	Till (2)	0.006	0.027	0.047
In-stream	I-4	Stream bottom sediment (1)	0.072	0.069	0.077
deposit	I-5	Slump, debris dam	0.003	0.004	0.008
	I-8	Sand bar	0.042	0.056	0.024
	I-11	Stream bottom sediment (2)	0.004	0.090	0.003
	I-12	Slump (1)	0.106	0.083	0.045
	I-13	Bar	0.017	0.018	0.019
Floodplain	F-1	Pasture	0.034	0.022	0.022
	F-9	Forest (1)	0.046	0.021	0.033
	F-10	Forest (2)	0.063	0.042	0.024
	F-14	Corn Field, tillage	0.026	0.027	0.035
	F-15	Soybean field	0.016	0.031	0.035
	F-16	Corn Field, no tillage	0.193	0.185	0.046

Appendix B11. Data of pH, Eh, PBC, and EPC for Table 15 and Fig.18. Nomenclatures refer to Appendix A.

Sediment type/ Replicate	pH			Eh (mV)			PBC (L kg^{-1})			EPC (mg L^{-1})		
	A	AN	ANG	A	AN	ANG	A	AN	ANG	A	AN	ANG
Camp Creek												
1	7.0	7.9	7.8	509.1	341.9	-21.3	178	377	38	0.035	0.069	0.775
2	6.9	7.8	7.6	499.5	330.8	-15.0	192	407	37	0.036	0.059	0.870
3	6.9	7.8	7.6	496.9	344.9	-13.4	194	378	31	0.036	0.062	0.859
Roberts Creek												
1	6.9	7.6	7.6	493.1	357.0	-2.7	298	711	35	0.029	0.048	1.000
2	6.9	7.7	7.5	479.4	355.7	15.5	347	521	51	0.033	0.046	0.972
3	6.9	7.6	7.6	463.6	367.6	7.2	334	334	50	0.027	0.048	1.006
Gunder												
1	7.9	8.2	7.8	463.6	346.4	16.2	150	187	18	0.029	0.085	1.279
2	8.0	8.2	7.7	473.3	334.5	1.7	127	161	14	0.011	0.087	1.347
3	8.0	8.2	7.8	467.0	340.6	7.5	120	188	16	0.048	0.083	1.314
Till												
1	8.2	8.1	7.9	427.6	333.7	20.4	990	170	205	0.011	0.011	0.019
2	8.2	8.1	7.9	415.8	350.2	25.8	1040	180	209	0.011	0.010	0.018
3	8.2	8.1	7.9	428.8	351.9	9.8	881	168	187	0.011	0.013	0.017

Appendix B12. Data of liquid-phase P (C, in mg L^{-1}) and solid-phase P (Q, in L kg^{-1}) for Fig. 19. Nomenclatures refer to Appendix A.

Replicate / Spike P level (mg L^{-1})	Camp Creek						Roberts Creek					
	A		AN		ANG		A		AN		ANG	
	C	Q	C	Q	C	Q	C	Q	C	Q	C	Q
Replicate 1												
0.00	0.041	0.632	0.069	-0.020	0.482	-8.230	0.032	0.823	0.050	0.361	0.607	-10.768
0.05	0.046	1.772	0.074	1.196	0.559	-8.479	0.033	2.014	0.051	1.667	0.705	-11.440
0.10	0.048	2.807	0.076	2.324	0.632	-8.839	0.043	2.895	0.053	2.787	0.752	-11.280
0.20	0.063	4.764	0.081	4.661	0.655	-6.948	0.042	5.186	0.054	5.224	0.763	-9.122
0.40	0.082	8.790	0.091	9.027	0.694	-3.208	0.068	9.066	0.060	9.731	0.844	-6.226
0.80	0.125	15.873	0.113	16.145	0.764	3.120	0.078	16.763	0.073	17.013	0.923	-0.053
Replicate 2												
0.00	0.046	0.531	0.063	0.109	0.545	-9.473	0.035	0.743	0.051	0.350	0.676	-12.162
0.05	0.045	1.776	0.063	1.425	0.612	-9.550	0.035	1.975	0.052	1.650	0.783	-12.992
0.10	0.047	2.823	0.066	2.516	0.675	-9.694	0.048	2.797	0.052	2.807	0.789	-12.007
0.20	0.060	4.823	0.071	4.866	0.708	-7.990	0.047	5.079	0.054	5.241	0.796	-9.771
0.40	0.079	8.843	0.076	9.341	0.750	-4.337	0.055	9.322	0.061	9.664	0.821	-5.773
0.80	0.121	15.904	0.101	16.325	0.849	1.408	0.081	16.696	0.081	16.880	0.932	-0.241
Replicate 3												
0.00	0.045	0.545	0.060	0.169	0.516	-8.893	0.032	0.808	0.049	0.380	0.724	-13.093
0.05	0.039	1.897	0.069	1.292	0.552	-8.330	0.036	1.972	0.053	1.633	0.748	-12.274
0.10	0.049	2.789	0.071	2.416	0.653	-9.244	0.037	3.015	0.057	2.701	0.781	-11.874
0.20	0.065	4.755	0.073	4.832	0.668	-7.171	0.040	5.240	0.063	5.049	0.833	-10.529
0.40	0.084	8.766	0.089	9.071	0.736	-4.058	0.053	9.377	0.083	9.256	0.865	-6.658
0.80	0.117	16.052	0.103	16.305	0.845	1.493	0.079	16.760	0.094	16.568	0.970	-1.010

Appendix B12. Continued.

Replicate / Spike P level (mg L^{-1})	Gunder						Till					
	A		AN		ANG		A		AN		ANG	
	C	Q	C	Q	C	Q	C	Q	C	Q	C	Q
Replicate 1												
0.00	0.045	0.542	0.090	-0.441	0.569	-9.995	0.013	1.183	0.024	0.862	0.024	0.914
0.05	0.048	1.723	0.095	0.792	0.680	-10.924	0.015	2.391	0.034	1.965	0.025	2.172
0.10	0.054	2.689	0.100	1.856	0.762	-11.438	0.016	3.458	0.021	3.384	0.058	2.642
0.20	0.045	5.137	0.102	4.276	0.857	-10.960	0.016	5.723	0.033	5.562	0.041	5.331
0.40	0.076	8.890	0.114	8.656	0.876	-6.869	0.019	10.073	0.068	9.416	0.054	9.542
0.80	0.136	15.619	0.171	15.114	1.003	-1.665	0.030	17.764	0.104	16.073	0.093	16.522
Replicate 2												
0.00	0.027	0.896	0.085	-0.341	0.528	-9.158	0.013	1.188	0.024	0.872	0.025	0.893
0.05	0.033	2.033	0.086	0.970	0.630	-9.921	0.015	2.393	0.029	2.070	0.037	1.937
0.10	0.023	3.295	0.106	1.720	0.744	-11.108	0.016	3.449	0.033	3.138	0.023	3.333
0.20	0.050	5.033	0.110	4.128	0.811	-10.038	0.015	5.746	0.035	5.531	0.059	4.969
0.40	0.082	8.776	0.152	7.893	0.896	-7.257	0.020	10.040	0.045	9.857	0.052	9.597
0.80	0.133	15.658	0.167	15.167	1.001	-1.609	0.029	17.830	0.105	16.143	0.092	16.540
Replicate 3												
0.00	0.047	0.496	0.080	-0.231	0.538	-9.358	0.013	1.183	0.023	0.894	0.025	0.906
0.05	0.067	1.339	0.080	1.080	0.673	-10.814	0.015	2.391	0.027	2.102	0.036	1.959
0.10	0.063	2.488	0.098	1.887	0.749	-11.169	0.016	3.458	0.032	3.136	0.047	2.851
0.20	0.081	4.415	0.122	3.883	0.806	-9.938	0.017	5.703	0.037	5.487	0.025	5.660
0.40	0.130	7.828	0.135	8.220	0.906	-7.440	0.019	10.073	0.070	9.386	0.076	9.135
0.80	0.162	15.114	0.148	15.530	1.004	-1.681	0.032	17.724	0.109	15.999	0.091	16.525

Appendix B13. Data of pH and Eh for Fig.22. Nomenclatures refer to Appendix A.

Sediment type/ Replicate	pH								Eh (mV)							
	Day 3		Day 6		Day 12		Day 24		Day 3		Day 6		Day 12		Day 24	
	OX	AN	OX	AN	OX	AN	OX	AN	OX	AN	OX	AN	OX	AN	OX	AN
Camp Creek																
1	7.26	8.58	7.07	8.43	6.85	8.03	6.85	7.26	568.4	377.1	526.8	322.1	578.3	349.6	560.6	295.1
2	7.26	8.51	7.06	8.49	6.98	8.12	6.85	7.50	511.8	363.2	511.4	314.7	557.1	348.7	539.2	298.3
3	7.32	8.85	7.11	8.61	6.92	8.29	6.86	7.50	466.3	347.7	466.4	304.8	514.9	346.8	504.8	292.7
Roberts Creek																
1	7.28	8.53	7.06	8.44	6.85	7.92	6.73	7.16	558.7	386.2	530.2	337.2	577.2	363.6	571.7	313.4
2	7.35	8.65	7.18	8.48	7.03	7.80	6.90	7.04	491.1	364.3	496.8	320.8	547.4	365.3	529.3	316.3
3	7.33	8.73	7.14	8.65	6.94	8.10	6.81	7.22	468.5	349.3	471.0	303.2	524.1	349.6	513.1	303.6
Gunder																
1	7.49	8.93	7.46	9.01	7.42	9.01	7.52	8.79	536.3	375.9	515.3	321.2	558.2	342.2	536.4	325.0
2	7.49	8.87	7.45	8.89	7.42	8.92	7.56	8.70	495.1	366.1	498.1	309.6	549.7	333.1	530.0	312.9
3	7.53	8.96	7.49	8.88	7.53	8.98	7.54	8.74	464.2	336.9	469.7	300.7	524.8	323.1	504.3	308.4
Till																
1	7.76	9.08	7.84	9.13	7.91	9.22	8.04	9.21	546.7	357.6	532.8	302.7	579.2	327.1	569.2	286.1
2	7.73	9.13	7.81	9.11	7.90	9.27	8.04	9.24	466.8	338.1	472.6	288.8	520.3	322.1	498.8	279.3
3	7.79	9.11	7.84	9.18	7.90	9.29	8.07	9.28	454.7	320.5	439.8	284.8	490.8	314.5	474.5	288.1

Appendix B14. Data of dissolved P and DOC for Fig.20. Nomenclatures refer to Appendix A.

Sediment type/ Replicate	Dissolved P (mg L^{-1})								DOC (mg L^{-1})							
	Day 3		Day 6		Day 12		Day 24		Day 3		Day 6		Day 12		Day 24	
	OX	AN	OX	AN	OX	AN	OX	AN	OX	AN	OX	AN	OX	AN	OX	AN
Camp Creek																
1	0.000	0.000	0.003	0.005	0.013	0.030	0.015	0.030	0.0	0.0	0.0	0.0	0.8	0.6	1.1	1.1
2	0.000	0.000	0.005	0.008	0.012	0.028	0.017	0.027	0.0	0.0	0.0	0.0	0.7	0.8	0.8	1.0
3	0.000	0.000	0.005	0.012	0.010	0.030	0.011	0.034	0.0	0.0	0.0	0.0	1.2	1.2	1.4	1.4
Roberts Creek																
1	0.000	0.000	0.006	0.015	0.010	0.033	0.011	0.035	0.0	0.0	0.0	0.0	0.8	1.1	1.3	1.3
2	0.000	0.000	0.003	0.007	0.011	0.032	0.013	0.030	0.0	0.0	0.0	0.0	0.8	1.3	1.1	1.7
3	0.000	0.000	0.004	0.007	0.010	0.031	0.011	0.032	0.0	0.0	0.0	0.0	0.7	1.2	0.8	1.2
Gunder																
1	0.000	0.000	0.006	0.006	0.009	0.012	0.011	0.013	0.0	0.0	0.0	0.0	0.9	1.4	1.0	1.4
2	0.000	0.000	0.004	0.009	0.010	0.013	0.010	0.012	0.0	0.0	0.0	0.0	0.7	1.1	0.8	1.1
3	0.000	0.000	0.007	0.006	0.011	0.011	0.010	0.012	0.0	0.0	0.0	0.0	0.8	1.2	0.9	1.2
Till																
1	0.000	0.000	0.008	0.005	0.011	0.011	0.012	0.014	0.0	0.0	0.0	0.0	0.7	1.2	0.7	1.1
2	0.000	0.000	0.004	0.007	0.012	0.014	0.010	0.015	0.0	0.0	0.0	0.0	0.7	1.2	0.7	1.1
3	0.000	0.000	0.005	0.004	0.011	0.013	0.012	0.016	0.0	0.0	0.0	0.0	1.0	1.3	0.9	1.5

Appendix B15. Data of pH, Eh, and P fractionation for Fig.22- Fig.29. Nomenclatures refer to Appendix A.

Sediment type/ treatments	Repli-cate	pH	Eh (mV)	P fractionation (mg kg-1)								
				P_{H2O}	*Pi*				*Po*			P_{Res}	P_{sum}
					P_{Lab}	Fe-P_{slow}	Ca-P_{slow}	P_{stab}	P_{Lab}	P_{slow}	P_{stab}		
Camp Creek													
A	1	5.6	636	9	42	73	105	87	11	65	21	53	466
A	2	5.7	590	8	37	70	103	86	12	70	22	57	465
A	3	5.9	579	7	37	71	103	88	15	66	24	52	463
AN	1	6.3	423	10	37	71	105	90	8	66	24	56	467
AN	2	6.2	419	9	35	68	105	87	11	65	25	57	462
AN	3	6.0	409	9	36	72	105	88	11	65	26	50	462
ANG	1	7.2	113	9	51	65	105	85	14	62	25	57	473
ANG	2	6.9	108	10	52	60	96	87	17	72	21	49	464
ANG	3	7.0	136	8	49	67	100	86	17	64	22	55	468
Roberts Creek													
A	1	5.6	636	9	42	73	105	87	11	65	21	53	466
A	2	5.7	590	8	37	70	103	86	12	70	22	57	465
A	3	5.9	579	7	37	71	103	88	15	66	24	52	463
AN	1	6.3	423	10	37	71	105	90	8	66	24	56	467
AN	2	6.2	419	9	35	68	105	87	11	65	25	57	462
AN	3	6.0	409	9	36	72	105	88	11	65	26	50	462
ANG	1	7.2	113	9	51	65	105	85	14	62	25	57	473
ANG	2	6.9	108	10	52	60	96	87	17	72	21	49	464
ANG	3	7.0	136	8	49	67	100	86	17	64	22	55	468

Appendix B15. Continued.

Sediment type/ treatments	Repli-cate	pH	Eh (mV)	P fractionation (mg kg-1)									
				P_{H2O}	*Pi*				*Po*			P_{Res}	P_{sum}
					P_{Lab}	Fe-P_{slow}	Ca-P_{slow}	P_{stab}	P_{Lab}	P_{slow}	P_{stab}		
Gunder													
A	1	6.2	575	7	22	25	322	58	0	3	1	40	478
A	2	6.2	540	7	21	24	329	58	1	3	2	38	483
A	3	6.2	531	8	22	26	329	59	0	1	4	37	486
AN	1	6.4	369	9	20	23	322	58	0	9	0	39	480
AN	2	6.5	354	10	20	23	323	58	0	7	1	38	480
AN	3	6.6	354	10	20	22	322	59	1	10	2	39	485
ANG	1	6.9	171	5	23	21	326	62	1	14	1	39	492
ANG	2	6.6	191	4	24	23	318	58	0	9	2	41	479
ANG	3	6.7	215	4	24	21	314	61	0	9	1	40	474
TIll													
A	1	7.2	493	6	7	9	269	110	0	4	4	31	440
A	2	7.2	444	7	6	11	284	116	0	3	3	30	460
A	3	7.3	423	9	6	9	265	110	1	4	3	31	438
AN	1	7.2	274	9	6	9	265	102	0	3	3	29	426
AN	2	7.3	282	9	7	9	272	113	0	2	2	28	442
AN	3	7.2	278	10	6	10	267	118	0	2	3	33	449
ANG	1	7.5	172	4	8	8	254	108	0	3	3	28	416
ANG	2	7.5	177	4	7	9	284	116	0	2	3	32	457
ANG	3	7.4	169	5	8	8	252	118	1	4	2	29	427

Appendix B16. P concentration (mg kg^{-1}) in each extracting solution, data for Fig.31 (Camp Creek). Nomenclatures refer to Appendix A.

Methods/ Replicate	Water	*Pi*				*Pt*			Conc. H_2SO_4
		0.5 *M* $NaHCO_3$	0.1 *M* NaOH	1 *M* HCl	Conc. HCl	0.5 *M* $NaHCO_3$	0.1 *M* NaOH	Conc. HCl	
Molybdate blue-ascorbic acid method (AA)									
1	8	38	67	96	75	54	115	108	47
2	7	37	67	100	74	53	115	106	47
3	10	45	73	102	73	61	120	104	46
4	10	40	74	101	78	57	124	108	50
5	9	37	65	96	77	53	123	106	50
6	7	41	72	106	79	57	127	105	47
Malachite green method (MG)									
1	7	35	66	96	72	55	120	106	46
2	7	35	65	100	73	53	117	107	48
3	10	44	73	99	71	64	113	104	46
4	10	41	74	102	73	57	121	111	49
5	10	38	65	94	72	49	115	105	48
6	8	40	73	102	80	60	127	110	46

Appendix B17. P concentration (mg kg^{-1}) in each extracting solution, data for Fig.32 (Roberts Creek). Nomenclatures refer to Appendix A.

Methods/ Replicate	Water	*Pi*				*Pt*			Conc. H_2SO_4
		0.5 *M* $NaHCO_3$	0.1 *M* NaOH	1 *M* HCl	Conc. HCl	0.5 *M* $NaHCO_3$	0.1 *M* NaOH	Conc. HCl	
Molybdate blue-ascorbic acid method (AA)									
1	7	52	87	121	66	69	165	95	47
2	7	53	88	125	69	74	162	102	45
3	10	51	93	121	71	68	154	100	48
4	6	53	96	125	70	70	158	102	49
5	7	51	88	123	69	69	154	98	47
6	9	49	96	128	67	68	159	98	43
Malachite green method (MG)									
1	8	51	87	117	59	71	152	93	45
2	7	52	88	125	61	75	170	98	45
3	10	49	91	123	65	75	150	101	48
4	6	54	94	130	63	69	166	101	47
5	7	49	87	121	60	72	151	98	46
6	9	52	97	128	62	70	171	104	46

Appendix B18. P concentration (mg kg^{-1}) in each extracting solution, data for Fig.33 (Gunder). Nomenclatures refer to Appendix A.

Methods/ Replicate	Water	*Pi*				*Pt*			Conc. H_2SO_4
		0.5 *M* $NaHCO_3$	0.1 *M* NaOH	1 *M* HCl	Conc. HCl	0.5 *M* $NaHCO_3$	0.1 *M* NaOH	Conc. HCl	
Molybdate blue-ascorbic acid method (AA)									
1	7	21	22	322	44	24	25	52	33
2	7	23	21	329	43	25	25	54	35
3	10	22	18	320	44	25	23	51	33
4	6	22	20	321	43	24	25	52	35
5	7	22	19	327	46	24	26	54	33
6	9	22	19	325	46	25	25	54	33
Malachite green method (MG)									
1	8	19	18	322	42	20	25	53	32
2	7	21	19	329	40	24	25	54	34
3	10	20	16	320	38	23	25	54	33
4	6	20	18	321	40	24	24	53	36
5	7	22	19	327	43	22	27	57	34
6	9	22	19	325	44	22	27	56	32

Appendix B19. P concentration (mg kg^{-1}) in each extracting solution, data for Fig.34 (Till). Nomenclatures refer to Appendix A.

Methods/ Replicate	Water	*Pi*				*Pt*			Conc. H_2SO_4
		0.5 *M* $NaHCO_3$	0.1 *M* NaOH	1 *M* HCl	Conc. HCl	0.5 *M* $NaHCO_3$	0.1 *M* NaOH	Conc. HCl	
Molybdate blue-ascorbic acid method (AA)									
1	8	7	6	267	107	8	12	114	24
2	6	6	8	266	108	8	10	117	26
3	9	7	7	236	105	8	12	113	28
4	7	5	7	263	107	8	10	115	28
5	10	6	7	242	107	7	14	122	24
6	7	6	7	264	110	7	11	121	25
Malachite green method (MG)									
1	7	5	5	267	102	7	12	112	24
2	7	4	6	266	110	5	11	119	26
3	9	3	5	236	110	8	13	119	28
4	8	4	5	263	102	5	12	117	28
5	10	4	5	242	102	7	12	119	25
6	8	4	6	264	106	4	11	121	25

Appendix B20. P concentration (mg L^{-1}) in water at different measurement time of malachite green method, data for Table 21.

Sediment type/ Replicate	Measurement time (hours)					
	t=0	t=0.5	t=2	t=6	t=12	t=24
Camp Creek						
1	0.122	0.122	0.124	0.127	0.127	0.130
2	0.122	0.123	0.125	0.129	0.130	0.133
3	0.171	0.172	0.174	0.177	0.175	0.178
4	0.167	0.168	0.172	0.174	0.175	0.179
5	0.182	0.183	0.185	0.187	0.188	0.191
6	0.132	0.133	0.133	0.137	0.137	0.139
Roberts Creek						
1	0.173	0.175	0.178	0.182	0.182	0.187
2	0.208	0.210	0.211	0.214	0.214	0.218
3	0.218	0.220	0.221	0.224	0.223	0.227
4	0.146	0.146	0.147	0.150	0.149	0.151
5	0.176	0.175	0.177	0.181	0.180	0.182
6	0.141	0.141	0.144	0.148	0.146	0.149
Gunder						
1	0.141	0.143	0.147	0.151	0.149	0.153
2	0.110	0.111	0.114	0.117	0.115	0.118
3	0.169	0.171	0.173	0.176	0.176	0.179
4	0.091	0.092	0.095	0.098	0.099	0.100
5	0.119	0.121	0.124	0.127	0.128	0.129
6	0.147	0.148	0.151	0.154	0.154	0.157
Till						
1	0.124	0.125	0.128	0.131	0.130	0.134
2	0.114	0.114	0.118	0.121	0.119	0.124
3	0.157	0.158	0.160	0.163	0.161	0.165
4	0.128	0.128	0.130	0.133	0.132	0.135
5	0.182	0.182	0.184	0.186	0.185	0.188
6	0.141	0.141	0.144	0.148	0.146	0.149

Appendix B21. *Pi* concentration (mg L^{-1}) in 0.5 *M* $NaHCO_3$ at different measurement time of malachite green method, data for Table 21.

Sediment type/ Replicate	Measurement time (hours)					
	t=0	t=0.5	t=2	t=6	t=12	t=24
Camp Creek						
1	0.096	0.096	0.096	0.096	0.097	0.098
2	0.096	0.096	0.097	0.097	0.098	0.099
3	0.117	0.116	0.117	0.118	0.119	0.120
4	0.110	0.111	0.112	0.113	0.114	0.115
5	0.104	0.104	0.105	0.105	0.106	0.107
6	0.108	0.108	0.108	0.109	0.110	0.111
Roberts Creek						
1	0.138	0.137	0.137	0.137	0.138	0.140
2	0.141	0.142	0.142	0.143	0.144	0.146
3	0.133	0.133	0.134	0.135	0.136	0.138
4	0.148	0.148	0.149	0.149	0.149	0.151
5	0.136	0.132	0.133	0.134	0.136	0.137
6	0.139	0.139	0.140	0.140	0.141	0.142
Gunder						
1	0.056	0.052	0.053	0.054	0.055	0.055
2	0.058	0.058	0.059	0.059	0.060	0.060
3	0.055	0.055	0.056	0.056	0.056	0.057
4	0.057	0.057	0.056	0.057	0.057	0.057
5	0.063	0.064	0.064	0.064	0.064	0.064
6	0.060	0.061	0.061	0.061	0.062	0.062
Till						
1	0.014	0.014	0.015	0.016	0.016	0.016
2	0.013	0.013	0.013	0.014	0.015	0.015
3	0.013	0.012	0.013	0.014	0.014	0.014
4	0.010	0.011	0.012	0.013	0.013	0.013
5	0.011	0.012	0.013	0.014	0.015	0.014
6	0.013	0.013	0.014	0.015	0.016	0.015

Appendix B22. *Pt* concentration (mg L^{-1}) in 0.5 *M* $NaHCO_3$ at different measurement time of malachite green method, data for Table 21.

Sediment type/ Replicate	Measurement time (hours)					
	t=0	t=0.5	t=2	t=6	t=12	t=24
Camp Creek						
1	0.184	0.185	0.184	0.185	0.184	0.186
2	0.176	0.176	0.177	0.176	0.176	0.179
3	0.212	0.212	0.212	0.212	0.212	0.216
4	0.191	0.191	0.191	0.190	0.190	0.195
5	0.153	0.153	0.153	0.153	0.154	0.155
6	0.200	0.201	0.201	0.201	0.200	0.202
Roberts Creek						
1	0.239	0.238	0.239	0.239	0.239	0.241
2	0.252	0.252	0.252	0.252	0.251	0.254
3	0.250	0.249	0.249	0.249	0.249	0.254
4	0.231	0.232	0.231	0.232	0.231	0.236
5	0.240	0.240	0.240	0.240	0.239	0.242
6	0.234	0.234	0.234	0.234	0.234	0.235
Gunder						
1	0.066	0.066	0.067	0.067	0.066	0.071
2	0.079	0.080	0.079	0.080	0.080	0.082
3	0.075	0.075	0.075	0.075	0.075	0.077
4	0.082	0.082	0.082	0.082	0.083	0.085
5	0.069	0.069	0.070	0.070	0.070	0.072
6	0.069	0.069	0.070	0.070	0.069	0.072
Till						
1	0.022	0.023	0.022	0.023	0.021	0.026
2	0.018	0.019	0.020	0.018	0.019	0.022
3	0.027	0.027	0.028	0.027	0.027	0.032
4	0.017	0.017	0.018	0.018	0.018	0.019
5	0.024	0.023	0.024	0.023	0.025	0.025
6	0.012	0.012	0.013	0.013	0.012	0.015

Appendix B23. *Pi* concentration (mg L^{-1}) in 0.1 *M* NaOH at different measurement time of malachite green method, data for Table 21.

Sediment type/ Replicate	Measurement time (hours)					
	t=0	t=0.5	t=2	t=6	t=12	t=24
Camp Creek						
1	0.276	0.270	0.274	0.274	0.276	0.280
2	0.274	0.271	0.273	0.276	0.278	0.283
3	0.304	0.300	0.302	0.303	0.305	0.308
4	0.314	0.309	0.311	0.313	0.316	0.319
5	0.272	0.267	0.270	0.271	0.272	0.275
6	0.303	0.297	0.302	0.303	0.306	0.312
Roberts Creek						
1	0.364	0.356	0.361	0.361	0.361	0.366
2	0.367	0.361	0.362	0.364	0.365	0.371
3	0.380	0.375	0.379	0.378	0.379	0.385
4	0.395	0.386	0.393	0.392	0.395	0.399
5	0.364	0.355	0.362	0.362	0.364	0.366
6	0.407	0.398	0.403	0.405	0.406	0.411
Gunder						
1	0.076	0.078	0.078	0.080	0.079	0.080
2	0.081	0.084	0.083	0.085	0.085	0.085
3	0.066	0.069	0.069	0.070	0.071	0.070
4	0.075	0.078	0.077	0.079	0.078	0.079
5	0.079	0.082	0.081	0.083	0.083	0.082
6	0.079	0.083	0.081	0.082	0.082	0.082
Till						
1	0.022	0.022	0.022	0.025	0.025	0.025
2	0.024	0.025	0.025	0.027	0.027	0.027
3	0.021	0.022	0.021	0.024	0.024	0.024
4	0.021	0.021	0.021	0.023	0.023	0.023
5	0.019	0.019	0.020	0.022	0.022	0.021
6	0.024	0.024	0.023	0.026	0.026	0.026

Appendix B24. *Pt* concentration (mg L^{-1}) in 0.1 *M* NaOH at different measurement time of malachite green method, data for Table 21.

Sediment type/ Replicate	Measurement time (hours)					
	t=0	t=0.5	t=2	t=6	t=12	t=24
Camp Creek						
1	0.282	0.285	0.280	0.281	0.281	0.289
2	0.275	0.272	0.276	0.280	0.279	0.277
3	0.264	0.268	0.264	0.263	0.264	0.265
4	0.286	0.289	0.281	0.289	0.290	0.288
5	0.270	0.276	0.278	0.276	0.279	0.276
6	0.296	0.300	0.313	0.302	0.304	0.301
Roberts Creek						
1	0.357	0.357	0.360	0.359	0.364	0.253
2	0.399	0.397	0.397	0.392	0.406	0.409
3	0.351	0.349	0.358	0.348	0.348	0.345
4	0.393	0.390	0.397	0.392	0.402	0.409
5	0.354	0.361	0.359	0.352	0.353	0.363
6	0.399	0.396	0.405	0.405	0.391	0.407
Gunder						
1	0.058	0.059	0.057	0.059	0.059	0.059
2	0.059	0.060	0.058	0.060	0.057	0.059
3	0.057	0.057	0.054	0.056	0.054	0.056
4	0.056	0.056	0.056	0.059	0.057	0.060
5	0.062	0.065	0.067	0.070	0.066	0.067
6	0.062	0.063	0.061	0.062	0.060	0.062
Till						
1	0.028	0.025	0.026	0.027	0.025	0.026
2	0.027	0.024	0.024	0.026	0.026	0.024
3	0.030	0.027	0.028	0.027	0.029	0.027
4	0.028	0.026	0.026	0.026	0.027	0.026
5	0.028	0.025	0.025	0.028	0.025	0.024
6	0.025	0.022	0.024	0.023	0.022	0.026

Appendix B25. P concentration (mg L^{-1}) in 1 *M* HCl at different measurement time of malachite green method, data for Table 21.

Sediment type/ Replicate	Measurement time (hours)					
	t=0	t=0.5	t=2	t=6	t=12	t=24
Camp Creek						
1	0.064	0.065	0.064	0.066	0.066	0.067
2	0.067	0.068	0.068	0.071	0.070	0.071
3	0.066	0.068	0.067	0.069	0.069	0.069
4	0.068	0.069	0.069	0.071	0.071	0.071
5	0.063	0.064	0.069	0.066	0.065	0.074
6	0.068	0.069	0.069	0.072	0.071	0.072
Roberts Creek						
1	0.078	0.078	0.078	0.080	0.079	0.081
2	0.084	0.084	0.084	0.085	0.085	0.086
3	0.082	0.082	0.082	0.084	0.083	0.084
4	0.087	0.087	0.088	0.089	0.088	0.089
5	0.081	0.081	0.081	0.082	0.081	0.082
6	0.086	0.086	0.086	0.087	0.087	0.089
Gunder						
1	0.216	0.216	0.216	0.217	0.216	0.219
2	0.220	0.219	0.218	0.220	0.219	0.220
3	0.217	0.217	0.215	0.216	0.215	0.215
4	0.221	0.220	0.219	0.220	0.220	0.221
5	0.221	0.221	0.221	0.221	0.219	0.222
6	0.220	0.219	0.220	0.220	0.220	0.222
Till						
1	0.179	0.179	0.179	0.179	0.179	0.180
2	0.183	0.183	0.184	0.184	0.183	0.185
3	0.156	0.156	0.157	0.157	0.156	0.157
4	0.175	0.175	0.174	0.175	0.174	0.176
5	0.160	0.159	0.159	0.159	0.159	0.160
6	0.178	0.178	0.178	0.179	0.177	0.179

Appendix B26. *Pi* concentration (mg L^{-1}) in concentrated HCl at different measurement time of malachite green method, data for Table 21.

Sediment type/ Replicate	Measurement time (hours)					
	t=0	t=0.5	t=2	t=6	t=12	t=24
Camp Creek						
1	0.073	0.073	0.074	0.075	0.075	0.075
2	0.074	0.074	0.075	0.077	0.077	0.078
3	0.071	0.072	0.073	0.074	0.074	0.075
4	0.074	0.074	0.075	0.077	0.077	0.077
5	0.073	0.073	0.074	0.075	0.076	0.076
6	0.080	0.081	0.081	0.083	0.084	0.084
Roberts Creek						
1	0.059	0.060	0.061	0.062	0.062	0.062
2	0.061	0.062	0.063	0.065	0.065	0.065
3	0.065	0.065	0.066	0.068	0.068	0.069
4	0.064	0.064	0.066	0.067	0.067	0.068
5	0.060	0.061	0.062	0.063	0.064	0.064
6	0.062	0.062	0.063	0.065	0.065	0.066
Gunder						
1	0.037	0.038	0.038	0.039	0.039	0.039
2	0.036	0.036	0.038	0.039	0.040	0.041
3	0.033	0.034	0.035	0.037	0.038	0.038
4	0.035	0.036	0.037	0.039	0.039	0.040
5	0.037	0.037	0.038	0.040	0.041	0.041
6	0.038	0.038	0.039	0.042	0.043	0.043
Till						
1	0.089	0.089	0.090	0.092	0.092	0.092
2	0.097	0.097	0.098	0.098	0.098	0.097
3	0.094	0.094	0.094	0.092	0.092	0.092
4	0.089	0.089	0.089	0.091	0.091	0.091
5	0.088	0.089	0.089	0.090	0.091	0.091
6	0.092	0.092	0.093	0.095	0.095	0.096

Appendix B27. *Pt* concentration (mg L^{-1}) in concentrated HCl at different measurement time of malachite green method, data for Table 21.

Sediment type/ Replicate	Measurement time (hours)					
	t=0	t=0.5	t=2	t=6	t=12	t=24
Camp Creek						
1	0.107	0.107	0.106	0.106	0.107	0.107
2	0.108	0.107	0.107	0.109	0.108	0.108
3	0.102	0.102	0.102	0.103	0.104	0.104
4	0.111	0.110	0.110	0.111	0.112	0.112
5	0.104	0.103	0.104	0.104	0.105	0.105
6	0.108	0.107	0.107	0.109	0.109	0.110
Roberts Creek						
1	0.092	0.092	0.092	0.093	0.093	0.094
2	0.097	0.096	0.097	0.097	0.098	0.098
3	0.098	0.098	0.099	0.101	0.101	0.101
4	0.100	0.100	0.100	0.101	0.102	0.102
5	0.098	0.097	0.097	0.098	0.098	0.098
6	0.103	0.103	0.102	0.103	0.103	0.104
Gunder						
1	0.044	0.044	0.044	0.045	0.046	0.046
2	0.045	0.045	0.044	0.045	0.046	0.046
3	0.045	0.044	0.045	0.046	0.047	0.046
4	0.044	0.044	0.044	0.045	0.046	0.046
5	0.048	0.048	0.046	0.047	0.048	0.048
6	0.046	0.046	0.046	0.047	0.048	0.048
Till						
1	0.095	0.095	0.095	0.096	0.097	0.097
2	0.100	0.100	0.100	0.102	0.102	0.102
3	0.098	0.098	0.099	0.102	0.102	0.102
4	0.101	0.100	0.101	0.102	0.101	0.101
5	0.103	0.102	0.101	0.102	0.103	0.103
6	0.103	0.103	0.102	0.103	0.103	0.104

Appendix B28. P concentration (mg L^{-1}) in concentrated H_2SO_4 at different measurement time of malachite green method, data for Table 21.

Sediment type/ Replicate	Measurement time (hours)					
	t=0	t=0.5	t=2	t=6	t=12	t=24
Camp Creek						
1	0.075	0.074	0.072	0.074	0.074	0.074
2	0.076	0.076	0.074	0.076	0.076	0.076
3	0.074	0.074	0.071	0.072	0.074	0.074
4	0.079	0.079	0.076	0.078	0.079	0.079
5	0.077	0.076	0.074	0.077	0.077	0.078
6	0.074	0.074	0.072	0.074	0.074	0.075
Roberts Creek						
1	0.073	0.073	0.070	0.072	0.072	0.072
2	0.072	0.072	0.068	0.070	0.071	0.071
3	0.077	0.076	0.074	0.075	0.076	0.076
4	0.077	0.076	0.075	0.074	0.076	0.076
5	0.075	0.074	0.072	0.075	0.073	0.073
6	0.070	0.070	0.067	0.068	0.070	0.070
Gunder						
1	0.052	0.052	0.049	0.052	0.052	0.052
2	0.055	0.054	0.051	0.052	0.054	0.054
3	0.053	0.053	0.050	0.052	0.052	0.053
4	0.058	0.057	0.054	0.056	0.057	0.057
5	0.055	0.055	0.053	0.057	0.056	0.056
6	0.052	0.052	0.049	0.051	0.052	0.052
Till						
1	0.039	0.039	0.036	0.042	0.040	0.040
2	0.042	0.042	0.039	0.041	0.043	0.043
3	0.045	0.044	0.041	0.045	0.045	0.045
4	0.045	0.045	0.042	0.044	0.045	0.046
5	0.040	0.040	0.036	0.040	0.040	0.039
6	0.040	0.040	0.036	0.038	0.040	0.040

APPENDIX C

CORRELATION BETWEEN TOTAL C AND ORGANIC MATTER CONTENT

Total C values determined using the dry combustion method were strongly correlated to organic matter (OM) values determined by the loss-on-ignition (LOI) method (see the graph below). The results agree with those of a study by Konen *et al.* (2002) for soil samples from major land resource areas in the north central US. This graph used 24 out of the 25 samples; sample B-20 (the till, calcareous, pH=8.1) was excluded due to the potential for inorganic carbon to contribute to the value determined by the loss-on-ignition method.

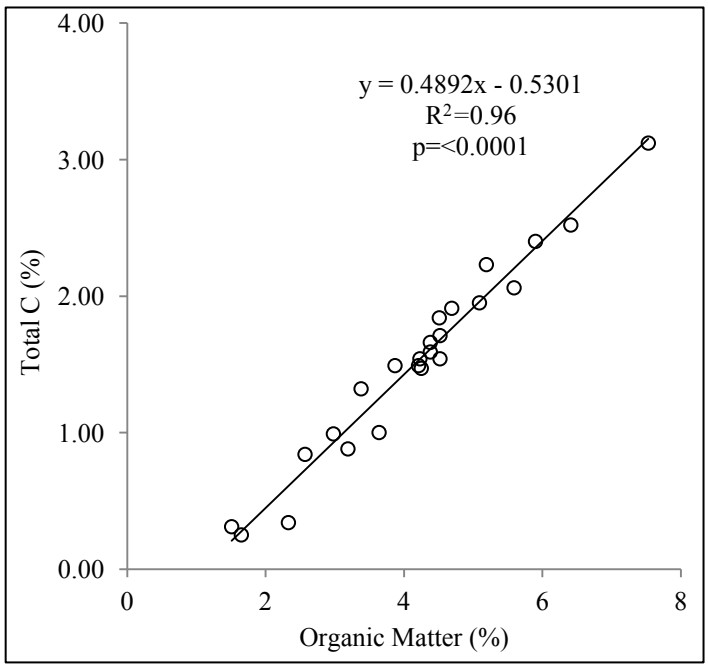

Correlation of organic matter and total C (*n=24*), data of B-20 were excluded.

A widely cited factor for converting soil organic carbon to soil organic matter is 1.724. It is based on studies based on the dichromate oxidation technique in the early part of

the 20th century, and assumes that soil organic matter contains about 58% carbon. However, if the conversion factor of 1.724 were used for sediments in this study, it is likely soil organic matter content would be underestimated. Based on the regression equation shown in this figure, it would be better to use a conversion factor of ~2 and include an adjustment corresponding to the intercept shown in the figure. Such a conversion factor suggests that organic matter is ~50% carbon, as proposed in a study by Pribyl (2010).